12-17-2018 1:00 PM

# Identifying and Targeting Cancer Stem Cells in Colorectal Cancer

Amber Harnett
*The University of Western Ontario*

Supervisor
Asfaha, Samuel.
*The University of Western Ontario*

Graduate Program in Pathology and Laboratory Medicine
A thesis submitted in partial fulfillment of the requirements for the degree in Master of Science

# ABSTRACT

The cancer stem cell hypothesis posits that cancer stem cells (CSCs) are the driving force behind tumour progression and metastasis, making them ideal therapeutic targets. Previous research identified Leucine-rich repeat-containing G-protein-coupled receptor 5 (Lgr5) as a marker of CSCs in colorectal cancer (CRC). However, it is not known whether more than one CSC population exists in CRC. Identifying and targeting CSCs in CRC is important for effective treatment of cancer patients. Here, I show that Keratin-19 (K19) labels intestinal CSCs in mouse tumours that recapitulate the early stages of CRC. Moreover, selective ablation of Lgr5 has no effect on tumour initiation or growth. These results demonstrate additional CSC populations exist besides those labeled by Lgr5, which are important for tumour initiation and growth. Consequently, these findings have important clinical implications for the development of new therapies targeting CSCs.



# KEYWORDS

Cancer stem cells, colorectal cancer, Keratin-19 (K19), Lgr5, cancer biology

# CO-AUTHORSHIP STATEMENT

The following individuals contributed to this thesis:

| | |
|---|---|
| Hayley Good | Help with animal care and tissue dissection for figures 16, 17 and 19. |
| Alice Shin | Help with animal care and tissue dissection for figures 16, 17 and 19. |
| Amanda Liddy | Help with image acquisition for figures 21-24. |
| Samuel Asfaha | Study design, data interpretation, and critical evaluation of thesis; grant funding, biosafety and animal use protocol. |

# ACKNOWLEDGEMENTS

This work was made possible by funding and support from the Cancer Research and Technology Transfer (CaRTT) strategic training program.

I would like to thank all of the members of the Asfaha lab, past and present, for their help and guidance throughout my MSc. Specifically, I'd like to thank Elena Fazio and Liyue Zhang for their advice and technical assistance with learning many essential laboratory techniques. I am also very grateful for the teaching, support and friendship provided over the past two years from my fellow lab mates Hayley Good and Alice Shin, as well as the friends I have met through the pathology department - in particular Milica Krstic. Thank you to Robert Gauthier for providing excellent care to the mice (as well as the humans of our lab). In addition, I'd like to thank safety officer Peter Ferguson for technical training and intellectual discussions every Friday over pizza lunch.

Finally, I cannot thank the members of my committee: Chris Pin and Chandan Chakraborty, as well as Zia Khan and my supervisor Samuel Asfaha enough for their extensive teaching, technical assistance, intellectual support and close guidance throughout my MSc. It has been fantastic to work with you over the last two years and I could not have achieved much of what I have done without your help.

Special mention must go to my parents, David Harnett and Mary Rixon, for their unconditional love and support throughout my MSc. All of my successes are dedicated to you, for they would not have been possible without you.

# TABLE OF CONTENTS

# LIST OF TABLES

# LIST OF FIGURES

## LIST OF APPENDICES

# LIST OF ABBREVIATIONS

| | |
|---|---|
| AOM | Azoxymethane |
| APC | Adenomatous polyposis coli |
| ASCL2 | Achaete-scute complex homolog 2 |
| AXIN | Axis inhibitor protein |
| BMI1 | B cell-specific Moloney murine leukemia virus integration site 1 |
| BMP | Bone morphogenic protein |
| CA-CRC | Colitis-associated colorectal cancer |
| CBC | Crypt base columnar |
| CD34 | cluster of differentiation 34 |
| CD38 | cluster of differentiation 38 |
| CD44 | cluster of differentiation 44 |
| CD133 | cluster of differentiation 133 |
| CRC | Colorectal cancer |
| Cre | Cre-recombinase |
| CreERT | Cre-recombinase estrogen-receptor fusion transgene |
| CSC | Cancer stem cell |
| CSL | Suppressor of Hairless, Lag-1 |
| DCLK1 | Double cortisone like kinase 1 |
| DCS | Deep crypt secretory cells |
| Dhh | Desert hedgehog |
| DMEM | Dulbecco's Modified Eagle's Medium |
| DSH | Dishevelled |
| DSS | Dextran sodium sulfate |
| DT | Diphtheria toxin |
| DTR | Diphtheria toxin receptor |
| EDTA | Ethylenediaminetetraacetic acid |
| EGF | Epidermal growth factor |
| eGFP | Enhanced green fluorescent protein |
| EphB2 | Ephrin type B receptor 2 |
| ER | Estrogen-receptor |
| FACS | Fluorescence activated cell sorting |
| FAP | Familial adenomatous polyposis |
| FBS | Fetal bovine serum |
| FoxL1 | Forkhead Box L1 |
| FZ | Frizzled |
| gDNA | Genomic deoxyribonucleic acid |
| GFP | Green fluorescent protein |
| Gli2/3 | Glioma associated oncogene |
| GSK3 | Glycogen Synthase Kinase 3 |
| GIST | Gastrointestinal stromal tumour |
| H&E | Hematoxylin and eosin |
| HNPCC | Hereditary nonpolyposis colorectal cancer |
| HOPX | Homeodomain only protein X |
| IBD | Irritable bowel disease |
| Ihh | Indian Hedgehog |
| ISC | Intestinal stem cell |
| K19 | Keratin-19 |
| KRAS | Kirsten Rat Sarcoma viral oncogene homolog |

| | |
|---|---|
| LDL | Low-density lipoprotein |
| LEF | Lymphoid enhancer-binding factor 1 |
| Lgr5 | Leucine rich repeat containing g coupled receptor 5 |
| LRP | Low density lipoprotein receptor related protein |
| L5DKA | Lgr5-DTR-eGFP;K19-CreERT;APCf/f mice |
| MIN | Multiple intestinal neoplasia |
| NICD | Notch intracellular domain |
| NOD | Non-obese diabetic |
| OCT | Optimal cutting temperature |
| Olfm4 | Olfactomedin 4 |
| p53 | Protein 53 |
| PBS | Phosphate-buffered saline |
| PCR | Polymerase chain reaction |
| RFP | Red fluorescent protein |
| Rnf43 | Ring finger 43 |
| rpm | Revolutions per minute |
| R-SMADS | Receptor-regulated SMADS (Drosophila mothers against decapentaplegic) |
| RT | Room temperature |
| SCID | Severe combined immune deficient |
| Shh | Sonic hedgehog |
| SMADs | Drosophila homologue of mothers against decapentalplegic proteins |
| SMOC2 | SPARC related modulator calcium binding 2 |
| TA | Transit amplifying |
| TACE | Tumour necrosis factor-α-converting enzyme |
| TAE | Tris-base, acetic acid and EDTA buffer |
| TCF | T cell-specific transcription factor |
| TdTomato | Tandem dimer tomato fluorescent protein |
| TGFβ | Transforming growth factor-β |
| TR-CRC | Therapy resistant colorectal cancer |
| Wnt | Wingless-related integration site |
| WT | Wild type |

# Chapter 1

# INTRODUCTION

## 1.1 The Healthy Colon

### 1.1.1 *Intestinal anatomy and function*

The mammalian intestinal tract can be divided into the small intestine and colon, which are two anatomically and functionally distinct segments (Barker et al., 2010). These segments share the same basic structure: an outer, middle and inner layer (Barker et al., 2010). The outer layer consists of smooth muscle that is innervated by the enteric nervous system (Barker et al., 2010). This layer is responsible for rhythmic peristaltic movements that direct food along the intestine (Barker et al., 2010). The middle layer consists of connective or stromal tissue (Barker et al. 2010). This tissue contains nerves, lymphatic vessels and capillaries which transport absorbed nutrients from the third structure, the innermost layer (Barker et al., 2010). The inner layer is composed of an absorptive epithelial lining called the mucosa (Barker et al., 2010). However, the architecture of the small intestine (duodenum, jejunum and ileum) and colon varies significantly reflecting their distinct functions *in vivo* (Barker et al., 2010). The luminal surface of the small intestine consists of a sheet of epithelial cells which are organized into numerous finger-like protrusions called villi that project into the lumen (Clevers, 2013). These villi maximize the available surface area for absorption, reflecting the major function of the small intestine - absorption of nutrients and minerals (Clevers, 2013). Each villus is surrounded at the base by multiple epithelial invaginations termed the crypts of Lieberkühn. These crypts were named after the scientist who discovered them - Jonathan Nathanael Lieberkühn (1711-1756) (Clevers, 2013). He injected wax into the small intestine and colon to reveal anatomical structures (Clevers, 2013). In contrast, the major function of the colon is dehydration and waste removal (Clevers, 2013). This is reflected by an essentially flat mucosal surface, with multiple crypts that penetrate deep into the underlying submucosa (Clevers, 2013).

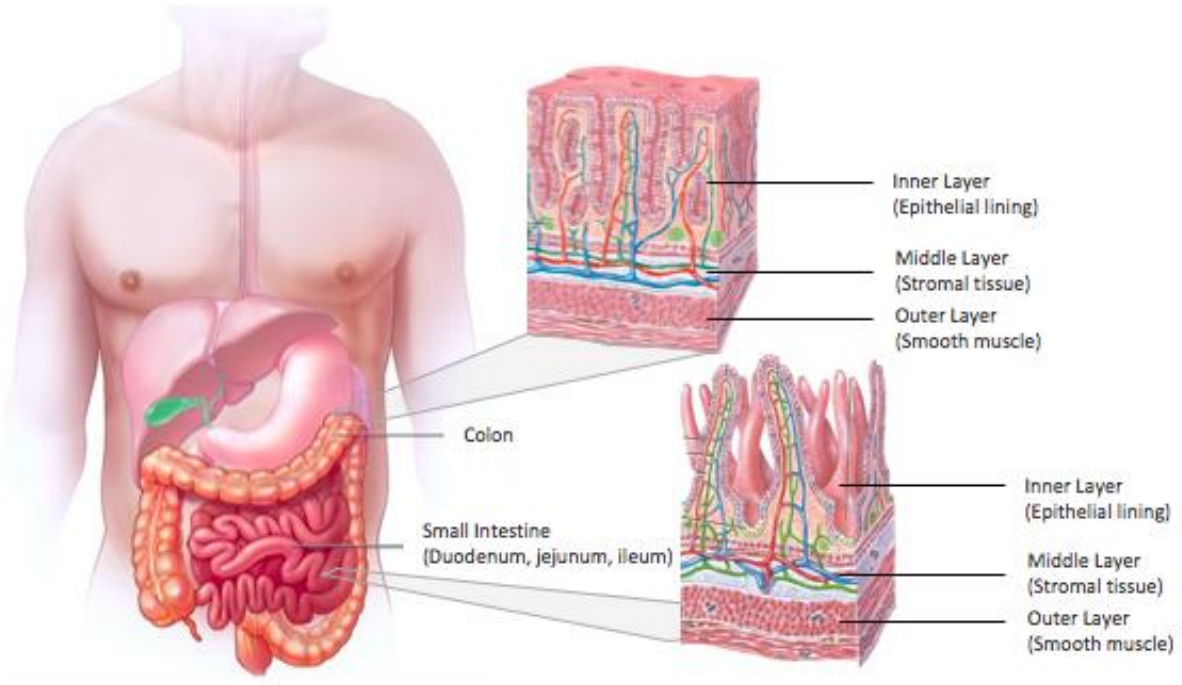


Figure 1 | **Anatomy of the small intestine and colon.** The intestinal tract is divided into two anatomically and functionally distinct segments: the small intestine (duodenum, jejunum, ileum) and colon. The colonic epithelium contains an essentially flat mucosal surface with multiple crypts that penetrate deep into the underlying submucosa. In contrast to the relatively flat surface of the colonic epithelium, the intestinal epithelium contains many finger like projections known as villi, surrounded by crypts. These anatomical differences reflect their differences in function, as the colon functions to compact stool and the small intestine functions to absorb nutrients. Cross sections of the colonic vs intestinal tissue highlight these differences. Moreover, each layer of the intestinal tract: outer, middle and inner is clearly defined. This figure was originally published online in *Mayo Foundation for Medical Education and Research. [https://www.mayoclinic.org/colon-and-small-intestine/img-20008226] and the Department of Zoology and Environmental Management, Faculty of Science, University of Kelaniya, Sri Lanka. Gastrointestinal histology. 2018 [http://science.kln.ac.lk/depts/zoology/index.php?option=com_content&view=article&id=46&Itemid=46]*. The figure is being reproduced for educational purposes only and not for any commercial use. Figure is included in the M.Sc. dissertation with attribution.

### 1.1.2 *Intestinal architecture*

The epithelial lining of the intestine and colon is subjected to extremely harsh environmental conditions (Barker et al., 2012). As such, it is highly susceptible to mechanical-, chemical- and pathogen-driven insults (Barker et al., 2012). This imposes a need for continuous renewal of the simple columnar cells that line the villi and crypts (Barker et al., 2012). Structurally, the intestinal epithelium is highly regulated, with up to ten crypts generating over 250 new

epithelial cells per day (Clevers, 2013) allowing for the entire epithelium to renew itself every 3-5 days for the duration of our lifetime (Leblond & Stevens, 1948). Due to the harsh conditions that exist in the intestinal lumen, this extreme turnover rate is necessary to maintain intestinal tissue homeostasis (Barker et al., 2010).

The cells responsible for driving tissue regeneration are vigorously proliferating epithelial cells – known as intestinal stem cells (ISCs) that reside at the bottom of crypts (Barker et al., 2012). The ISC population is capable of self-renewal and asymmetric division and gives rise to rapidly expanding progenitors known as transit amplifying (TA) cells (Barker et al., 2012). TA cells in the crypt divide and move toward the crypt/villus border to differentiate into six main epithelial cell types: enterocytes, enteroendocrine cells, goblet cells, tuft cells, Paneth cells (small intestine) and deep secretory cells (colon), whose function is outlined below (Figure 2) (Van der flier & Clevers, 2009). These differentiated epithelial cells continue migrating up the villus axis until they undergo apoptosis and are shed into the lumen of the intestine (Van der flier & Clevers, 2009). The only post-mitotic cell types excluded from this upward mobility are the Paneth cells (small intestine) and deep secretory cells (colon) (Van der flier & Clevers, 2009). They migrate to the crypt base, where they reside for 6-8 weeks (Van der flier & Clevers, 2009).

**Enterocytes**

Enterocytes comprise the majority of differentiated cells found in the villi of the small intestine (Clevers, 2013). They are characterized by a luminal brush border and function as absorptive cells responsible for nutrient uptake (Clevers, 2013). Due to their cellular organization, they also prevent microbes from entering the bloodstream as they are tightly packed together forming cell-to-cell adhesions, which act as a protective epithelial barrier (Clevers, 2013). Enterocytes can be identified histologically by the expression of the enzyme alkaline phosphatase.

**Enteroendocrine cells**

In comparison to other differentiated cell types, enteroendocrine cells are more rare and are found throughout the whole crypt-villus axis (Gunawardene, 2011). Their function is to secrete

hormones that regulate numerous processes, such as controlling glucose levels and food intake, as well as signaling to empty food from the stomach (Gunawardene, 2011). They can be identified histologically by staining for the presence of secretory vesicles using Chromogranin A.

**Goblet cells**

Goblet cells are found throughout the villus and secrete mucins, which function to aid in the lubrication of the epithelium (Clevers, 2013). Mucins serve to protect the epithelial lining from extreme mechanical stress that results from the movement of food through the intestine (Clevers, 2013). Goblet cells have also been found to secrete trefoil proteins that contribute to tissue repair (Mashimo et al. 1996). These cells can be identified histologically by staining for mucins using Alcian Blue.

**Tuft cells**

Tuft cells are also referred to as brush cells and are found anywhere throughout the crypt-villus axis (Middlehoff et al., 2017). Their exact function and importance for intestinal homeostasis are controversial (Middlehoff et al., 2017). However, they may act as chemosensory cells that detect and sense the luminal contents (Middlehoff et al., 2017). Tuft cells can be identified histologically through staining for a variety of different markers including Doublecortin Like Kinase 1 (DCLK-1) (Middlehoff et al., 2017).

**Paneth cells**

Paneth cells are found exclusively in the small intestine, where they reside at the base of the intestinal crypt (Clevers, 2013). They protect the intestinal crypt by providing microbial immunity through the secretion of a variety of antimicrobial peptides such as lysosomes and defensins (Clevers, 2013). Paneth cells may also play a role in tissue maintenance through the secretion of growth factors that support the ISC population (Clevers, 2013). Unlike the other differentiated cell types, Paneth cells are long-lived (6-8 weeks) and migrate back down to the crypt-villus axis as they differentiate (Clevers, 2013). They can be identified histologically by the presence of eosinophilic granules or staining for secreted lysozyme.

**Deep crypt secretory cells**

Deep crypt secretory cells (DCS) are found exclusively in the colon, where they reside at the base of the crypt (Sasaki et al., 2016) They may represent the colonic counterpart of Paneth cells (Sasaki et al., 2016). DCS cells can be identified through the expression of Reg4+ (Sasaki et al., 2016).

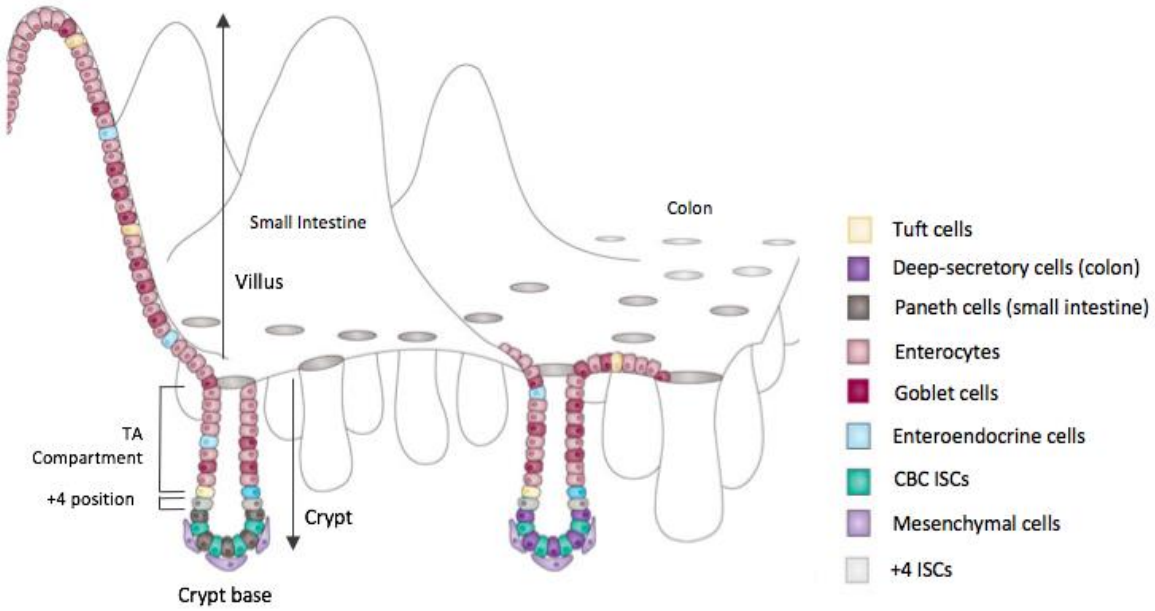


Figure 2 | **The intestinal and colonic epithelium.** The intestinal epithelium consists of crypts and villi. The crypt base contains rapidly cycling intestinal stem cells (ISCs) as well as transit-amplifying (TA) progenitors. The major differentiated cell types are enterocytes, enteroendocrine cells, goblet cells, tuft cells and Paneth cells. Except for Paneth cells, these cell types migrate as clonal lineages to the tip of the villi in 4-5 days where they are shed into the lumen. Post-mitotic Paneth cells are relatively long lived (6-8 weeks) and intermingle at crypt bottoms to secrete ISC niche factors and support innate immunity. In contrast to the small intestine the colonic epithelium has a flat epithelial surface and lacks Paneth cells. Instead of Paneth cells, deep secretory crypt cells are thought to be responsible for the ISC niche function. This figure was originally published in *Nature. Vermeulen L., and Snippert H. J. Stem cell dynamics in homeostasis and cancer of the intestine. 2014; 14(7), 468-480.* This figure is being reproduced for educational purposes only and not for commercial use. Figure is included in the M. Sc. dissertation with attribution.

Key points 1 | **The intestinal and colonic epithelium**

- The intestinal epithelium is lined with crypts and villi (finger like projections) that function to absorb nutrients.
- Crypts contain rapidly proliferating intestinal stem cells that drive regeneration of the epithelium.
- There are 6 main types of differentiated epithelial cells that arise from intestinal stem cells.
- The colonic epithelium has a flat surface and lacks villi reflecting its role in waste dehydration and removal.

### 1.1.3 *Intestinal stem cells*

**Models of intestinal stem cell identity**

Although it is widely accepted that intestinal stem cells are multipotent adult stem cells, which give rise to all epithelial cell lineages, the exact identity of ISCs (location and gene expression patterns) is controversial. Over time, technological innovation has enabled the identification of multiple candidate stem cell populations and provided insight into the function of the ISC compartment. However, the lack of definitive markers to identify ISCs has been a major obstacle in the field of intestinal stem cell biology. This created a long-lasting debate on the true identity of ISCs, which remains confusing partially due to the use of many different terms for the same cell or cellular processes.

Previously, it was reported that ISCs can be categorized into two distinct populations: crypt base columnar and +4 stem cells. This led to the emergence of two opposing intestinal stem cell models: the stem cell zone model and the +4 model (Barker et al., 2010). The stem cell zone model argues that crypt base columnar (CBC) stem cells are the actual stem cells, which rapidly divide at the base of the crypt and are responsible for intestinal homeostasis (Cheng & Leblond, 1974). In contrast, the +4 model argues that the actual stem cells responsible for intestinal homeostasis reside at the +4 position as discovered by Potten and colleagues (Potten et al. 1997; Barker et al., 2010). A number of different stem cell markers have been proposed for each model, only to be refuted later, making this a dynamic and evolving area of research.

**Crypt base columnar stem cells**

The first marker for CBC cells, leucine-rich-repeat containing G-protein coupled receptor 5 (Lgr5), was identified as a Wnt target gene selectively expressed at the base of intestinal crypts (Figure 5) (Barker et al., 2007; Stevens and Leblond, 1947; Koo and Clevers, 2014). Lgr5-positive CBC cells are considered fast-cycling as they divide every day and are the driving force of intestinal tissue renewal (Barker et al., 2010). Several experimental approaches have been used to validate the stem cell-like nature of these cells that are outlined below, including lineage tracing, gene expression studies, stem cell activity assays, and *in vitro* organoid culture.

**In vivo lineage tracing using the Lgr5 marker**

The current 'gold standard' to identify candidate stem cells in their native microenvironments is lineage tracing (Barker, 2013). In this technique, a permanent heritable genetic mark, such as the expression of a fluorescent protein, is introduced into candidate stem cells (Barker, 2013). Subsequently, these marks are inherited by descendants of that cell enabling their characterization in the epithelium (Figure 3) (Barker, 2013). If the presence of all differentiated lineages is observed in a single traced clone that is capable of long-term labelling of cell lineages, it may reveal multipotency and self-renewal (Barker, 2013). Taken together, these characteristics fulfil the basic definition of a stem cell, as a cell capable of self-renewal and multipotency (Barker, 2013). The stem cell activity of Lgr5+ CBCs was confirmed via lineage tracing in mice, which demonstrated that CBC cells produced clonal ribbons containing all the major epithelial cell lineages and persisted for the lifetime of the mouse (Barker et al., 2007). These results validated Lgr5+ CBC cells as self-renewing multipotent adult intestinal stem cells (Barker et al., 2007).

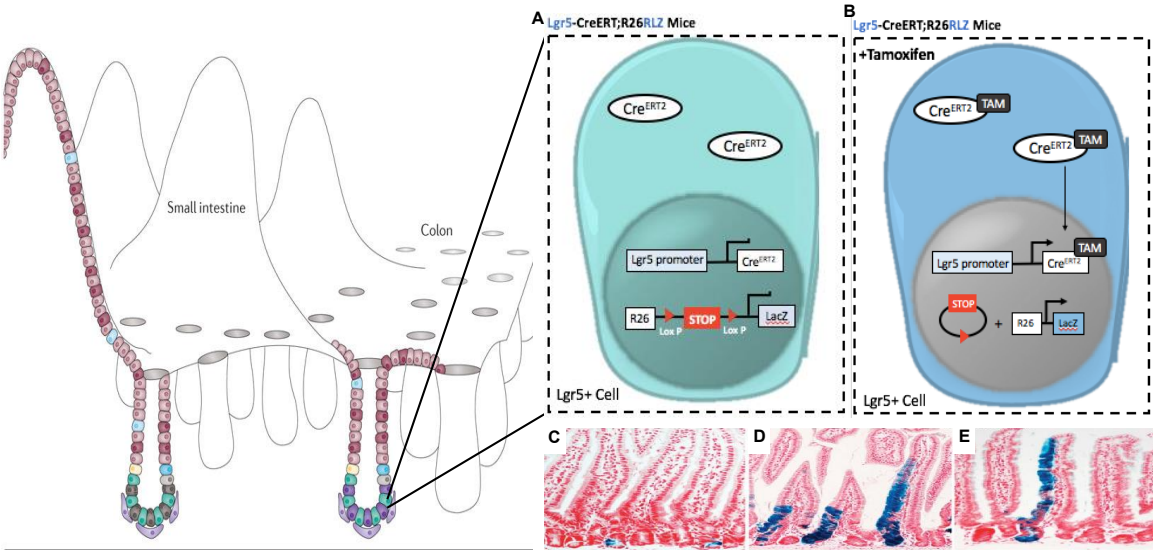


Figure 3 | **Genetic lineage tracing using Lgr5.** (A) Cre recombinase expression is spatially restricted by expressing it under the control of a tissue-specific promoter (Lgr5), while temporal restriction is achieved by fusion of a tamoxifen-responsive hormone-binding domain of the estrogen receptor (Cre-ERT). To visualize Lgr5 expressing cells as well as their progeny, the Cre construct was used in conjunction with a reporter gene LacZ. This reporter is ubiquitously expressed under the control of the Rosa26 promoter and placed downstream of a STOP codon flanked by cre recombinase recognition sites (loxp). In the absence of tamoxifen, the Cre enzyme is in an inactive state. Therefore, no expression of the reporter gene is observed due to the presence of the STOP codon upstream of the reporter gene. (B) However, when tamoxifen is administered the Cre enzyme is activated and capable of translocating to the nucleus to mediate recombination between the loxp sites in Lgr5 expressing cells. As a consequence, the STOP codon is excised and the cells are permanently marked by the reporter gene. Part of this figure was originally published in *Nature. Vermeulen L., and Snippert H. J. Stem cell dynamics in homeostasis and cancer of the intestine. 2014; 14(7), 468-480.* This figure is being reproduced for educational purposes only and not for commercial use. Figure is included in the M. Sc. dissertation with attribution. (C) Histological analysis of LacZ activity in the small intestine of Lgr5-CreERT;Rosa26-RLZ mice one day after induction, five days after induction (D), and 60 days after induction (E) This figure was originally published in *Nature. Barker et al. Identification of stem cells in small intestine and colon by marker gene Lgr5. 449(7165), 10003.* This figure is being reproduced for educational purposes only and not for commercial use. Figure is included in the M. Sc. Dissertation with attribution.

### Lgr5+ CBC stem cell expression signature

Through a combination of microarray and proteomic experimental techniques, researchers were able to establish a molecular signature for Lgr5+ CBC stem cells (Munoz et al., 2012;Van der Flier et al., 2007). Sorted intestinal Lgr5-eGFP stem cells (high eGFP expression) and their progeny (low eGFP expression) were analyzed to reveal approximately 500 differential genes upregulated in stem cells (Van der Flier et al., 2007).

As expected, a strong Wnt signature was present, including many Wnt target genes such as Achaete-scute complex homolog 2 (Ascl2), EphB2, and Tory and axis inhibition (axin)-2 (Van der Flier et al., 2007). Interestingly, this expression profile also revealed novel markers of Lgr5+ CBCs including Olfactomedin 4 (Olfm4) and SPARC related modulator calcium binding 2 (SMOC2), as well as ring finger 43 (Rnf43) (Van der Flier et al., 2007).

**Regulation of CBC stem cell activity and fate**

Many of the genes identified from the Lgr5+ CBC stem cell expression signature have been used to provide functional insight into the regulation of intestinal stem cell activity and fate *in vivo*. In particular, ASCL2 was found to be highly upregulated in the Lgr5+ stem cell fraction and was identified as a critical regulator of intestinal stem cell fate (Van der Flier et al., 2009). ASCL2 is commonly known as a transcription factor that promotes neuroblast differentiation. However, conditional ablation of ASCL2 in the intestinal epithelium resulted in a rapid loss of the stem cell compartment (Van der Flier et al., 2009). Two other genes that were found to be highly expressed in stem cells were Rnf43 and Troy (Barker, 2013). These genes play an important role in regulating endogenous Wnt signaling which is critical in the maintenance of the stem cell compartment. Accordingly, Lgr5 was identified as a component of the Wnt signaling complex at the plasma membrane (Barker, 2013). Lgr5 recruits secreted Wnt agonists (roof plate-specific spondin (R-spondin) 1-4), thus amplifying canonical Wnt signaling and ensuring stem cell homeostasis *in vivo* (Barker, 2013).

**In vitro culture of Lgr5+ CBC stem cells**

Further proof of Lgr5 labelling a stem cell population arose from the development of a novel *in vitro* method known as organoid culture. In this method, single Lgr5+ CBC cells were isolated from Lgr5-eGFP reporter mice using fluorescence activated cell sorting (FACS) and plated in a Matrigel-based three-dimensional culture system (Sato et al., 2009). The Matrigel is supplemented with media that contains a cocktail of growth factors found in the endogenous stem cell niche including: Noggin (a bone morphogenic protein inhibitor), R-spondin (Wnt agonist), epidermal growth factor (EGF) and Notch ligand (Sato et al., 2009). This generates self-renewing epithelial organoids also known as “mini-guts”

that are organized into crypts (containing CBC cells intercalated with Paneth cells) and a villus-like region (containing differentiated cell lineages) (Figure 4) (Sato et al., 2009). This system was also adapted to culture the colonic epithelium. However, these cultures require WNT3A in the media, most likely reflecting differences in the stem cell niche between the small intestine and colon.

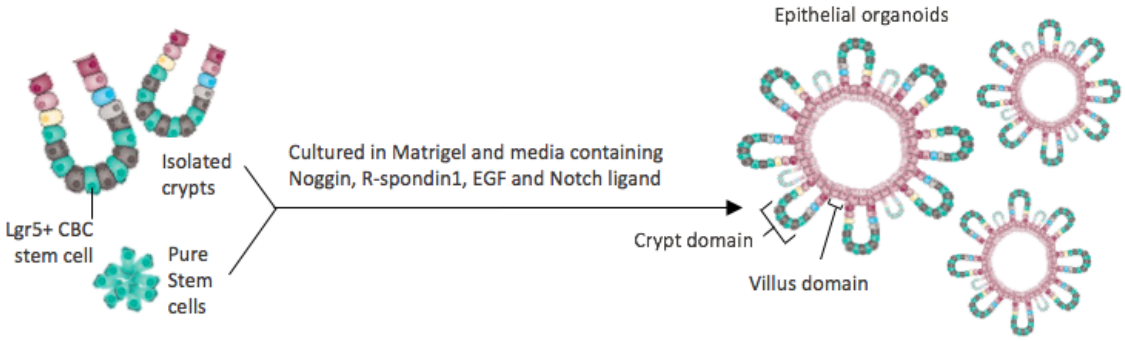


Figure 4 | **Generation of organoids via intestinal stem cell culture.** Isolated intestinal crypts containing Lgr5+ CBC stem cells or purified Lgr5+ CBC stem cells are plated into Matrigel containing Noggin, R-spondin1, EGF and Notch ligand. This results in the generation of self-renewing epithelial organoids organized into crypt and villus like domains. The crypts contain stem cells intercalated with Paneth cells at their base, while the villi contain differentiated cell lineages. This protocol was adapted for culturing the colonic epithelium, although these cultures require exogenous WNT3A. This figure was originally published in *Nature. Vermeulen L., and Snippert H. J. Stem cell dynamics in homeostasis and cancer of the intestine. 2014; 14(7), 468-480.* Modified figure shown here is substantially different from the original and is being included for educational purposes only.

**+4 stem cells**

A number of genes have been reported to selectively identify the +4 stem cell position using *in vivo* lineage tracing including B cell-specific Moloney murine leukemia integration-1 (BMI1), keratin-19 (K19) and homeodomain-only (HOPX), which are briefly outlined below and in figure 5.

**BMI1**

BMI1 was first implicated in regulating hematopoietic and neural stem cell regulation through encoding a component of the Polycomb repressor complex (Sangiorgi & Capecchi, 2008). However, analysis of BMI1 expression in the small intestine using *in situ* hybridization revealed that it was predominantly expressed at the +4 ISC position (Sangiorgi & Capecchi, 2008). This was further validated using a Bmi1-eGFP reporter mouse model (Tian, H. et al 2011), as well as *in vivo* fate-mapping studies using a Bmi1-CreERT/R26R-lacz mouse model. These experiments demonstrated that BMI1+/ +4 position cells produced clonal ribbons containing all the major epithelial cell lineages and persisted for the lifetime of the mouse (Tian, H. et al 2011), thus validating BMI1+/ +4 cells as self-renewing multipotent adult ISCs. Additionally, when BMI1+ cells were ablated *in vivo*, epithelial renewal was prevented, suggesting BMI1+ ISCs play an important role in intestinal homeostasis (Tian, H. et al 2011). Further evidence demonstrated that isolated BMI1+ cells could generate epithelial organoids in culture that capitulated functional intestinal tissue (Yan et al., 2012), providing support that BMI1 labels an ISC population.

**K19**

Keratin-19 (K19) was first implicated as a cytokeratin (a multigene family of intermediate filaments), critical in the maintenance of the cytoskeleton but expressed in different lineages in the epithelium (Moll et al., 1982). To investigate the role of K19 in the small intestine and colon, a K19-mApple reporter mouse was generated. Upon histological analysis of the small intestine and colon, K19-mApple was expressed at the +4-position extending up the isthmus, labelling a population of cells including long-lived stem cells that were distinct from rapidly cycling Lgr5+ CBC stem cells. Of note, unlike BMI1, K19 is expressed in both the small intestine and colon (Asfaha et al., 2015). Furthermore, genetic lineage tracing experiments using K19-BAC-CreERT;R26-LacZ mice revealed labelled cells expanded clonally and persisted for the lifetime of the mouse, consistent with K19 labeling long-lived ISCs (Asfaha et al., 2015).

**HOPX**

HOPX was first implicated in regulating developmental processes as the gene encodes an atypical homeobox protein. However, analysis of HOPX expression in the intestine using HOPX-Lacz reporter mice revealed it labels a +4 position ISC population that is quiescent and radiation-resistant (Takeda et al., 2011). This was further validated through *in vivo* lineage tracing studies using HOPX-CreERT;R26R-Lacz mice (Takeda et al., 2011). These studies revealed reporter gene activation at the +4 position followed by the production of clonal ribbons containing all the major epithelial cell lineages that persisted for the lifetime of the mouse (Takeda et al., 2011). This indicated that HOPX labels a multipotent, self-renewing adult ISC. When the progeny of HOPX+ cells were analyzed using expression profiling, Lgr5 and other CBC genes were found to be highly expressed. This suggested that HOPX is capable of giving rise to Lgr5+ CBC cells. Of note, when Lgr5+ CBC stem cells were cultured they gave rise to HOPX+ cells (Takeda et al., 2011). These findings support a unique model of ISC identity, whereby stem cell populations may interconvert.

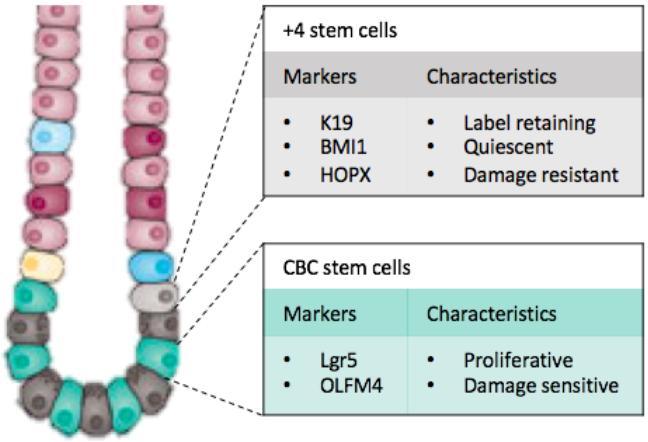


Figure 5 |**Markers & characteristics of intestinal stem cells**. +4 ISC can be identified through the markers K19, BMI1 and HOPX. This stem cell population is typically characterized as label retaining, quiescent and damage resistant. CBC stem cells can be identified through the expression of Lgr5 and OLFM4. This stem cell population is typically characterized as proliferative and damage sensitive. This figure was originally published in *Nature. Vermeulen L., and Snippert H. J. Stem cell dynamics in homeostasis and cancer of the intestine. 2014; 14(7), 468-480.* Modified figure shown here is substantially different from the original and is being included for educational purposes only.

**Current view on intestinal stem cell identity**

Although specific markers have been identified for both the CBC and +4 stem cell populations, neither model has been definitively true. Recently, a more plastic model of stem cell identity has emerged. In this model, the crypt base contains two types of ISCs (1) the CBC stem cells that act as a dedicated and active ISC population responsible for daily epithelial homeostasis, and (2) the relatively quiescent +4 cells, which act as a secondary "reserve" stem cell population capable of activating upon tissue injury. Furthermore, this model suggests that cells residing in the lower portion of the TA compartment may dedifferentiate to acquire stem cell properties in the case of catastrophic injury to the crypt base. Accordingly, it has been proposed that many of the markers discussed above define pools of dedicated or reserve ISC that are selectively activated in response to various injuries. Importantly, many irradiation-induced injury models have provided important mechanistic insight into this theory. In one study, short-term loss of Lgr5+ CBC cells through targeted conditional ablation *in vivo*, revealed no negative effects on the intestinal epithelium despite the critical role of CBC cells in homeostasis (Tian et al., 2011). This suggested that another damage-resistant "reserve" stem cell may be capable of maintaining intestinal homeostasis (Tian et al., 2011). Based on the inherent characteristics of +4 ISCs such as quiescence and radiation-resistance, they are the likely reserve stem cell candidates (Yan et al., 2012). Moreover, there is evidence that BMI1 as well as K19 label a reserve stem cell population as *in vivo* lineage tracing from BMI1 (Tian et al., 2011) and K19 (Asfaha et al., 2015) was observed following targeted ablation of the Lgr5+ CBC stem cell population or radiation injury. Challenging the traditional models of ISC identity, these findings support a unique model whereby epithelial homeostasis is maintained by a heterogeneous pool of both dedicated and reserve ISCs.

Key points 2 | **Intestinal stem cells**

- ISCs are considered adult tissue stem cells capable of self-renewal and multipotentcy.
- Experimental methods for validating stem cells include: immunohistochemistry, lineage tracing, gene expression, and in vitro organoid culture.
- The gold standard to identify stem cells in their natural environment is lineage tracing.
- Two models of intestinal stem cell identity were proposed with a number of stem cell markers and characteristics identified for each model:
    1. Stem cell zone model – whereby CBC stem cells are the actual stem cells.
        - Markers for CBCs include Lgr5 and OLFM4 as well as others.
        - Characteristics of this ISC include active proliferation and damage sensitivity.
    2. +4 model – whereby +4 stem cells are the actual stem cells.
        - Markers for +4 ISC include K19, BMI1 and HOPX as well as others.
        - Characteristics of this ISC include the ability to retain DNA labels, quiescence (in some cases) and resistance to damage.
- Both models may be true, as studies have shown mature intestinal cells emerge from different cell populations.
- This led to the formation of a new theory, whereby CBC stem cells act as the dedicated and active ISC population responsible for daily homeostasis and +4 ISCs act as a secondary reserve stem cells capable of activating upon tissue injury.

### 1.1.4 *Signaling pathways involved in intestinal homeostasis*

The maintenance of intestinal structure and function depends upon a delicate balance of cell proliferation, migration and apoptosis that must be carefully regulated. These processes are regulated by controlling gene expression through four main signaling pathways: Wnt, Notch, TGFβ/BMP and the Hedgehog pathway that are outlined below, as well as in Figure 6.

**Wnt**

The Wnt signaling pathway plays an essential role in the maintenance of cellular hierarchy throughout the intestinal and colonic epithelium. A gradient of Wnt activity is observed along the crypt-villus axis, with the highest level of Wnt pathway activation occurring at the base of the intestinal crypts where the ISC population resides (Spit et al., 2018). The

ISC population remains in close contact to stromal tissue capable of providing an abundance of Wnt factors (Spit et al., 2018). Subsequently, when a Wnt ligand binds to its receptor complex containing Frizzled (FZ)/low-density lipoprotein (LDL) receptor-related protein (LRP), a signal is transduced to intracellular proteins that stimulates interaction between Dishevelled (Dsh) and Axin (Spit et al., 2018). This prevents the breakdown of β-catenin and results in an accumulation of β-catenin in the cytoplasm and nucleus. β-catenin is then able to interact with a member of the lymphoid enhancer-binding factor 1 or T cell-specific transcription factor (LEF/TCF) to enhance transcription of Wnt target genes (Spit et al., 2018).

A variety of Wnt target genes function to enhance cell proliferation, migration and adhesion processes that are essential for intestinal and colonic epithelium homeostasis. Thus, the expression of Wnt target genes increases the proportion of stem cells (Spit et al., 2018). As cells differentiate and migrate up the crypt-villus axis towards the lumen of the intestine, they lose their proximity to Wnt factors. In the absence of Wnt, a β-catenin destruction complex is formed preventing the downstream activation of Wnt target genes (Spit et al., 2018). Briefly, the intracellular proteins adenomatous polyposis coli (APC) and Axin are phosphorylated by glycogen synthase kinase-3 (GSK3), resulting in the breakdown of β-catenin (Spit et al., 2018). Subsequently, this decrease in Wnt signaling is thought to drive differentiation of the intestinal and colonic epithelium. Interestingly, conditional homozygous deletion of β-catenin in mice results in increased apoptosis, catastrophic destruction of crypts, reduced numbers of goblet cells and detachment of entire sheets of enterocytes (Sansom et al., 2004). These results highlight the important role of Wnt in maintaining the ISC compartment.

**Notch**

Similar to Wnt signaling, Notch also plays a role in maintaining the undifferentiated and proliferative stem cell compartment at the base of the crypt (Van der Fliers and Clevers, 2009). This is supported by the high levels of Notch ligands found at the base of the crypt compared to the rest of the crypt-villus axis (Spit et al., 2018). In contrast to the Wnt pathway, Notch signaling can only occur via direct cell-to-cell contact of adjacent cells

(Spit et al., 2018). When Notch ligands (such as Jagged or Delta) interact with the Notch receptor, two proteolytic cleavage events are initiated (Spit et al., 2018). Firstly, tumour necrosis factor-α-converting enzyme (TACE), cleaves the extracellular domain of the Notch receptor (Spit et al., 2018). Then a second cleavage event takes place, which frees the Notch intracellular domain (NICD), enabling it to enter the nucleus (Spit et al., 2018). Once NICD enters the nucleus, it is able to activate the transcription factor CSL, resulting in the expression of Notch target genes (Spit et al., 2018). Similar to Wnt, Notch target genes influence apoptosis, proliferation, spatial patterning and cell fate determination (Artavanis-Tsakanoas et al., 1999). Inhibition of Notch signaling in mice results in a decrease of epithelial stemness and an increase in the goblet cell population (Sikander et al., 2010). This reinforces Notch's role in maintaining the ISC compartment.

**TGFβ/BMP**

In contrast to Wnt and Notch signaling, the TGFβ/BMP signaling pathway is a negative regulator of intestinal stem cell renewal (He et al., 2004; Spit et al., 2018). In this role, the expression of TGFβ is concentrated at the villus tip where cells are differentiated and not proliferating (Spit et al., 2018). TGFβ and BMP pathways are activated in a similar manner: a ligand binds to the membrane-bound type II receptor that enables the type II receptor to dimerize with type I receptors and phosphorylate its cytoplasmic domain (Spit et al., 2018). Upon phosphorylation, type I receptors recruit and phosphorylate SMAD2/3 (TGFβ), or SMAD1/5/8 (BMP) proteins (Spit et al., 2018). Once phosphorylated these complexes are referred to as receptor regulated SMADS (R-SMADS) (Spit et al., 2018). To enable translocation into the nucleus, R-SMADS dissociate from the receptor and form a complex with SMAD4 (Spit et al., 2018). Once in the nucleus, SMAD4 interacts with regulatory proteins to activate transcription factors and downstream TGFβ/BMP genes (Spit et al., 2018). The target genes of the TGFβ/BMP pathways are most commonly associated with inhibition of cellular growth and proliferation. Interestingly, inhibition of TGFβ/BMP signaling in mice increases the proportion of stem and progenitor cell populations, eventually leading to cancer (He et al., 2004). These findings highlight the inhibitory function of this pathway under homeostatic conditions and explains the ability of TGFβ/BMP to inactivate stem cells.

**Hedgehog**

Hedgehog signaling has been found to primarily regulate the intestinal mesenchyme. However, it plays an important role as an indirect regulator of BMP and Wnt signaling (Kaestner et al., 1997; Spit et al., 2018). The hedgehog pathway is controlled by two transmembrane proteins known as Patched and Smoothened. When a ligand (Sonic Hedgehog (Shh), Indian Hedgehog (Ihh) or Desert hedgehog (Dhh)) binds to Patched, Smoothened inhibition is prevented, allowing for active Smoothened to prevent phosphorylation and degradation of Gli2/3 (Spit et al., 2018). Subsequently, Gli2/3 is able to enter the nucleus and act as a transcription factor for Hedgehog target genes. In particular, one important target gene of the Hedgehog pathway is FoxL1. FoxL1 has been shown to regulate BMP and Wnt signaling (Kaestner et al. 1997). Interestingly, FoxL1 deficit results in increased intestinal epithelial proliferation and distorted crypt architecture (Kaestner et al. 1997). More recently, Kosinski and colleagues demonstrated a similar effect is caused by the loss of the Hedgehog ligand Ihh in the intestinal epithelium, manifesting as increased proliferation and expansion of the ISC compartment (Kosinski et al., 2010). The Hedgehog pathway also indirectly affects the ISC compartment through modulation of the adjacent mesenchymal tissue that makes up the supportive structure of the crypts (Kosinski et al., 2010). When Ihh was depleted, the mesenchymal architecture was disrupted and the extracellular matrix deteriorated. This lead to a loss of crypt architecture and an increase in the ISC population, highlighting the important link between interactions of the epithelium and mesenchymal tissue in ISC homeostasis (Kosinski et al., 2010).

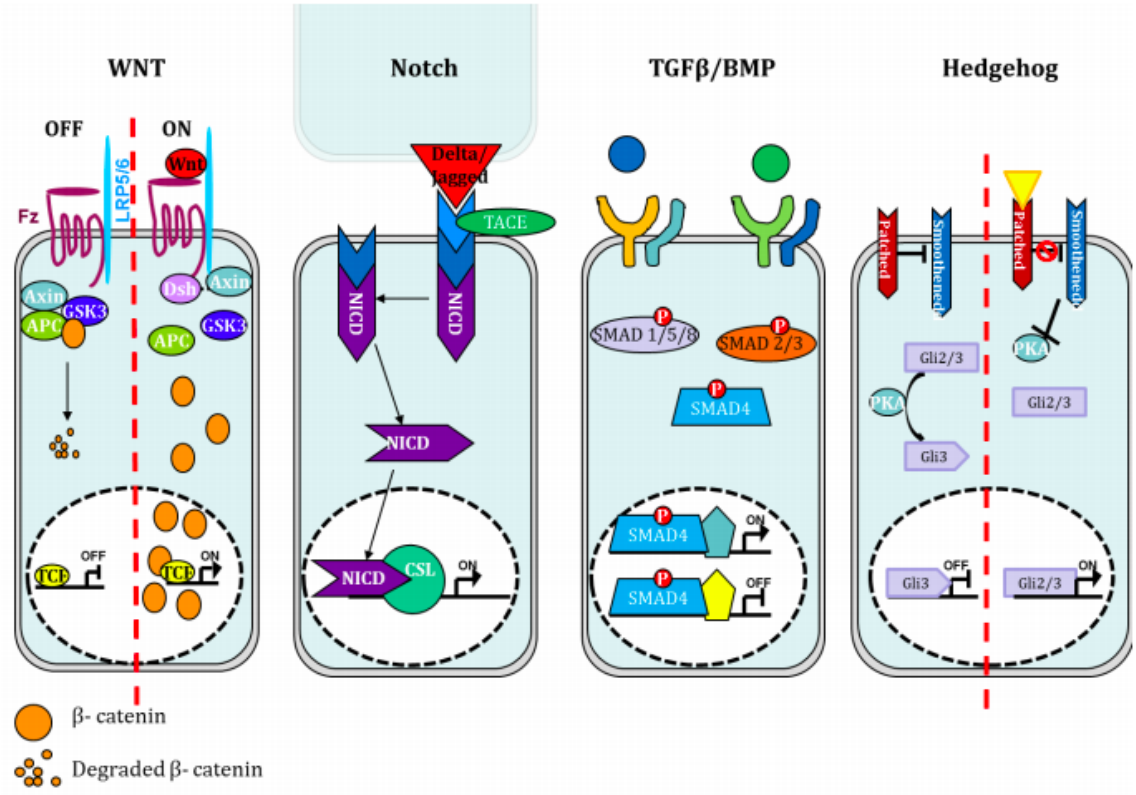


Figure 6 | **The four main signaling pathways involved in intestinal homeostasis.** From left to right: WNT, Notch, TGFB/BMP and hedgehog signaling. These pathways all control the expression of genes associated with homeostatic processes such as proliferation, apoptosis, differentiation, growth and migration This figure was originally published in *Current molecular medicine. Radtke, F., Clevers, H. & Riccio, O. From gut homeostasis to cancer. 2006; 6(3), 275-289.* Modified figure shown here is different from the original and is being included for educational purposes only.

Key points 3 | **Signaling pathways involved in intestinal homeostasis**

- Four main signaling pathways are involved in regulating intestinal homeostasis: Wnt, Notch, TGFβ /BMP and Hedgehog.
- Wnt maintains the ISC compartment.
    - Highest levels of Wnt are found at the crypt base.
    - As Wnt expression decreases cells differentiate.
- Notch maintains the ISC compartment in addition to Wnt.
    - Highest levels of Notch are found at the crypt base.
    - Also plays a role in differentiation of secretory cell lineages.
- TGFβ /BMP plays a role in differentiated cells and inactivates ISCs.
    - Highest levels are found at the villus tip.
- Hedgehog maintains the intestinal mesenchyme to indirectly modulate ISCs through BMP and Wnt signaling.

## 1.2 Colorectal Cancer

Colorectal cancer (CRC) is one of the most common cancers worldwide, with over 1.2 million new cases diagnosed each year (Zeuner et al., 2014). In Canada, CRC is highly prevalent with an estimated 27,000 Canadians diagnosed in 2017 (Bromfield et al., 2017). Although aggressive treatment options such as surgery, radiation and chemotherapy are available, approximately 30-50% of patients will develop therapy-resistant CRC (TR-CRC) leading to recurrent disease (Ragnahammar et al., 2001; O'Connell et al., 2008). Unfortunately, when TR-CRC is treated unsuccessfully, recurrent tumours that arise are often much more aggressive than primary tumours, resulting in poor survival rates (O'Connell et al., 2008). Other factors that have been found to impact patient survival include detection of CRC in advanced stages as well as high recurrence rates and tendency to metastasize. Due to this, CRC remains the second and third leading cause of death in men and women, respectively (Bromfield et al., 2017).

By etiology, human CRC can be classified as inherited, colitis-associated, or sporadic. Inherited CRC can be categorized into: familial, hereditary nonpolyposis, familial adenomatous polyposis (FAP) and rare CRC syndromes. Familial CRC accounts for 10-30% of all CRC cases and is defined by family history of non-syndromic CRC (Figure 7)

(Jasperson et al., 2010). It is caused by an accumulation of mutations in intestinal epithelial cells and progresses through a well-characterized sequence (described in section 1.2.1) (Jasperson et al., 2010). Hereditary nonpolyposis CRC (HNPCC) or Lynch syndrome accounts for 5% of all CRC cases (Jasperson et al., 2010). It is an autosomal dominant condition that is caused by mutations in genes involved in the DNA mismatch repair pathway including MSH2, MLH1 and MSH6 (Jasperson et al., 2010). Familial adenomatous polyposis (FAP) accounts for 5% of all CRC cases and is caused by a germline mutation in the adenomatous polyposis coli gene (APC) (Jasperson et al., 2010). A subset of inherited CRCs is very rare and accounts for 0.1% of all cases. These include leiomyosarcomas, colorectal lymphomas, neuroendocrine tumours, as well as gastrointestinal stromal tumours (GISTs) (Jasperson et al., 2010). Colitis-associated CRC (CA-CRC) arises from areas of active colonic inflammation caused by inflammatory bowel disease (IBD) and accounts for 2% of all CRC cases (Van Der Kraak et al., 2015). It is caused by an accumulation of mutations in intestinal epithelial cells and progresses through a well-characterized inflammation to dysplasia to carcinoma sequence (described in section 1.2.1) (Van Der Kraak et al., 2015). Lastly, the majority of colorectal cancer cases are considered sporadic (~80%). However, the etiology of sporadic CRC remains elusive. In addition to hereditary- or disease-related aspects, a likely contributing factor to the development of CRC may be a number of lifestyle factors including: obesity, physical inactivity, dietary influences and smoking (World Cancer Research Fund, 2011).

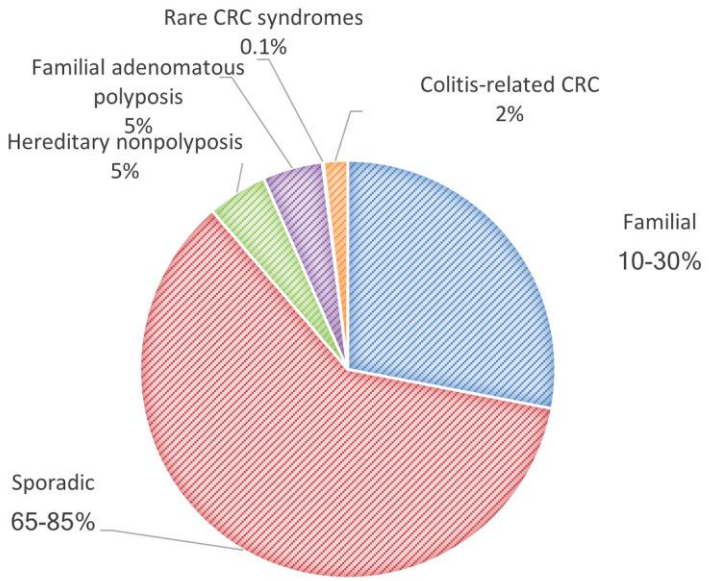


Figure 7 | **Etiology of colorectal cancer.** The etiology of human CRC can be classified as rare CRC syndromes (0.1%), colitis-related (2%), familial adenomatous polyposis (5%), Hereditary nonpolyposis (5%), familial (10-30%) or sporadic (65-85%).

### 1.2.1 *A model of colorectal carcinogenesis*

Early observations in human cancers and animal models reported that a successive accumulation of multiple genetic mutations is necessary to convert a normal human cell into a cancer cell (Foulds, 1954; Nowell, 1976). Following these initial observations, Fearon and Vogelstein proposed a model of colorectal carcinogenesis based on studies of the frequency of gene mutations at various stages of progression in human tumours (Fearon and Vogelstein, 1990). In this model, CRC development is a multistep process, whereby a series of genetic mutations leads to progression from the normal intestinal epithelium to dysplastic tissue to benign adenomas through to metastatic carcinoma (Figure 8). The initial step in colorectal carcinogenesis involves loss of function of APC resulting in constitutive activation of the Wnt-pathway and formation of a benign lesion (Fearon and Vogelstein, 1990). This is followed by an activating mutation in the small GTPase KRAS and subsequent inactivation of SMAD2/4 in adenomas and early carcinomas, respectively (Fearon and Vogelstein, 1990). Lastly, inactivating mutation in p53 lead to invasion and metastatic lesions (Fearon and Vogelstein, 1990) (Figure 8). Initial research on invasive

carcinomas from familial and colitis-associated CRC showed a similar genetic pattern of acquired mutations in APC, KRAS, SMAD2/4 and p53. This led to the assumption that genes important in the initiation and progression of familial CRC were also important in CA-CRC. Although the accumulated mutations were similar, the timing of these genetic mutations was found to vary greatly between familial and CA-CRC. In CA-CRC, the order of progression is reversed, whereby the initiating mutation tends to occur in p53, followed by SMAD2/4, KRAS and lastly APC (Van Der Kraak et al., 2015). Interestingly, the frequency of APC mutation in high grade dysplasia is also reduced (27.5%) compared to non-CA-CRC adenomas (50%) (Foersch et al., 2014). Thus highlighting the genetic differences in colorectal carcinogenesis between familial and colitis associated colorectal cancer.

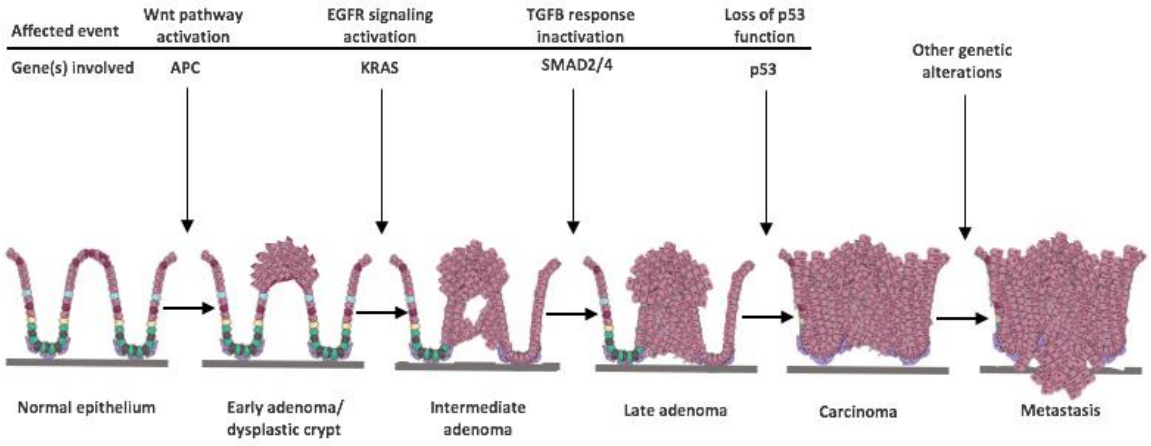


Figure 8| **Model of colorectal carcinogenesis as proposed by Fearon and Vogelstein**. Progression from normal epithelium to colorectal cancer requires an accumulation of mutations in particular genes that affect the balance between proliferation and apoptosis. The steps shown above occur during the development of sporadic colorectal cancer in normal colonic epithelium. However, not all colorectal tumours exhibit all the mutations shown in the above figure. Part of this figure was originally published in *Nature. Vermeulen L., and Snippert H. J. Stem cell dynamics in homeostasis and cancer of the intestine. 2014; 14(7), 468-480 and Nature reviews cancer. Davies, R. J., Miller, R., & Coleman, N. Colorectal cancer screening: prospects for molecular stool analysis. 2005; 5(3), 199.* Modified figure shown here is different from the original and is being included for educational purposes only.

### 1.2.2 *Cell of origin theory*

In colorectal cancer research, two theories about the cell of origin exist: the bottom-up and top-down model. The bottom-up model proposes that stem cells are the cell of origin; i.e. stem cells acquire the initial mutations necessary for malignant conversion (Visvader, 2011). Evidence for the malignant conversion of stem cells has been demonstrated using mouse models that allow for the induction of specific mutations in ISCs. In 2009, Barker et al. found that deleting the APC tumour suppressor gene in Lgr5-expressing CBC stem cells lead to rapid adenoma formation throughout the small intestine and colon (Barker et al., 2009). Further studies also demonstrated rapid adenoma formation upon aberrant Wnt activation in BMI1+ and K19+ cells, supporting the bottom-up model as transformation was initiated in a stem cell at the bottom of the crypt (Preston, Wong et al. 2003). In contrast, the top-down model opposes the unidirectional development of tumours from stem cells. In this model, transformation is initiated in a differentiated cell that spreads laterally, thus initiating tumour growth from the top down. Recently, it was demonstrated that loss of APC in a differentiated cell population followed by aberrant activation of nuclear factor-κB (NF-κB) through intestinal inflammation or KRAS mutation, leads to transformation of these cells (Schwitalla et al. 2013; Asfaha et al. 2015). However, APC inactivation alone was not sufficient to initiate tumorigenesis. This suggests that additional signals are required for malignant conversion of differentiated cells in the top-down model of carcinogenesis.

### 1.2.3 *Wnt signaling in cancer*

Wnt target genes play a key role in a number of regulatory processes associated with tumorigenesis, such as cell proliferation and adhesion (Staal et al., 2004). As such, abnormalities in the Wnt pathway are closely associated with cancer including CRC (Bienz and Clevers, 2000; Polakis, 2000). This important role of Wnt pathway in CRC was highlighted by the detection of truncating mutations in the tumour suppressor gene APC in 1989 (Ashton-Rickardt et al., 1989). APC is an important negative regulator of the Wnt pathway and mutations in this gene often initiate the formation of CRC, as loss of APC occurs early on in carcinogenesis for sporadic and hereditary familial adenomatous polyposis (FAP) tumours (Ashton-Rickardt et al., 1989; Groden et al., 1991; Kinzler et al.,

1991). Moreover, it was found that mutations that result in activated Wnt signaling occur in about 80% of sporadic CRCs (Powell et al., 1992). Ultimately, loss of APC function prevents phosphorylation and degradation of β-Catenin (Miyaki et al., 1994). This leads to the accumulation and subsequent translocation of β-Catenin to the nucleus, driving uncontrolled LEF/TCF-mediated gene transcription (Polakis, 1999). As outlined in section 1.1.4, target genes of LEF/TCF transcription are associated with the "stem cell signature" and enhance cell proliferation, migration and adhesion processes (Sansom et al., 2004; Gregorieff and Clevers, 2005; Van der Flier et al., 2007). Therefore, activation of Wnt signaling drives tumorigenic processes.

### 1.2.4 *Mouse models of colorectal cancer*

Mouse models addressing different CRC subtypes have been developed over several decades to closely approximate the molecular, histopathological, and etiological characteristics observed in human CRC. Moreover, many of the molecular interactions and signaling strategies in the Wnt pathway are highly conserved between humans and mice enhancing mouse models as faithful models of human CRC.

**Mouse models of FAP**

The APCmin mouse model was first reported in 1990 as a model of FAP after a mouse with multiple intestinal neoplasia was discovered from an ethyl-N-nitrosourea chemical mutagenesis screen (Moser et al. 1990). Sequencing of this mouse, revealed it carried a truncation mutation of one allele of APC (Moser et al. 1990). Therefore, the mouse line was termed APCmin (multiple intestinal neoplasia). Interestingly, one allele of the APC gene remains intact and capable of maintaining a functional β-catenin destruction complex to prevent tumourigenesis. However, sporadic loss of the functional allele over time leads to the activation of β-catenin and expression of Wnt target genes. The most common cause of loss of heterozygosity of APC is mitotic nondisjunction of chromosome 18 where the APC gene is located (Dalton et al., 2007; Powell et al., 1992).

The APCmin model recapitulates many aspects of FAP. Tumourigenesis in this model is driven by truncation mutations in the APC gene. APCmin tumours also share

histopathological characteristics with early human CRC (Zasadil et al., 2016). However, there are slight discrepancies between human FAP and the APCmin mouse model. Firstly, APCmin mice primarily develop tumours in the small intestine, in contrast to humans where polyps are primarily observed in the colon (Cunningham et al., 2010; Kettunen et al., 2003). The reasons for this are not fully understood. Secondly, it is not uncommon to see hundreds of tumours lining the colonic epithelium in human FAP (Cunningham et al., 2010). However, APCmin model shows approximately 30 polyps in the ileum of the small intestine (Moser et al. 1990). Over time, human FAP tumours may metastasize, however, this phenomenon is rarely observed in APCmin mice. APCmin tumours may occasionally invade the underlying mucosa and muscularis externa but they do not metastasize. A possible explanation for this may be the relatively short lifespan of these mice (30 weeks), which does not allow sufficient time for more advanced stages of the disease to develop. Despite this, the APCmin mouse model is one of the most commonly used mouse models of CRC.

**Cre-lox mouse models of CRC**

Although the APCmin model is useful for studying intestinal tumourigenesis, it has limited utility when investigating the earliest stages of CRC. Initial onset of CRC is caused by inactivation of both alleles of APC, while in the APCmin mouse model, the time that heterozygosity is lost is unknown (Gryfe et al. 1997). Therefore, a model in which both alleles of APC could be deleted at specific time points was created using a conditional Cre-loxP recombination system (Evans et al., 2016). The Cre-loxP system recombines DNA between any two loxP sites in the same orientation when Cre-recombinase is expressed by a tissue-specific promoter (Evans et al., 2016). For example, to direct conditional APC loss in a K19-expressing cell, tamoxifen mediated cre-expression would be directed from a tissue specific promoter K19 to an essential exon (exon 14) of APC flanked by loxP sites. As the K19-CreERT transgene encodes a cre-recombinase estrogen-receptor (ER) linked protein, it will remain inactive until tamoxifen is present and binds to the ER, freeing the Cre-recombinase and activating the enzyme to cut the loxP sites surrounding exon 14 of APC. This results in loss of functional APC protein in K19 expressing cells and

subsequently tissue specific/conditional knockout of APC with tamoxifen induction. An advantage to using this model is the ability to drive expression of Cre-recombinase from different tissue-specific promoters, thereby driving recombination of a number of genes in different tissues or cellular compartments. Accordingly, this model has enabled the initial stages of intestinal tumorigenesis to be studied in detail. In particular, this model was used to identify Lgr5 as a cellular origin of CRC, as mentioned in section 1.2.2.

Besides altering the function of genes in a specific tissue or cell compartment, Cre-Lox technology has enabled cell lineage tracing to determine the genetic origin of a tumour. For example, LacZ reporter gene crossed to a K19-Cre mouse will express B-galactosidase when recombined (Asfaha et al., 2015). Additionally, daughter cells of the recombined cells will inherit the genetic marker, which can then be stained using X-gal. This allows for visualization of K19 cells and progeny when crossed to a tumour model. This model was used to identify K19 as a cellular origin of CRC, as detailed in section 1.2.2. Furthermore, the same principle of genetic lineage tracing has also been used in the non-mutated intestine to identify ISCs as described in section 1.1.3.

**Mouse models of colitis-associated CRC**

The AOM/DSS model is a well-established animal model of colitis-associated cancer, whereby colorectal cancer is induced chemically. In this model, a single intraperitoneal (i.p.) injection of a genotoxic colonic carcinogen, azoxymethane (AOM) (10 mg/kg body weight) and exposure to a non-genotoxic inflammatory agent, dextran sodium sulfate (DSS) (2.5%) in the drinking water for five days results in the development of multiple colonic tumours in approximately 9-12 weeks, with mice becoming moribund at 20 weeks with an average of 7 tumours (Rosenberg, 2008). DSS is toxic to the epithelial lining of the colon and produces severe colitis similar to what is seen in patients with inflammatory bowel disease (IBD) (Rosenberg, 2008). The pathogenesis of tumours induced in mice exposed to AOM/DSS is similar to that observed in human colitis-associated cancer. For instance, tumours are frequently found in the distal part of the colon, which is also the predominant location of colitis-associated cancer in humans (Rosenberg, 2008). Likewise, AOM/DSS tumours have been reported to share molecular features with human CRC, such

as dysregulation of β-catenin-signaling pathway (Takahashi et al., 1998; Takahashi et al., 2000) and mutations in K-Ras (Takahashi and Wakabayashi, 2004). However, they rarely display mutations in p53 or Smad4 and detailed molecular mechanisms of the AOM/DSS model are still very limited (Rosenberg, 2008). Regardless, the AOM/DSS model is representative of the colitis-associated colorectal cancer observed in humans.

Key points 4 | **Colorectal Cancer**

- Colorectal cancer (CRC) is highly prevalent in Canada.
- 30-50% of patients will develop therapy resistant CRC that results in poor survival rates.
- Human CRC can be classified as inherited (familial, hereditary nonpolyposis, familial adenomatous polyposis (FAP) and rare CRC syndromes), colitis associated or sporadic.
- Sporadic CRC is the most common CRC.
- Fearon and Volgelstein proposed that CRC development is a multistep process where a series of genetic mutations (APC → KRAS → SMAD2/4 → p53) leads to the progression of CRC from normal epithelium to metastatic carcinoma.
- Mutations in the Wnt pathway are closely associated with CRC and occur in ~80% of sporadic cancers.
- Two theories on the cell of origin in CRC exist:
    1. Bottom-up model suggests stem cells acquire mutations for malignant conversion.
    2. Top-down model suggests differentiated cells acquire mutations for malignant conversion.
- A variety of mouse models are used to study CRC.
- The APCmin mouse model is the most commonly used model of FAP.
    - Spontaneous loss of heterozygosity of APC leads to the formation of 30+ intestinal and 2-3 colonic tumours within 6 months.
- Conditional Cre-loxP recombination systems are used to study early stages of CRC by introducing a mutation in APC into a cell population of interest.
- The AOM/DSS model is the most commonly used model of colitis-associated CRC.
    - Azoxymethane (AOM) is a chemical carcinogen injected intraperitoneal.
    - Dextran sodium sulfate (DSS) causes inflammation when administered in the drinking water.
    - Together they cause tumourigenesis and tumour formation within 20 weeks.

## 1.3 Cancer Stem Cells

The cellular composition of CRCs maintains a high degree of similarity to normal intestinal tissue, with the appearance of glandular structures, although structurally disorganized in comparison to normal tissue (Medema and Vermeulen, 2011). Moreover, a variety of differentiated cell types are found in CRCs that are also present in the normal intestinal tissue (Blank et al., 1994; Grabowski et al., 2004; Marsh et al., 1993; Pierce et al., 1977; West et al., 1988). These findings can also be interpreted to suggest that like their normal tissue of origin, tumour cells are organized into a hierarchy of potency. Support for this interpretation was enforced by the discovery of stem cell-like cancer cells that expressed ISC markers (see section 1.1.3), which were multipotent and capable of self-renewal (Ricci-Vitiani et al., 1988; O'Brien et al., 2007; Dalebra et al., 2011). These findings support the cancer stem cell (CSC) hypothesis, which posits only a small subpopulation of cancer cells are capable of driving tumour growth and progression. Furthermore, it is postulated that therapy-resistant CRC arises from CSCs capable of evading treatment and persisting in tumours to cause relapse (Sarkar et al., 2009; Yu et al., 2012). Therefore, CSCs represent a novel therapeutic target for the treatment and/or prevention of tumour progression. However, there are still many uncertainties regarding their identification, functional properties and importance, which are outlined below (Medema, 2013).

### 1.3.1 *History and Identification*

CSCs were first identified nearly 20 years ago in acute myeloid leukemia through serial transplantation assays (Lapidor et al., 1994). In this assay, subpopulations of tumour cells expressing identified surface markers are sorted via FACS, transplanted into immunocompromised mice and evaluated for tumour formation (Figure 9). Using this experimental technique, Bonnet & colleagues were able to identify a small subpopulation of CD34+/CD38- leukemic cells capable of establishing human leukemia (Bonnet et al., 1997). Interestingly, the other cell populations failed to form tumours. These results indicated that CD34+/CD38- cell population labelled cancer initiating cells or CSCs (Bonnet et al., 1997). Accordingly, serial transplantation assays using xenografts have become the gold standard to define CSCs, and many CSCs have been identified in several solid tumour types including: medulloblastoma/glioblastoma (Singh et al., 2004), breast

(Al-Hajj et al., 2003), pancreatic (Fredebohm et al., 2012), prostate (Collins et al., 2005), and colorectal (Ricci-Vitiani et al., 2007; O'Brien et al., 2007) cancers, among many others. However, there are many limitations with this assay when applied to epithelial cancers, such as colorectal cancers (Nguyen et al., 2012; Zeuner et al., 2014; Plaks et al., 2015). This assay has identified the existence of CSCs in CRC but these cells often show poor engraftment, even after enrichment for CSC markers (Ricci-Vitiani et al., 2012; O'brien et al., 2007; Kobayashi et al., 2012; Kemper et al., 2012). This may largely be due to sorted epithelial cells undergoing anoikis during detachment from the tissue (Fuji et al., 2017). Moreover, epithelial stem cells are passively regulated by their microenvironment (niche), suggesting that repopulation efficiency may reflect the robustness or fitness of the transplanted cells into the recipient niche rather than stemness (Fuji et al., 2017). Interestingly, this phenomenon was observed in serial transplantation assays performed with melanoma cells. Quintana et al. found that the tumorigenic capacity of transplanted melanoma cells changed with the level of immune deficiency of host animals (Quintana et al. 2008).

To circumvent the drawbacks of serial transplantation assays, lineage tracing of genetically marked cells has been used to identify colorectal CSCs in genetically traceable mouse tumour models (Driessens et al., 2012; Schepers et al., 2011; Asfaha et al., 2015). The first evidence to support the existence of CSCs using this method, was demonstrated in three independent lineage tracing studies of brain (Chen Li et al., 2012), skin (Driessens et al., 2012) and intestinal (Schepers et al., 2011) cancers. In regards to colorectal cancer, Schepers et al. employed the confetti mouse model to initiate "lineage retracing" in intestinal adenomas. They demonstrated that a small subpopulation (5-10%) of tumour cells was labelled by the ISC marker Lgr5 which fueled the growth of established intestinal adenomas and displayed multi-lineage differentiation potential indicative of CSC activity. However, it is important to note that sorted Lgr5+ intestinal tumour cells have not been shown to form tumours using the traditional method of serial transplantation assays.

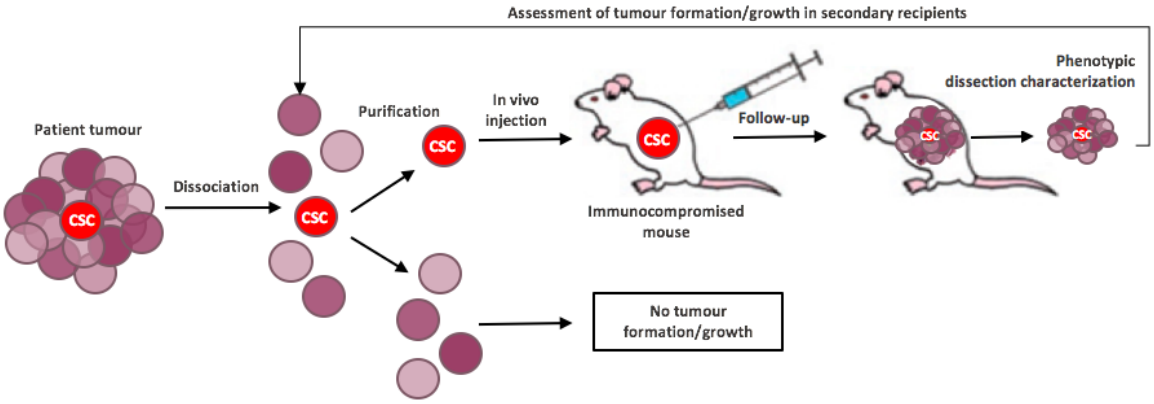


Figure 9 | **Identification of cancer stem cells.** Serial transplantation assays allow for the identification of cancer stem cell populations. Patient tumours are dissociated into single cell populations and injected into immunocompromised mice to assess the formation of tumours. Only the injection of CSCs will yield tumours, whereas injection of tumour cells that lack cancer stem cell properties will not result in tumour formation or growth. To determine whether the cancer stem cell population is capable of self-renewal, xenografted tumours are removed and put through this process again to assess tumour formation/growth in secondary recipients. Only the cancer stem cell population will possess long-term self-renewal capacity and it will regenerate the tumour, whereas injection of non-CSCs will not re-initiate tumour growth.

### 1.3.2 *Colorectal cancer stem cell markers*

Identification of colorectal CSCs relies heavily on the expression of cell surface or ISC markers. As such, many CSC markers have been proposed and their ability to robustly identify the colorectal CSC population is discussed below.

### 1.3.3 *Cell surface markers*

A number of cell surface markers have been proposed to identify colorectal CSCs including CD133 (Ricci-Vitiani et al., 2007; O'Brien et al., 2007), CD44 (Chu et al., 2009) and ALDH1 (Huang et al., 2009). Using serial transplantation assays, these markers were identified on the basis that enriched populations initiate tumours in xenograft models, whereas depleted populations did not. However, many of the CSC markers identified from these assays were chosen because the proteins were expressed in colorectal cancer tumours. Unlike this reasoning, the original studies conducted on leukemic CSCs relied heavily on the understanding of stem-progenitor hierarchies in the healthy bone marrow to establish relevant highly reliable CSC markers (Lapidot et al., 1994; Bonnet et al. 1997). However, few studies have employed this methodology. In fact, one study implicated CD44 as a CSC

in breast cancer despite the lack of CD44 in normal breast epithelial stem-progenitor hierarchies (Al-Hajj et al., 2003). This suggests that CD44 was incorrectly chosen for its differential expression in breast tumours. In addition to CD44, CD133 or prominin 1 has been suggested as a CSC marker in a variety of cancers, which shares expression with its normal stem-progenitor tissue counterparts. Although recently, it was revealed that CD133 is widely expressed in many tissues (Shmelkov et al., 2008). Therefore, there is considerable disagreement over the validity and usefulness of this CSC marker. Initially, CD133 was proposed as a useful CSC marker in CRC (O'Brien et al., 2007; Ricci-Vitiani et al., 2007), as well as brain cancers (Singh et al., 2004; Bao et al., 2006). However, these findings were later refuted in subsequent studies (Dalebra et al., 2007; Shmelkov et al., 2008; Joo et al., 2008; Ogden et al., 2008; Wang et al., 2010; Chen et al. 2010). These studies highlight the need for selection of CSCs that are relevant and specific to the underlying stem cell biology of normal tissues from which the cancer originates.

The following sections outline a select few cell surface proteins that may function as CSC markers in CRC.

**CD133**

CD133 or prominin-1 expression has been used to identify CSCs in a number of different cancers including medulloblastoma/glioblastoma (Singh et al., 2004), prostate (Collins et al., 2005; Richardson et al., 2004), pancreatic (Hermann et al., 2007) and colorectal cancers (Ricci-Vitiani et al., 2007; O'Brien et al., 2007). CD133 is a 120kDa five-transmembrane cell surface protein that has been reported to affect many cellular processes including stemness, tumourigenesis, chemo/radioresistance, metabolism, autophagy and apoptosis (Li, 2013). In the colon, CD133 was the first CSC marker used. It was found that 1000-3000 CD133+ cells were capable of initiating tumours in immunodeficient mice (Ricci-Vitiani et al. 2007; O'Brien et al. 2007). However, recent studies have suggested that CD133 may not be a robust CSC marker. Importantly, it was found that when the CD133 negative population was transplanted into NOD/SCID mice, tumour formation was initiated (Shmelkov et al. 2008). Moreover, knockdown of CD133 does not affect colony

formation efficiency or tumorigenic capacity, highlighting the need for a more pertinent CSC marker in CRC (Du et al., 2008).

**CD44**

Another commonly employed CSC marker is CD44. CD44 has been identified as a CSC marker in breast (Al-Hajj et al., 2003; Pham et al., 2011), prostate (Collins et al., 2005), gastric (Yoon et al., 2014) and colorectal (Du et al., 2008; Dalebra et al., 2007) cancer. Functionally, CD44 is a receptor for hyaluronic acid and plays a role in normal cell-cell adhesion as well as proliferation, motility, adhesion and cell survival in cancer (Keysar and Jimeno, 2010; Afify et al., 2009; Marharba and Zoeller, 2004). In comparison to normal tissue, CD44 has been found to be upregulated in colorectal cancer tissue. Moreover, CD44+ cells isolated from primary colorectal tumours demonstrate increased tumorigenic capacity, with as few as 100 CD44+ cells leading to tumour initiation in mice (Du et al., 2008; Dalebra et al., 2007). In contrast to CD133, CD44+ cells demonstrate enhanced colony formation efficiency indicating self-renewal (Chu et al., 2009; Du et al. 2008; Wang et al., 2012). Furthermore, CD44+ cells formed heterogeneous tumours containing CD44- cells *in vivo*, demonstrating the ability of this population to differentiate into other cancer cell types (Chu et al., 2009). Importantly, when CD44 was knocked down in primary tumour samples, colony formation and tumourigencity was inhibited. Thus, highlighting the role of CD44 as a functional marker of colorectal CSCs.

**ALDH1**

In addition to CD133 and CD44, aldehyde dehydrogenase 1 (ALDH1) is a commonly used marker of CSCs. It has been detected in numerous cancers including ovarian (Deng et al., 2010), bladder (Su et al., 2010) and colorectal (Huang et al., 2009). Functionally, ALDH1 is a member of the ALDH gene family, which catalyzes the oxidation of acetaldehydes and retinal (retinaldehyde) (Tomita et al., 2016), and it contributes to a variety of cellular processes through activation of retinoid signaling. The expression of ALDH1 is detectable by antibody based methods or enzymatic assay. However, the enzymatic assay lacks specificity for different ALDH isoforms. The activity of ALDH1 is elevated in normal stem/progenitor cells including ISCs (Dalebra et al., 2007). In several studies, when cancer

cells were sorted based on ALDH1 activity, a tumour initiating population was revealed (Tanei et al., 2009; Su et a.l, 2010; Kim et al., 2011; Sullivan et al., 2010). These results suggest that high activity or expression of ALDH1 is a useful method for identifying and isolating CSC populations in a variety of cancer types (Tanei et al., 2009; Su et al., 2010; Kim et al., 2011;Huang et al., 2009).

## Known intestinal stem cell markers

### Lgr5

In 2012, Clevers *et al.* provided the first *in vivo* validation of a colorectal CSCs using a novel transgenic mouse model, which allowed them to visualize lineage re-tracing in established tumours (Schepers et al., 2011). This work stemmed from earlier genetic fate mapping studies in the normal intestine. In this study, they identified Lgr5-expressing crypt base columnar cells as a stem cell population able to give rise to all intestinal cell types (Barker et al., 2007). Interestingly, upon ablation of Lgr5+ cells in the normal intestine, other stem cells have been shown to regenerate Lgr5+ cells and their progeny (Tian et al., 2011). This demonstrates the presence of a heterogeneous pool of stem cell populations in the normal intestinal epithelium. Though it is not known whether CSCs represent a heterogeneous pool encompassing different cell types in a much like the normal intestinal epithelium.

## Proposed intestinal stem cell markers

### K19

Our laboratory recently identified Keratin-19 (K19) as a potential CSC marker. Cytokeratins are a multigene family of intermediate filaments, critical in the maintenance of the cytoskeleton but expressed in different lineages in the epithelium (Moll et al., 1982). Keratin-19 is the smallest known acid keratin (approximately 40kDa) and is epithelial-specific, found in a broad range of epithelial tissues (Lapouge et al., 2011). In the small intestine and colon, our laboratory identified K19+ cells as radioresistant tissue stem cells capable of giving rise to Lgr5+ cells (Asfaha et al., 2015). Interestingly, K19 is also amplified in many solid tumours making it an ideal candidate marker for CSCs (Lapouge

et al., 2011). Our preliminary data (not included here) further demonstrated that K19 identifies CSCs in established colonic tumours.

### 1.3.4 *Targeting cancer stem cells*

CSCs are believed to play an important role in the maintenance of tumour growth, metastasis, as well as therapy resistance. Therefore, from a therapeutic standpoint, the elimination of CSCs is necessary to eliminate the tumours. However, treatments that are currently used in CRC are aimed at targeting rapidly dividing cells that make up the bulk of the tumour via chemotherapy or radiation. Unfortunately, these treatments are often unsuccessful at targeting slow-cycling CSCs. As a result, CSCs are thought to evade treatment, causing relapse of disease and the emergence of therapy-resistant CRC (Figure 10). This notion, has led to multiple studies targeting CSCs in CRC. Recently, Shimokawa et al and de Sousa e Melo et al investigated targeted ablation of Lgr5 expressing CSCs in two different models of colorectal cancer. Initially, both groups observed tumour regression, as one would expect to see if the source of cancer growth is being ablated. However, upon discontinuing ablation of Lgr5+ cells in established tumours, Lgr5+ cells reappeared and growth rapidly resumed (de Sousa e Melo et al., 2017; Shimokawa et al., 2017). Moreover, targeted ablation of Lgr5+ cells using an antibody-directed chemotherapeutic in APCmin mouse model had no effect on tumour burden (Juntila et al., 2015). This demonstrates that depending on the tumour model, the CSC pool might encompass different cell phenotypes and that elimination of Lgr5+ CSCs might alter tumour growth but may not eradicate the disease. This highlights the need to identify other CSC populations that may exist in CRCs.

From what we know about the functional role of CSCs in CRC, it is evident that a method of targeting CSCs is necessary to eradicate disease. However, this presents a number of difficulties related to the stem cell niche and *bona fide* markers. It is likely that the tumour environment regulates CSCs, much like what is observed in the normal intestinal environment. However, it remains unknown whether the tumour initiating activity is inherent to CSCs. This has major implications in terms of targeting CSCs. If the latter is correct, simply ablating CSCs will likely have non-significant effect on tumour growth other stem cells in the environment may assume the role of CSCs. Secondly, a major

challenge in targeting CSCs remains the lack our understanding of definitive markers identifying CSCs. The markers that have been used to identify CSCs thus far are poor candidates for antibody-directed therapy, as they are broadly expressed in healthy tissue. Together these challenges highlight the need to increase our understanding of normal ISCs and CSCs, as well as the seemingly interconnected relationship between niche environments and CSC plasticity to develop effective therapeutic targets.

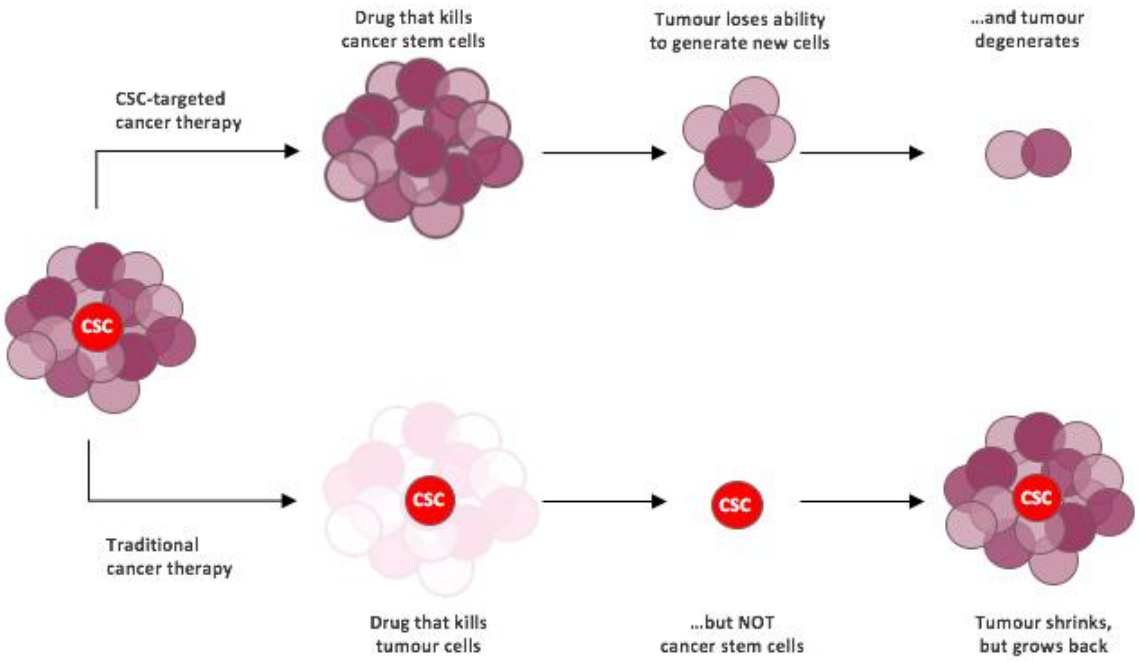


**Figure 10** | CSC-targeted therapy versus traditional cancer therapy. This figure was originally published online in *Sigma-Aldrich. Cancer stem cells: new targets for cancer therapy [https://www.sigmaaldrich.com/technical-documents/articles/biofiles/the-cancer-stem-cell.html]*. Modified figure is being reproduced for educational purposes only and not for any commercial use. Figure is included in the M.Sc. dissertation with attribution.

Key points 5 | **Cancer Stem Cells**

- The cancer stem cell (CSC) hypothesis posits that only a small subpopulation of cancer cells is capable of driving tumour growth and progression.
- Therapy resistant CRC may arise from CSCs capable of evading treatment to persist in tumours and cause relapse.
- Two critical properties of CSCs that contribute to their tumourigenic potential are (1) self-renewal (2) multipotentcy.
- CSCs may represent a novel therapeutic target for the treatment and/or prevention of tumour progression.
- CSCs are identified through the expression of various markers cell surface (CD133, CD44, ALDH1) and intestinal stem cell markers (Lgr5).
- Within the normal intestinal epithelium it has been shown that ablation of Lgr5 cells has no effect on intestinal homeostasis. This suggests that a reserve stem cell population exists to compensate for the loss of Lgr5.
- However, it is not known whether cancer stem cells represent a heterogeneous pool, similar to the normal intestine, whereby an Lgr5- CSC population could be important for tumour growth and progression.

## 1.4 Rationale

Evidence in the normal intestinal epithelium reveals stem cell populations represent a heterogeneous pool encompassing different cell types in a dynamic equilibrium (Barker et al., 2007). For example, stem cell activity is observed at the base of intestinal crypts in rapidly dividing cells that express leucine-rich repeat-containing G protein-coupled receptor (Lgr5) (Tian et al., 2011). However, genetic ablation of Lgr5+ cells *in vivo* does not appear to drastically alter tissue homeostasis, suggesting that their loss can be compensated for by the recruitment of a different Lgr5 negative stem cell populations which are capable of regenerating Lgr5+ cells (Ricci-Vitiani et al., 2007; O'Brien et al., 2007; Rizk et al., 2012; Moll et al., 1982). Our laboratory has identified Keratin-19 (K19) expressing cells as tissue stem cells at the apex of cellular hierarchy able to give rise to Lgr5+ cells (O'Brien et al., 2007). However, the extent to which these processes are paralleled in malignant tissues through CSC activity remains unclear. In 2012, Clevers and colleagues identified Lgr5 as a marker of colorectal CSC using a model of lineage re-tracing in established tumours (Ricci-Vitiani et al., 2007). Based on the results and

implications of these studies, I aim to determine if K19 labels a cancer stem cell population in an *in vivo* model of colorectal cancer.

### 1.4.1 *Hypothesis*

I hypothesize that K19 will label a cancer stem cell population that is distinct from previously identified Lgr5+ cancer stem cells and contributes to colorectal tumour growth.

### 1.4.2 *Objectives*

1. Determine if K19 labels a cancer stem cell population in colorectal cancer
2. Assess the effects of Lgr5+ ablation on tumour growth, both *in vivo* and *in vitro*.

# Chapter 2

# MATERIALS AND METHODS

## 2.1 Experimental Animals

All animal care and experimental procedures were approved by the Canadian Council of Animal Care and the Animal Use Subcommittee of the University of Western Ontario.

### 2.1.1 *Animal husbandry*

Mice were housed in transparent plastic cages in a room with a 12h light/12 h dark cycle. The mice were fed standard laboratory chow (Lab Diet) and tap water ad libitum.

### 2.1.2 *Breeding*

All strains were generated on a C57BL/6 background. Mice were bred at approximately 6 weeks of age. Pups were weaned at approximately 4 weeks old when feeding independently. Pups were sexed and separated at weaning, and ear-tagged for identification. At this time, small tail biopsies (3-4 mm) were collected for genotyping.

### 2.1.3 *Genetic mouse models*

A number of transgenic mouse models were utilized in this study (Table 1). The transgenes used contained exons of the gene of interest flanked with loxP sites, or insertion of human diphtheria toxin receptor to enable conditional deletion of genes, or cre-recombinase-driven by a tissue specific promoter to induce lineage tracing.

Table 1| **Transgenic mouse models**

| Model | Type of transgene | Expression | Mutation | Effect | Reference |
|---|---|---|---|---|---|
| **K19-CreERT2** | BAC | Inducible | Tamoxifen inducible CreERT2 fusion gene inserted into K19 gene coding region of K19 containing BAC clone (BAC RP-23-24N13). | Label K19+ expressing cells and progeny when combined with a reporter gene under control of the Rosa 26 locus. | (Asfaha et al., 2015) |
| **Rosa26-TdTomato** | Knock-in | Inducible | Cre reporter allele with loxP flanked stop cassette preventing transcription of CAG promoter-driven red fluorescent protein variant (TdTomato) inserted into the Rosa 26 locus. | Spatiotemporally label cells and progeny red when crossed to a cre recombinase gene under the control of a promoter of interest | (Luche et al., 2007) |
| **Lgr5-DTR-eGFP** | Knock-in | Constitutive | Exon 1 in the Lgr5 gene is linked in frame to eGFP and a human DTR cDNA, producing a fusion protein | Expression of eGFP functions as a reporter for Lgr5 expression and diphtheria toxin receptor confers diphtheria toxin sensitivity to Lgr5+ expressing crypt base columnar cells. | (Tian et al., 2011) |

| | | | | | |
|---|---|---|---|---|---|
| **APCf/f** | Knock-in | Inducible | Exon 14 in the APC gene is flanked by loxP sites | Ablation of APC functional protein when crossed to mice a cre recombinase gene under the control of a promoter of interest | (Colnot et al., 2004) |
| **APCmin** | Chemically induced mutation | Constitutive | Germline nonsense mutation at codon 850 of APC | Spontaneous loss of heterozygosity leads to tumour formation in small intestine and colon in ~6 months | (Moser et al., 1990) |

### 2.1.4 *Mouse lines*

To address the aims of this thesis, a number of mouse lines were generated from the mouse models outlined in Table 1. The mouse lines generated were used to visualize progeny of K19 and ablate Lgr5 cells in various CRC models. The details of these mouse lines are outlined in Table 2.

Table 2 | **Mouse lines**

| **Mouse line** | **Effect** |
|---|---|
| **K19-CreERT;Rosa26-TdTomato** | Treatment with tamoxifen induces excision of the STOP codon preventing TdTomato expression in K19 expressing cells resulting in robust TdTomato fluorescence. When these mice are treated with AOM/DSS, this allows for lineage tracing of K19+ cells and progeny in tumours. |
| **K19-CreERT;Rosa26-TdTomato;APCmin** | When crossed to APCmin mice which spontaneously form tumours, we are able to lineage trace K19 cells in tumours using a similar principle to the above mouse line. |
| **Lgr5-DTR-eGFP** | When these mice are treated with AOM/DSS, this mouse model allows for specific ablation of all Lgr5+ cells in tumours. |
| **Lgr5-DTR-eGFP; K19-CreERT;APCf/f** | Treatment with tamoxifen induces a loss of functional APC protein in K19 expressing cells, resulting in tumour formation. Additionally, with the presence of Lgr5-DTR, this allows for specific ablation of all Lgr5+ cells in K19 $APC^{f/f}$ derived tumours. |

| | |
|---|---|
| **K19-CreERT$^2$;APCf/f** | Treatment with tamoxifen induces a loss of functional APC protein in K19 expressing cells, resulting in tumour formation. |

### 2.1.5 *Experimental design*

**K19-CreERT;R26TdTomato;APCmin**

To induce cre-mediated lineage tracing of TdTomato in *established adenomas*, 3mg of tamoxifen in 200 µL corn oil was administered to 20 week-old mice by oral gavage (Figure 11). Following tamoxifen induction of Cre recombinase in K19+ cells, TdTomato labelling was assessed by immunofluorescence microscopy. Mice were sacrificed at 24 hours, 10 days and 4 weeks post-tamoxifen. Tissue sections were counterstained with DAPI (Fisher).

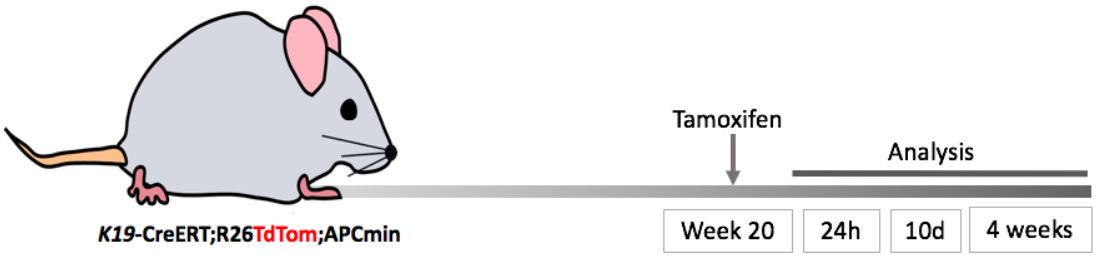


Figure 11 | **Experimental protocol for K19-CreERT$^2$;R26TdTom;APCmin mice**

**K19-CreERT;R26TdTomato**

To assess CSC properties of K19+ cells *in vivo*, I performed lineage tracing analysis of adenomas K19-CreERT;R26TdTomato mice treated with AOM/DSS mice. To induce cre-mediated lineage tracing of TdTomato in *established adenomas*, 3mg tamoxifen (K19) in 200 µL corn oil was administered to 15-week old mice by oral gavage (Figure 12). Following tamoxifen induction of Cre recombinase in K19+cells, TdTomato labelling was assessed as described above.


**Figure 12** | Experimental protocol for K19-CreERT$^2$;R26TdTom AOM/DSS mice

**Lgr5-DTR-eGFP AOM/DSS**

To examine the effect of Lgr5+ cancer stem cell ablation on tumour initiation and growth *in vivo*, I administered 500ng of diphtheria toxin 2x per week from week 3 post-AOM (Sigma) until the experimental endpoint at 20 weeks, to selectively ablate Lgr5+ cells in Lgr5-DTR-eGFP mice treated with AOM/DSS (Figure 13). Administration of DT (Sigma) from week 3 onwards ensured Lgr5+ cells are ablated for the duration of tumour initiation and growth. Therefore, cohorts of experimental (DT-treated) and control (saline- treated) mice (n > 10 per group) were compared with respect to tumour burden (number and size) and histology at 20 weeks.

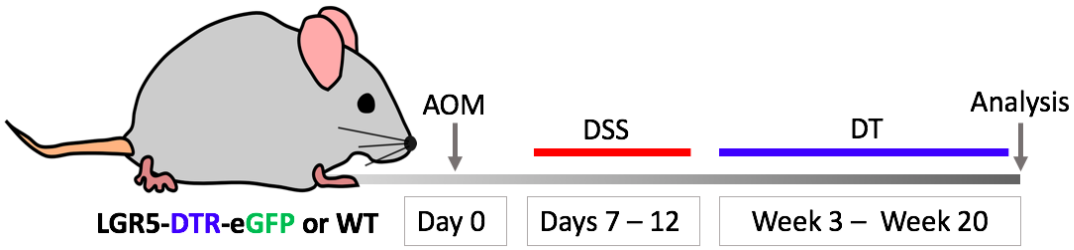


Figure 13 | **Experimental protocol for Lgr5-DTR-eGFP AOM/DSS mice**

## 2.2 Genotyping of mice

Polymerase chain reaction (PCR) was performed to genotype weaned mice using genomic DNA (gDNA) extracted from tail biopsy. Confirmatory genotyping was also performed at the time of death to ensure the mouse was assigned to the correct experimental cohort.

### 2.2.1 *Nucleic acid isolation*

Tail samples were placed in 1.5 mL centrifuge tube and stored at 4°C until use. 75 μL of tail lysis buffer (Appendix II) was added to tubes and incubated at 98°C for one hour. Samples were cooled on ice for 5 minutes and 75 μL of neutralization buffer was added (Appendix II). Following neutralization, samples were centrifuged at 4000 rpm for 3 minutes at 4°C and the supernatant was used for PCR. gDNA was stored at room temperature (RT) for short term use and at 4°C for long term storage.

### 2.2.2 *PCR protocol*

PCR was carried out in thin-wall 12-well strip tubes (Fisher). Two μL of gDNA, extracted as described above, was added to each tube with 18 μL of PCR mix (described in Table 3) containing the DNA polymerase (FroggaBio), $H_2O$ (FroggaBio), and gene-specific primers. One negative control ($H_2O$ only) and positive control tube was run with every PCR reaction. Primers were used as described from previous publications (Appendix III). The caps were placed firmly on tubes and the PCR reactions were on a thermocycler (Life Technologies, Verti PCR machine). PCR conditions and primers are listed in Appendix IV.

Table 3 | **Constituents of PCR mix**

| ***Component*** | **20 μL reaction** |
|---|---|
| *Taq polymerase (FroggaBio)* | 10 μL |
| *Forward primer* | 0.5 μL |
| *Reverse primer* | 0.5 μL |
| *Template DNA* | 2 μL |
| *Nuclease-free $H_2O$ (FroggaBio)* | 7 μL |

### 2.2.3 *Visualization of PCR products*

PCR products were visualized by gel electrophoresis. Agarose gels were made by dissolving 8 g of agarose (Fisher) in 400 mL TAE buffer [40mM Tris; 19mM Acetic Acid (Fisher)] in a conical flask by heating in a microwave until boiling. Ten μL of ethidium bromide (Sigma) was added to the melted gel and agitated carefully to ensure even distribution without incorporating air bubbles into the gel. One hundred fifty mL of gel

solution was poured into each mold (Bio-Rad) and combs inserted to create wells. Once the gels were set, the combs were removed and they were placed into gel electrophoresis tanks and covered with TAE.

Ten µL PCR product was added to each well of the agarose gel and run alongside a molecular weight ladder (Fisher). The gel was run at 140 V for approximately 30 minutes, and visualized using a GelDoc UV trans illuminator (Bio-Rad).

## 2.3 AOM/DSS Administration

To induce colonic tumours, K19-CreERT/R26TdTomato, Lgr5-DTR-eGFP and WT mice were subjected to a well-established, chemically-induced inflammation protocol (Wirtz et al., 2007; Tanaka, 2003). Mice (6-8 weeks old) were injected intraperitoneally (i.p.) with a single dose of AOM (with 10 mg/kg, (Sigma)) diluted in saline. After one week, 2.5% DSS (Gojira) was administered in the drinking water for 5 days, followed by regular drinking water. Throughout DSS administration, mice were assessed for health condition by using a scoring system. Mice were euthanized if endpoints were reached or 16-20 weeks post AOM administration.

## 2.4 Tamoxifen Preparation and Administration

Tamoxifen (Sigma) was dissolved in corn oil (Sigma) to a final concentration of 20 mg/mL. The sample was placed in a rotor and heated at 37°C until the tamoxifen was completely dissolved. In order to induce Cre expression in Cre-ERT mice, tamoxifen was administered via oral gavage. For tamoxifen dosing of each mouse line, please refer to Table 4.

Table 4 | **Doses of tamoxifen used for each mouse line**

| *Mouse Line* | *Dose of Tamoxifen* |
|---|---|
| *APCmin/K19-CreERT/Rosa26-tdTomato* | 3mg |
| *K19-CreERT/Rosa26-tdTomato* | 3mg |
| *Lgr5-DTR-eGFP/K19/APCf/f/Rosa26-tdTomato* | 6mg |
| *K19-CreERT/APCf/f/Rosa26-tdTomato* | 6mg |

## 2.5 Diphtheria Toxin Preparation and Administration

Diphtheria toxin stock solution was prepared from 1 mg of solid powder (Sigma). The powder was first dissolved in 1 mL of 0.9% saline. The solution was then diluted to a final concentration of 500 ng/200 µL and transferred to centrifuge tubes. Final prepared toxin solution was stored at -80°C and thawed directly before application.

## 2.6 Tissue Preparation

### 2.6.1 *Tissue dissection*

Mice were euthanized in a $CO_2$ chamber for 4-5 minutes, followed by cervical dislocation. Mice were sprayed with 70% ethanol and the skin and muscle of the abdomen cut through to open the abdominal cavity. The small intestine and colon were removed and flushed with PBS (Fisher). For organoid culture studies, 5-10 cm of the proximal small intestine and the entire colon was collected. For lineage tracing in AOM/DSS experiments only, the colon was collected. For APCmin lineage tracing experiments, both the small intestine and colon were collected. For Lgr5-DTR AOM/DSS experiments, small intestine and colon were collected. All tissues were collected into 4% paraformaldehyde (PFA; Santa Cruz) on ice.

### 2.6.2 *Tissue fixation*

For histological analysis, the organs were cut longitudinally, “Swiss rolled” (Moolenbeek and Ruitenberg 1981), inserted into embedding cassettes and fixed 6-8 hours in 4% paraformaldehyde in PBS at 4°C.

### 2.6.3 *Preparation of tissues*

Tissues were cryopreserved in 30% sucrose in PBS at 4°C for 48 hours. For subsequent histological analysis, tissues were embedded in Optimal Cutting Temperature (OCT) (Fisher) and stored at -80°C overnight before being cut to 5 µm slices with a microtome-cryostat (Leica) at -21°C and picked up on glass slides (Fisher). Slides were stored at -20°C. For all imaging studies, 4 serial sections of tissues were collected for analysis.

For long-term cohorts where an accurate tumour count was required, small and large intestines were flushed with cold 1 X PBS and opened longitudinally on filter paper (Fisher). Tumour number and volume (calculated as length x width x width) counts were performed and the gut was rolled using dissection tweezers and placed into cassettes and fixed as described above.

## 2.7 Histology

### 2.7.1 *Hematoxylin & Eosin (H&E) staining*

For routine histological analysis, frozen slides were warmed to room temperature for 10 minutes and rehydrated for two minutes in descending gradient of ethanol (100%, 95%, 70% and 50%). The tissue slides were washed in dd$H_2O$ and stained for 7 minutes in a ready to use hematoxylin solution (Cedarlane). Residual stain was washed off in tap water. In order to stain eosinophilic structures and the cytoplasm, slides were stained for 10 s in a 1.5% eosin (Fisher) solution. Residual staining solution was washed off in distilled water. The tissue was dehydrated in ascending ethanol gradient (50%, 70%, 95%, and 100%) and then incubated in xylenes (Fisher) for 5 min. The tissue slides were air-dried and mounted using toluene-based mounting medium (Fisher).

### 2.7.2 *Nuclear counterstaining for immunofluorescence microscopy*

Slides were washed with PBS for 5 minutes twice, incubated in 0.25% Triton X-100 (Fisher) in PBS for 10 minutes, rinsed in PBS for 5 minutes, and then counterstained with 1:1000 DAPI (Fisher). Slides were preserved in water-based mounting medium (Vectashield) and covered with a glass coverslip (Fisher).

### 2.7.3 *Image acquisition & analysis of slides*

Prepared slides were observed using EVOS FL Auto microscope (Life Technologies). DAPI UV (357-447 nm) filter was used to observe nuclei (blue), and RFP (red) were visualized under the 530-595 and 470-510 nm excitation filters, respectively. The percentage of lineage tracing was quantified using ImageJ. The area of lineage tracing or tumors was determined by outlining areas on ImageJ using the freehand area outlining tool.

Raw values were transferred to excel, and the percentage of lineage tracing was determined with the following formula ([total area of lineage tracing in tumours/total area of tumour] x 100).

## 2.8 Organoid Culture

The methods outlined below for intestinal organoid culture were modified from the methods originally presented by Sato et al., to increase efficiency (Sato et al., 2009).

### 2.8.1 *Experimental protocol*

Eight-week old Lgr5-DTR-eGFP;K19-CreERT;APCf/f and K19-CreERT;APCf/f mice were treated with 6 mg of tamoxifen via oral gavage. Two days post-tamoxifen treatment, small intestine and colonic tissues were cultured. R-spondin was removed from the media at day 5 to select for APCf/f organoids (normal organoids with intact APC require R-spondin for survival, while APCf/f organoids do not). Organoids were passaged and treated with 20 ng/mL DT or vehicle (0.9% saline) from day 10 until day 30. At day 20, a subset of organoids had DT removed from the media (Figure 14). All experiments were repeated in triplicate.

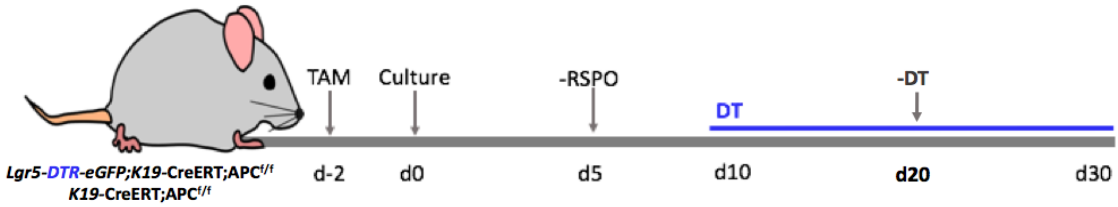


Figure 14 | **Experimental protocol for in vitro Lgr5 ablation experiments.**

### 2.8.2 *Isolation of intestinal crypts*

Fifteen cm of small intestine was flushed with PBS (Fisher). The intestine was then opened longitudinally and scraped firmly using a glass cover slip to remove the villi. Once scraped, the intestine was transferred to a centrifuge tube and washed vigorously with PBS. The intestine was resuspended in 10 mL of 2.5 mM EDTA (Fisher) in PBS and incubated at 4°C in a rotator for one hour. The intestine was removed from solution and cut into 0.5 mm pieces and resuspended in 10 mL fetal bovine serum (FBS; Fisher) in PBS. To release

crypts from intestinal tissue fragments, the solution was vigorously pipetted 10-20 times. The solution was passed through a 70 μM cell strainer to remove clumps and centrifuged at 800 rpm for 5 minutes. The pellet was resuspended in 5 mL DMEM (Fisher) containing Glutamax (Life Tech), (4-(2-hydroxyethyl)-1-piperazineethanesulfonic acid) (Hepes; Life Tech), and antibiotic/mycotic penicillin and streptomycin solution (Life Tech).

### 2.8.3 *Isolation of colonic crypts*

The entire colon was collected and flushed with PBS (Fisher). The colon was then opened longitudinally and scraped using a glass cover slip. Once scraped, the colon was transferred to a centrifuge tube and washed vigorously with PBS. The colon was resuspended in 10 mL of 3 mM EDTA in PBS and incubated at 4°C in a rotator for one hour. The colon was removed from solution and cut into 0.5 mm pieces and resuspended in 10 mL of FBS. To release crypts from colonic tissue fragments, the solution was vigorously pipetted 15-25 times. The solution was passed through a 100 μm cell strainer to remove clumps and centrifuged at 800 rpm for 5 minutes. The pellet was resuspended in 5 mL DMEM containing Glutamax, Hepes, and penicillin/streptomycin .

### 2.8.4 *Counting and seeding crypts*

The number of crypts in three 10 mL aliquots were counted and the appropriate volume of solution to seed the number of wells required was calculated. This volume was taken and resuspended in a 50:50 ratio with DMEM, followed by 50:50 dilution into the appropriate volume of Matrigel (Fisher). Ninety-six well plates were pre-warmed in the incubator prior to adding Matrigel.

### 2.8.5 *Organoid media*

Ninety-nine μL of organoid growth media (Table 5) was added to each well of the 96-well plates. Plates were returned to the incubator immediately, and the media was changed every 4 days.

Table 5 | **Recipe for complete organoid culture medium.**

| *Organoid Culture Medium* | *Volume* |
|---|---|
| *Penicillin/Streptomycin (100x )* | 1 mL |
| *Hepes Buffer (100x)* | 1 mL |
| *Glutamax (100x)* | 1 mL |
| *N2 Supplement (100x)* | 1 mL |
| *B27 Supplement (50x)* | 2 mL |
| *Rspondin* | 2 mL |
| *DMEM* | 100 mL |

### 2.8.6 *Diphtheria toxin treatment of organoids*

Organoids were treated with 20 ng/mL of Diphtheria toxin (DT) every two days from day 10 to day 30 (Figure 15). Thirty µL aliquots of 2 ng/mL DT were prepared on ice from 100X stock (Sigma). Aliquots were stored at -80°C until ready for use. One µL stock was added to 99 µL of media in each well.

### 2.8.7 *Passaging organoids*

Organoids were passaged every 10 days. Briefly, media was removed from each well and resuspended with 100 µL of cold DMEM. Matrigel was disrupted using a 200 µL pipette tip and pipetted up and down to free the organoids from the Matrigel. It was then pipetted into a 15 mL centrifuge tube, wells were rinsed with an additional 100 µL of cold DMEM and transferred to the tube. The organoids were centrifuged at 600 rpm for 5 minutes and the pellet was resuspended in growth media and re-seeded.

### 2.8.8 *Image acquisition & analysis of organoids*

Phase contrast images of organoid wells were obtained at days 10, 20, and 30 using EVOS FL Auto. Images were analyzed using ImageJ to quantify organoid number, area covered, as well as organoid-formation efficiency. Organoid-formation efficiency was defined as the ratio of the number of large colonies prior to passaging on day 20 and day 30 to the number of clones on day 10. The threshold area for total colonies on day 10 was set as $<2 \times 10^5$ µm$^2$ and for large colonies on day 30 as $>2 \times 10^5$ µm$^2$ (equivalent to 20 cells).

## 2.9 Statistical analysis

Descriptive data analysis was performed using Microsoft Excel. Comparison of means was carried out using GraphPad Prism 6.0. Following normality testing, the appropriate statistical test was carried out, as indicated in figures.

# Chapter 3

# RESULTS

## 3.1 K19 labels a CSC population in an APCmin model

The presence of CSCs in CRC as well as many other cancers has become apparent over the past years. Different populations of CSCs have been proposed in the literature based on the expression of different markers. The most well-known population has been defined as expressing Lgr5. However, it remains to be determined whether more than one CSC population exists in tumours. Our preliminary data indicated that K19 may label a CSC population. Therefore, to investigate whether K19 marks CSC population in a familial model of colorectal cancer, K19-CreERT;R26TdTomato;APCmin mice were used. In this model, the TdTomato gene is fused with a stop codon cassette that is floxed by two loxP sites and is downstream of the R26 promoter region. In the absence of Cre, the TdTomato gene is not transcribed due to the stop codon and K19-driven fluorescence is not evident. When tamoxifen is administered, Cre is transcribed from the K19 promoter and the recombination of the loxP sites takes place leading to the excision of STOP cassette, followed by robust TdTomato fluorescence in K19 cells. To visualize K19 lineage tracing in a familial model of colorectal cancer, these mice were crossed with the APCmin mice. APCmin mice spontaneously generate tumours due to loss of heterozygosity of the APC allele. The majority of these tumours are found in the small intestine, however a small proportion arise in the colon.

Tumours from 6-month old K19-CreERT;R26TdTomato;APCmin mice were analyzed for lineage tracing via histological analysis at 24 hours (n = 3) , 10 days (n = 2) and 4 weeks (n = 3) post-tamoxifen. The percentage of tumour area traced was calculated using ImageJ. In the small intestine, we found that a small proportion of tumour area was traced red 24 hours after administration of tamoxifen (2.913 ± 1.547). From 24 hours to 10 days post-tamoxifen, the red cell population expanded to encompass an average of 21.59 ± 2.143% of tumours, which was not significantly different compared to 4 weeks post-tamoxifen

(18.26 ± 3.903%) (Figure 15). This indicates that K19+ stem cells clonally expanded in established tumours, suggesting K19 may label a CSC population.

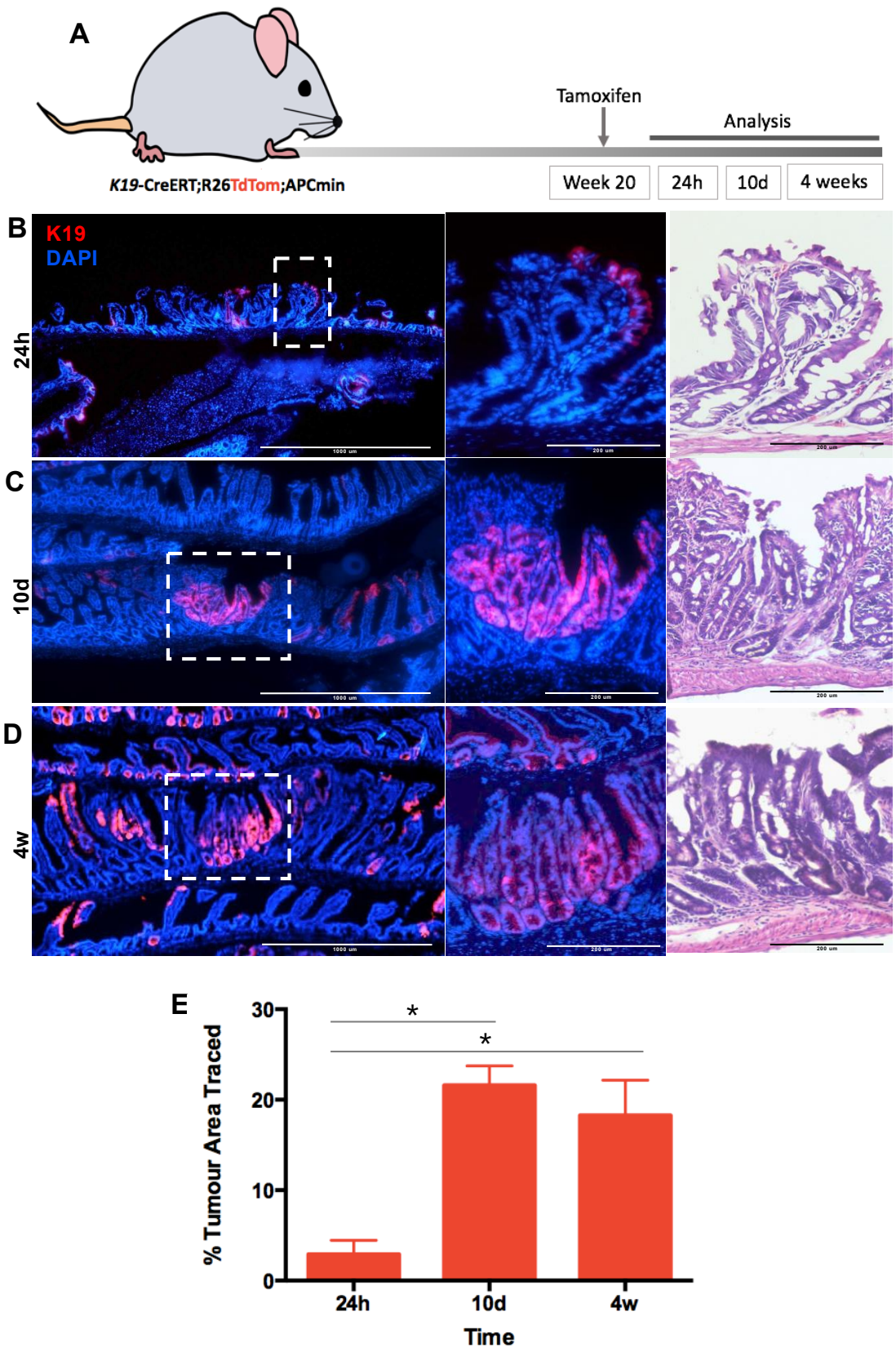
A
Tamoxifen
Analysis
K19-CreERT;R26TdTom;APCmin
Week 20
24h
10d
4 weeks
B
K19
DAPI
24h
C
10d
D
4w
E
% Tumour Area Traced
30
20
10
0
*
*
24h
10d
4w
Time

Figure 15 | **K19 labels a cancer stem cell population in the small intestine of APCmin mice**. Experimental protocol (A) used to analyze K19+ cells in adenomas from K19-CreERT;TdTomato;APCmin mice. Low power representative images of adenomas (Scale bars, 1000 μm) in the small intestine at 24h (B), 10d (C) and 4 weeks (D) post tamoxifen are shown. High power view of adenomas (Scale bars, 200 μm) in the small intestine are shown by immunofluorescence (left) and H&E (right). (E) Quantification of K19+ cells traced in adenomas as area over time. There was a significant increase in the area of tumour traced between 24h and 10d, while no significant was observed between 10d and 4w. Although significant between 24h and 10d, it is important to note that this comparison may have low power due to an n of 2 in the 10d group. Data is presented as mean ± SE; $n \geq 2$; analyzed by one-way ANOVA followed by Tukey's post hoc test for multiple comparisons; * $p < 0.05$.

## 3.2 K19 may label a CSC population in an AOM DSS model

In order to address whether K19 labels a CSC population in a colitis-associated model of colorectal cancer, tumours from AOM/DSS treated K19-CreERT;TdTomato mice were analyzed for lineage tracing at 24 hours (n = 4) , 10 days (n = 4) and 4 weeks (n = 4) post-tamoxifen. At 24 hours post-tamoxifen, a small proportion of tumour area was traced red (2.034 ± 1.551%). However, the proportion of red cells did not significantly increase from 24 hours to 10 days (7.083 ± 2.692%) and 4 weeks (5.025 ± 4.085%) (Figure 16). These results show lack of clonal expansion in K19 cells in the AOM/DSS-derived tumours.

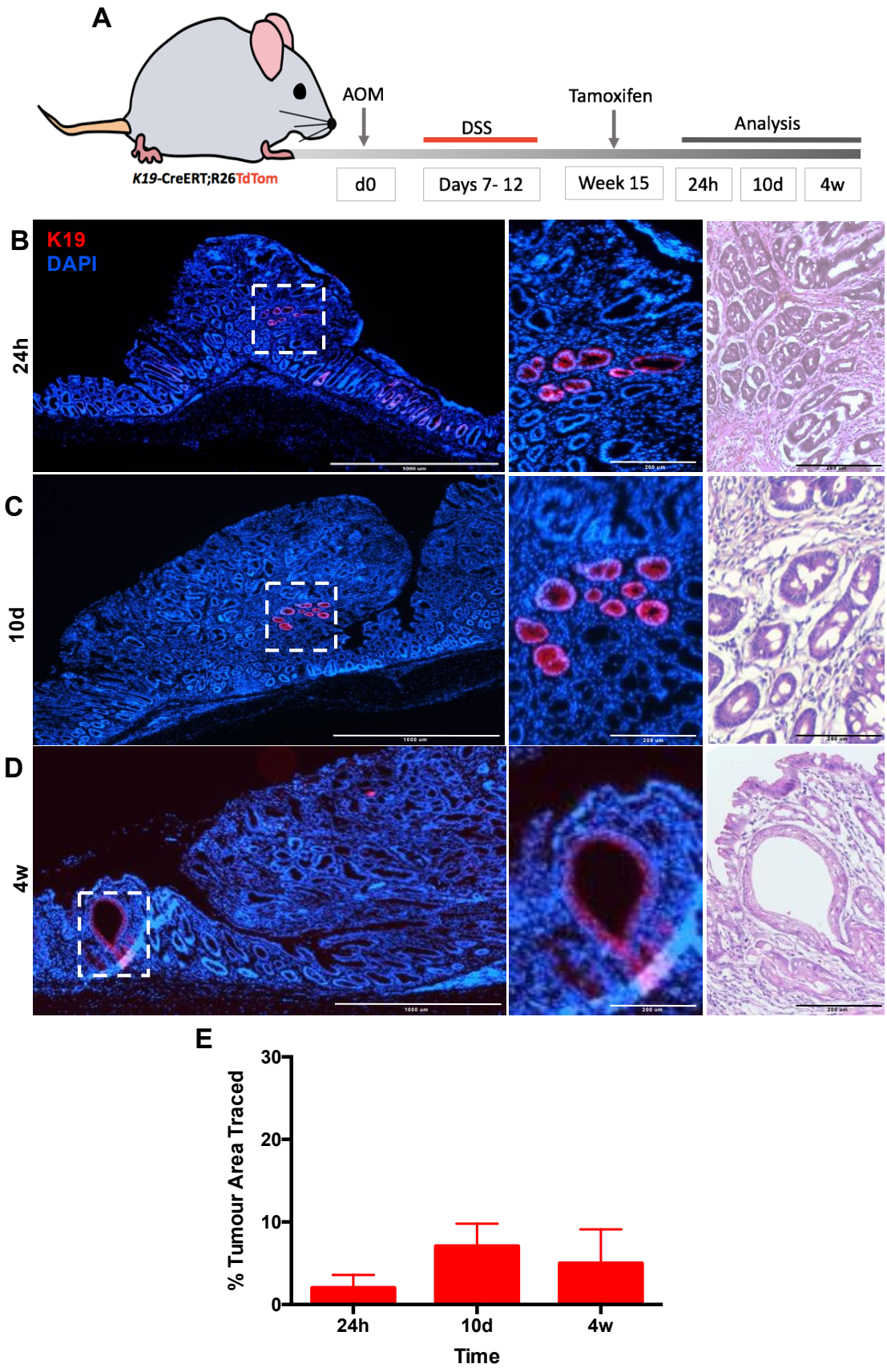
A
AOM
DSS
Tamoxifen
Analysis
K19-CreERT;R26TdTom
d0
Days 7- 12
Week 15
24h
10d
4w
B
K19
DAPI
24h
C
10d
D
4w
E
% Tumour Area Traced
30
20
10
0
24h
10d
4w
Time

Figure 16 | **K19 may label a CSC population in an AOM DSS model.** Experimental protocol (A) used to analyze K19+ cells in adenomas from AOM DSS treated K19-CreERT;TdTomato mice. Low power representative images of adenomas (Scale bars, 1000 μm) in the colon at 24h (B), 10d (C) and 4 weeks (D) post-tamoxifen are shown. High power view of adenomas (Scale bars, 200 μm) in the colon are shown by immunofluorescence (left) and H&E (right). (E) Quantification of K19+ cells traced in adenomas as % area over time. No significant increase in the area of tumour traced over time was observed. Data is presented as mean ± SE; n = 4 per group; analyzed by one-way ANOVA; * $p < 0.05$.

## 3.3 Ablation of Lgr5+ cells has no effect on tumour initiation or growth *in vivo*

### 3.3.1 *Diphtheria toxin dose characterization*

To confirm effective ablation of Lgr5+ cells in the intestine and colon of Lgr5-DTR-eGFP mice, 200 mL or 500ng of DT dissolved in 200 mL 0.9% saline was administered i.p. twice a week for two weeks (Figure 17; A). Twenty-four hours post administration of the last dose, tissues were prepared for histological analysis and analyzed for the presence of eGFP. As expected in the DT treated group, no eGFP (green) cells were present (Figure 17; B). This is compared to the saline treated group, where an abundance of eGFP (green cells) were found in the crypt base where Lgr5+ cells reside.

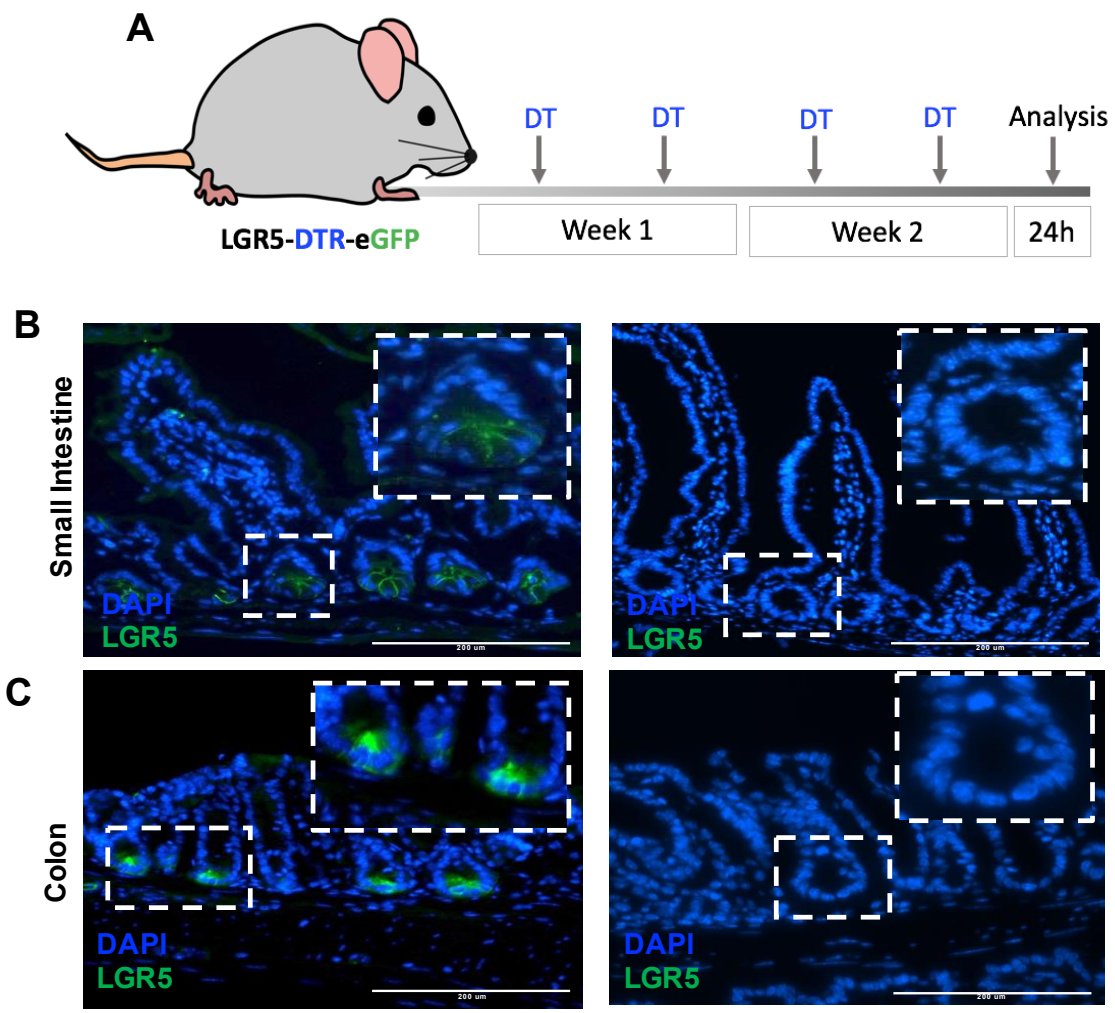


Figure 17 | **Diphtheria toxin dose characterization.** (A) Experimental protocol. (B) Low power representative immunofluorescence (Scale bars, 200 μm) of small intestine and (C) colonic crypts in control (left) versus DT treated (right) Lgr5-DTR-eGFP mice (insets 20x magnification). As expected with administration of DT, all Lgr5+ cells are ablated.

### 3.3.2 *Ablation of Lgr5+ cells has no effect on tumour initiation or growth in vivo*

To examine the effect of Lgr5+ cell ablation on tumour initiation and growth *in vivo*, AOM/DSS treated WT and Lgr5-DTR-eGFP mice were administered 500 ng of DT or saline i.p twice a week, 3-weeks after AOM and until the end of the experiment (20 weeks post-AOM) (Figure 18, A). Mice do not express the diphtheria toxin receptor (DTR) and, therefore, are not susceptible to diphtheria toxin (DT). Thus expression of DTR in a Lgr5 cell population allows for selective ablation of these cells upon DT administration. Cohorts of WT or Lgr5-DTR-eGFP experimental (DT treated) and control (saline treated) mice were compared (n > 10 per group) with respect to histology and tumour burden (number

and volume) at 20 weeks. As expected, histological analysis of adenomas from Lgr5 negative WT mice revealed no GFP expression (Figure 18, B and C), while adenomas of Lgr5 positive mice treated with saline had robust GFP signal (Figure 18, D). This is in contrast to Lgr5 positive mice treated with DT that did not express GFP (Figure 18, E). These results indicate that Lgr5 + cells were effectively ablated. Importantly, when tumour burden was analyzed, no significant differences were observed in tumour number (Figure 18, F) or tumour volume (Figure 18, G). This suggests that another CSC population besides Lgr5+ may contribute to tumour initiation and growth, as a complete loss of Lgr5+ cells has no effect on tumour burden.

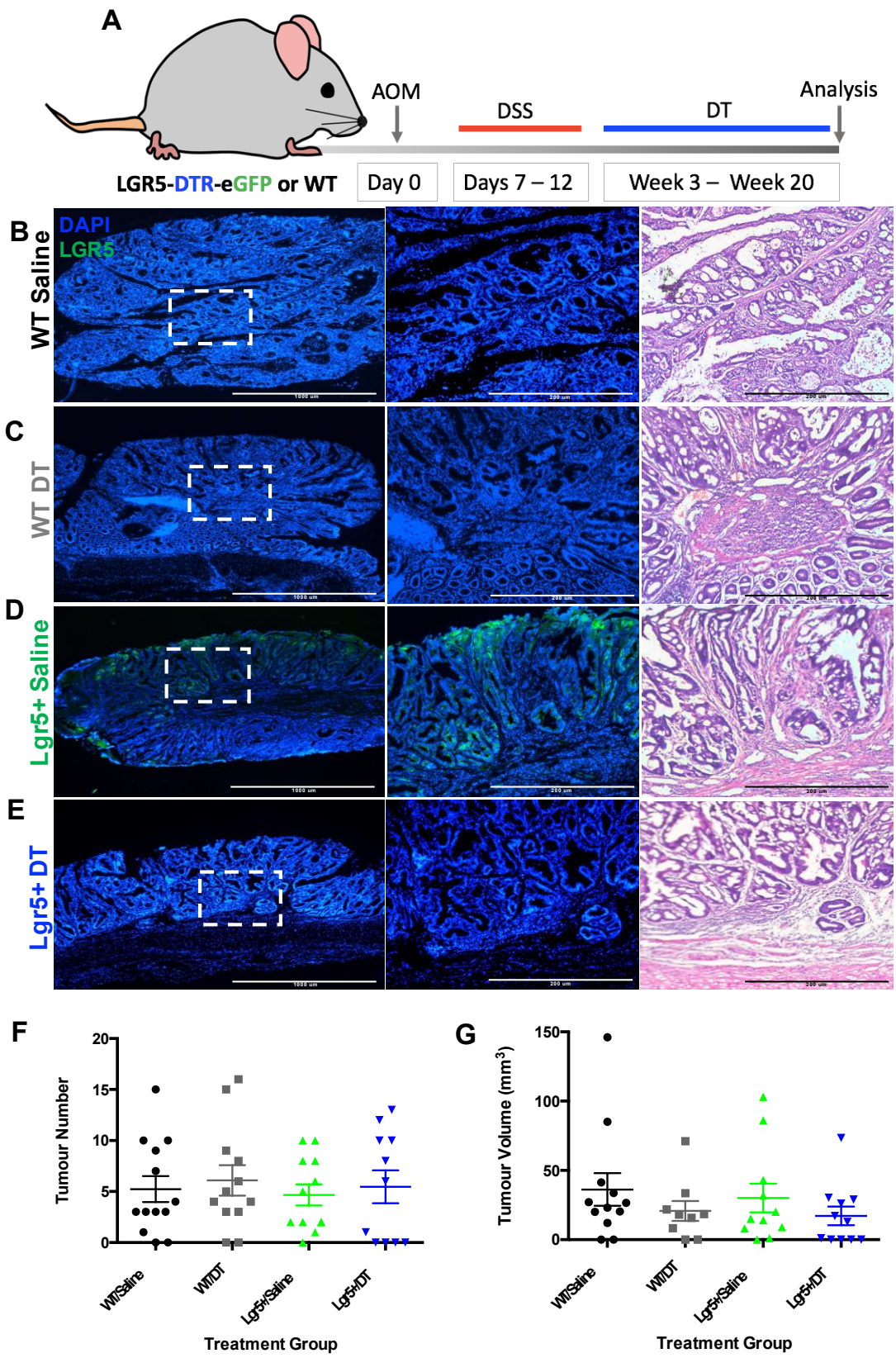
A
AOM
DSS
DT
Analysis
LGR5-DTR-eGFP or WT
Day 0
Days 7 – 12
Week 3 – Week 20
B
WT Saline
DAPI
LGR5
C
WT DT
D
Lgr5+ Saline
E
Lgr5+ DT
F
Tumour Number
20
15
10
5
0
WT/Saline
WT/DT
Lgr5+/Saline
Lgr5+/DT
Treatment Group
G
Tumour Volume (mm3)
150
100
50
0
WT/Saline
WT/DT
Lgr5+/Saline
Lgr5+/DT
Treatment Group

Figure 18 | **Ablation of Lgr5 cells has no effect on tumour initiation or growth.** (A) Experimental protocol. Low power representative immunofluorescence (Scale bars, 1000 μm) of colonic tumours from (B) WT/Saline, (C) WT DT, (D) Lgr5+/Saline and (E) Lgr5+/DT treated mice are shown. High power images (Scale bars, 200 μm) are shown by immunflourescence (left) and histology (right) for colonic tumours (F) The number of tumours and (G) tumour volume did not vary significantly between groups; $p > 0.05$. Results presented as mean ± SE; $n \geq 10$. One-way ANOVA was used for statistical analyses.

## 3.4 Intestinal and colonic K19+ APC floxed organoids give rise to spheroids

Asfaha et al. (2015) reported that when intestinal crypts from K19-CreERT;APCf/f mice were cultured following tamoxifen administration, recombined APC floxed organoids appeared as spherical structures, which were easily distinguishable morphologically from normal budding crypt structures. However, it was unclear whether *colonic* APC floxed crypts cultured from K19-CreERT;APCf/f mice would give rise to spheroids *in vitro*. To investigate this, intestinal and colonic crypts from K19-CreERT;APCf/f mice were cultured 48 hours after tamoxifen administration (Figure 19, A). As expected intestinal crypts contained APC floxed K19+ cells gave rise to spheroid structures that were easily distinguished from normal wild-type budding crypt structures (Figure 19, B). Similarly, colonic crypts from recombined APC floxed K19+ cells appeared as spheroid structures, which were also easily distinguishable morphologically from normal budding crypt structures (Figure 19, C). Moreover, K19+ cells in which APC was floxed produced organoids that could be maintained in culture even in the absence of R-spondin (Figure 20/21).

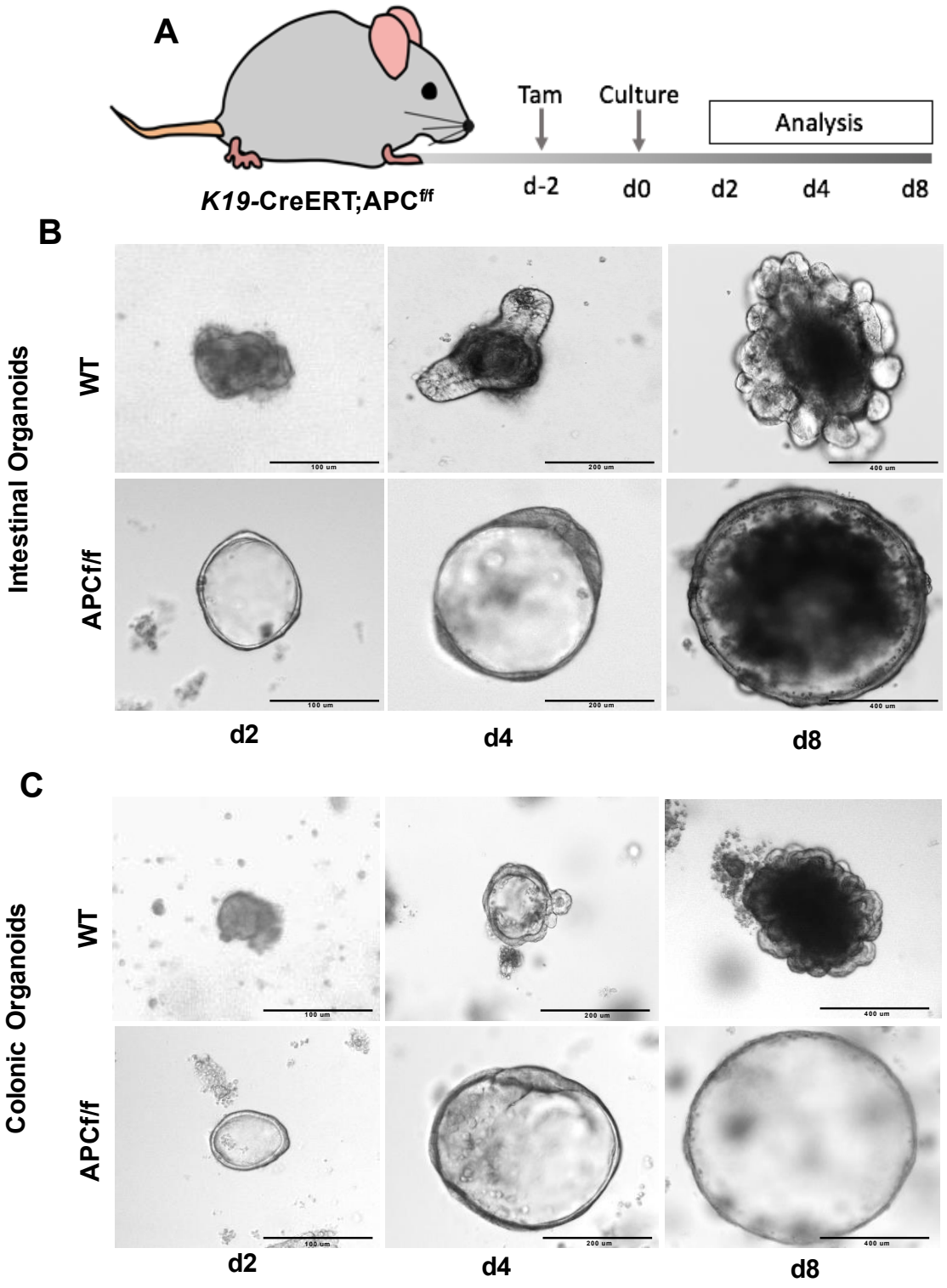


Figure 19 | **Intestinal and colonic K19+ floxed organoids give rise to spheroids.** (A) Experimental protocol. (B) Representative phase contrast images of intestinal and colonic (C) crypts cultured from K19-CreERT;APCf/f mice 48 hours after tamoxifen. Note Wild

Type (WT) organoids display a budding morphology while APCf/f organoids form spheroids. Scale bars, day two (100 μm), day four (200 μm) and day eight (400 μm).

## 3.5 Ablation of Lgr5+ cells has no effect on intestinal or colonic spheroid growth

To determine the effect of Lgr5+ cell ablation on tumour growth in established K19 tumours *in vitro*, Lgr5-DTR-eGFP mice were crossed to K19-CreERT;APCf/f mice to generate Lgr5-DTR-eGFP;K19-CreERT;APCf/f (L5DKA) mice. Briefly, treatment of these L5DKA mice with tamoxifen induces a loss of APC specifically in K19 cells and allows for ablation of Lgr5+ cells with DT administration. Our lab previously demonstrated that following tamoxifen treatment, intestinal cells cultured from L5DKA mice give rise to spherical "tumour" organoids *in vitro* in 48 hours. To determine the effects of Lgr5+ cell ablation on K19 spheroids, both intestinal and colonic crypts from tamoxifen treated L5DKA mice were cultured to monitor their growth and spheroid forming capacity with administration of DT. The organoids generated were treated with 20 ng/mL of DT (experimental) or vehicle (control) from d10 to d30. Additionally, a subset of spheroids was treated with DT from d10 to d20 and vehicle from d20 to d30 (Figure 20, A). Subsequently, the total number of spheroids, spheroid area and spheroid formation capacity were analyzed over time for small intestine and colonic spheroids. In the small intestine and colon, there was no significant difference ($p > 0.05$) in the total number of spheroids, tumour area or organoid forming efficiency between control, DT or DT removed groups at D10, D20 or D30 (Figure 20 and 21, C, D, E). Interestingly, there also was no change in tumour area between all groups ($p > 0.05$) (Figure 20 and 21 D).

As a control, intestinal and colonic crypts from tamoxifen-treated K19-CreERT;APCf/f mice were cultured at the same time as L5DKA mice using the same protocol to monitor their growth and spheroid forming capacity with administration of DT or vehicle. My results show no significant difference ($p > 0.05$) in the total number of spheroids, tumour area or organoid forming efficiency between control, DT or DT removed groups at D10, D20 or D30 (Figure 22 and 23, C, D, E). This demonstrates the DT administration itself

has no effect on intestinal or colonic spheroids, providing further support to the findings in Figure 20.

These results highlight that with a complete loss of Lgr5+ cells in K19+ APC floxed intestinal and colonic spheroids, there is no effect on tumour number, growth, or organoid forming efficiency. This suggests that another CSC population besides Lgr5+ CSC may establish intestinal and colonic tumours and contribute to tumour growth. Moreover, organoid-forming efficiency reflects the surviving fraction of stem cells among crypt cells as organoids are derived from stem cells. Therefore, despite continuous ablation of Lgr5+ CSCs (even after passaging), another CSC population must exist in intestinal and colonic tumours, that allows spheroids to establish themselves. Taken together, these results suggest that K19+ APC floxed spheroids are composed of a heterogeneous population whereby Lgr5 may be dispensable.

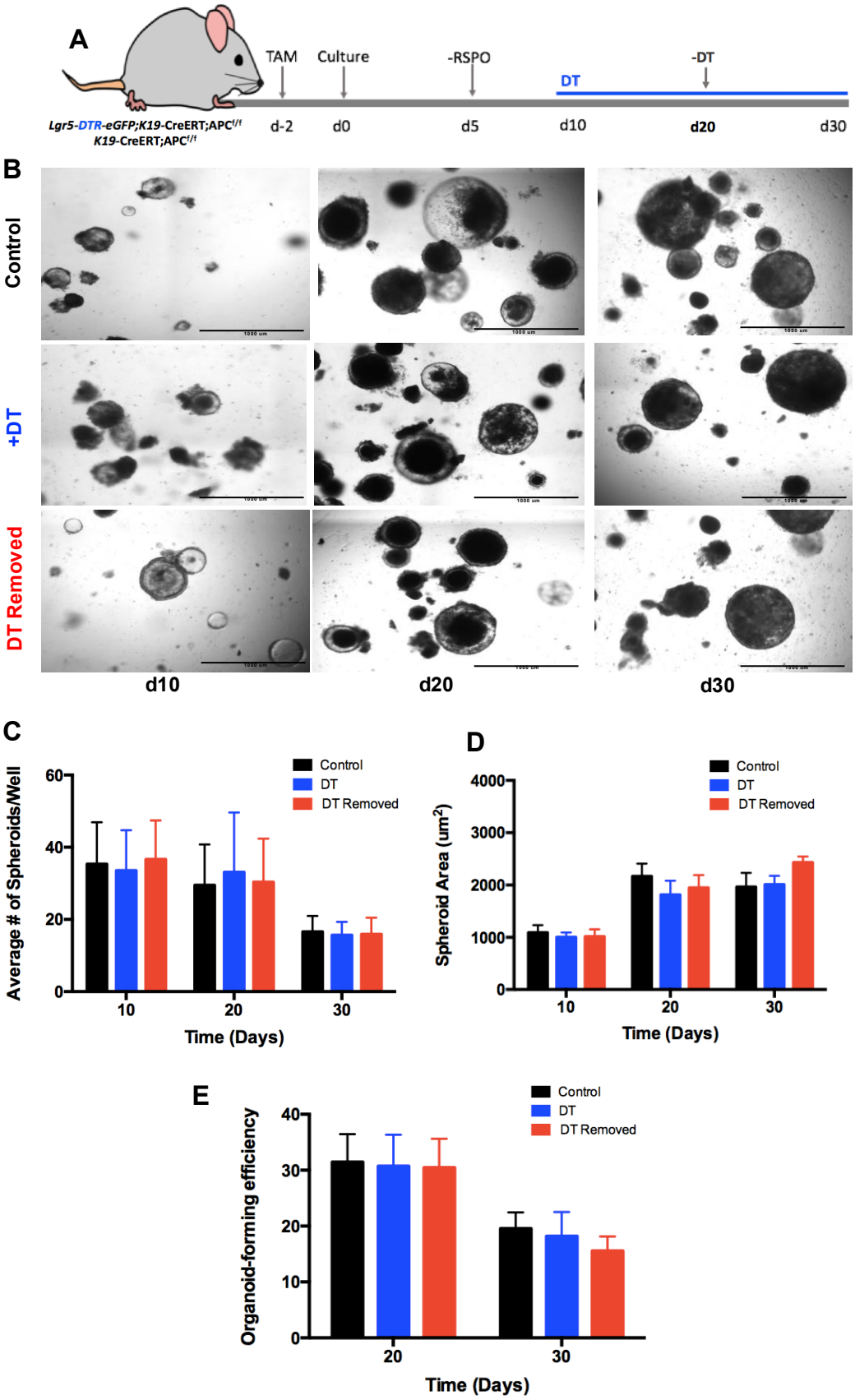
A
TAM
Culture
-RSPO
DT
-DT
Lgr5-DTR-eGFP;K19-CreERT;APC f/f
K19-CreERT;APC f/f
d-2
d0
d5
d10
d20
d30
B
Control
+DT
DT Removed
d10
d20
d30
C
Average # of Spheroids/Well
Control
DT
DT Removed
Time (Days)
D
Spheroid Area (um2)
Control
DT
DT Removed
Time (Days)
E
Organoid-forming efficiency
Control
DT
DT Removed
Time (Days)

Figure 20 | **Ablation of Lgr5 cells has no effect on small intestine spheroid growth.** (A) Experimental protocol. (B) Representative phase contrast images of organoid cultures (scale bars, 1000 μm). (C) Quantification of the number of spheroids, spheroid area (D), and spheroid forming efficiency (E). No significant differences were observed between treatment groups. Results presented as mean ± SE; n = 3. A two-way ANOVA followed by Tukey's post-hoc test for multiple comparisons was used for statistical analyses.

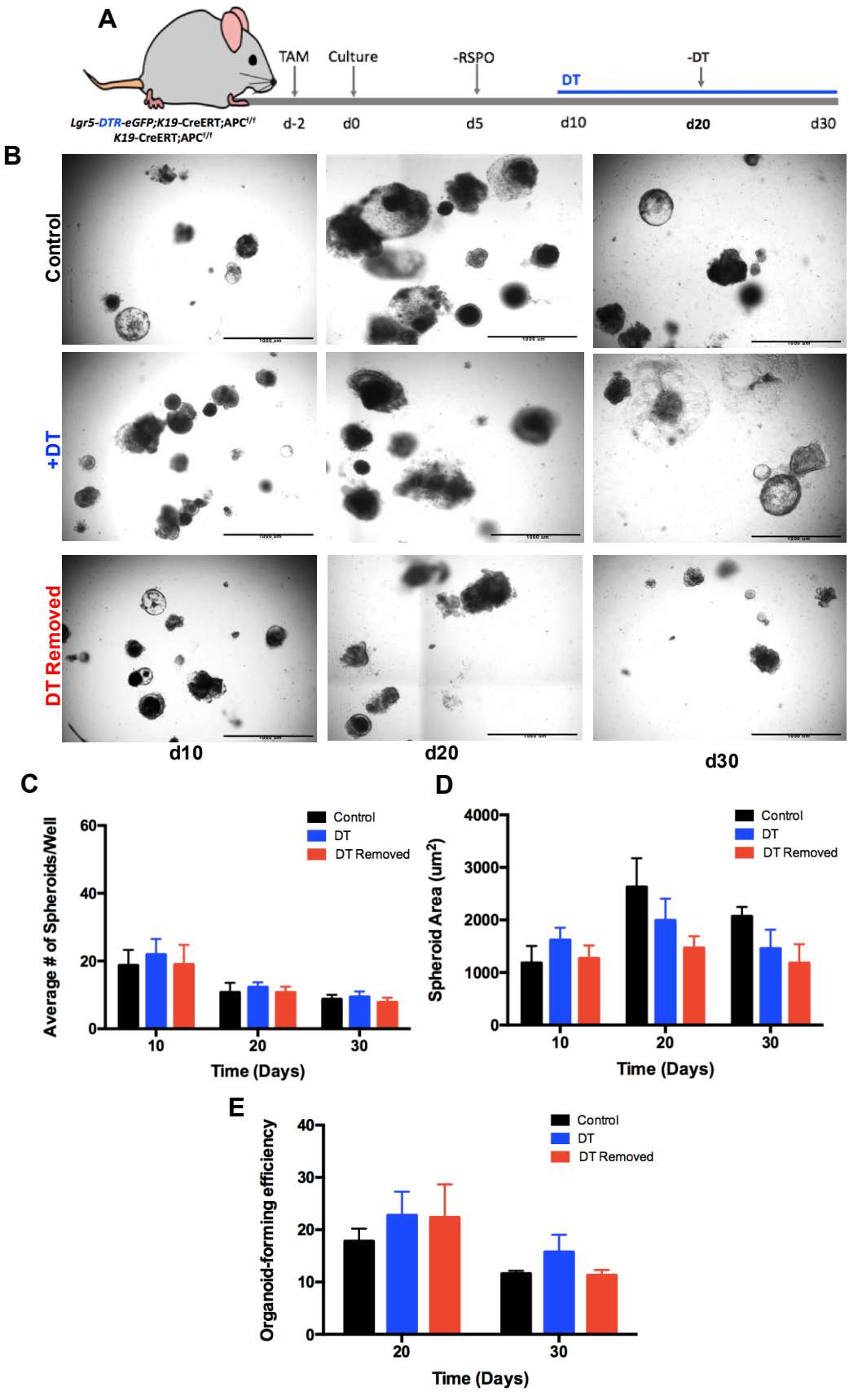
A
TAM
Culture
-RSPO
DT
-DT
Lgr5-DTR-eGFP;K19-CreERT;APC f/f
K19-CreERT;APC f/f
d-2
d0
d5
d10
d20
d30
B
Control
+DT
DT Removed
d10
d20
d30
C
Average # of Spheroids/Well
Control
DT
DT Removed
Time (Days)
D
Spheroid Area (um2)
Control
DT
DT Removed
Time (Days)
E
Organoid-forming efficiency
Control
DT
DT Removed
Time (Days)

Figure 21 | **Ablation of Lgr5 cells has no effect on colonic spheroid growth.** (A) Experimental protocol. (B) Representative phase contrast images (scale bars, 1000 μm) of organoid cultures. (C) Quantification of the number of spheroids, spheroid area (D), and spheroid formation efficiency (E). Results presented as mean ± standard error of the mean; n = 3. No significant differences were observed between treatment groups. A two-way ANOVA followed by Tukey's post-hoc test for multiple comparisons was used for statistical analyses.

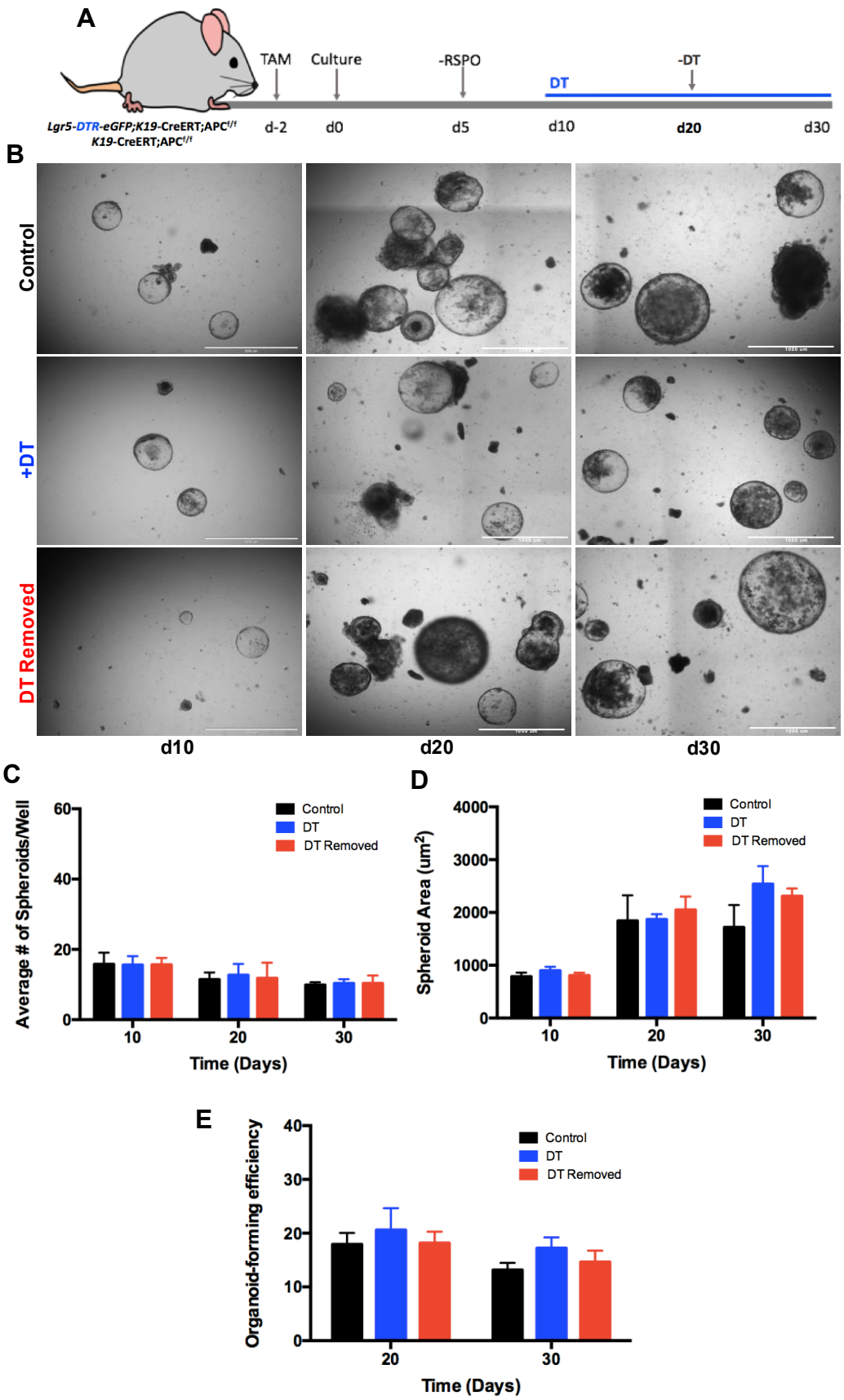
A
TAM
Culture
-RSPO
DT
-DT
Lgr5-DTR-eGFP;K19-CreERT;APC f/f
K19-CreERT;APC f/f
d-2
d0
d5
d10
d20
d30
B
Control
+DT
DT Removed
d10
d20
d30
C
Average # of Spheroids/Well
Control
DT
DT Removed
Time (Days)
D
Spheroid Area (um2)
Control
DT
DT Removed
Time (Days)
E
Organoid-forming efficiency
Control
DT
DT Removed
Time (Days)

Figure 22 | **Diphtheria toxin has no effect on WT small intestine spheroids.** (A) Experimental protocol. (B) Representative images of organoid cultures (scale bars, 1000 μm). (C) Quantification of the number of spheroids, spheroid area (D), and spheroid formation efficiency (E). Results presented as mean ± standard error of the mean; n = 3. No significant differences were observed between treatment groups. A two-way ANOVA followed by Tukey's post-hoc test for multiple comparisons was used for statistical analyses.

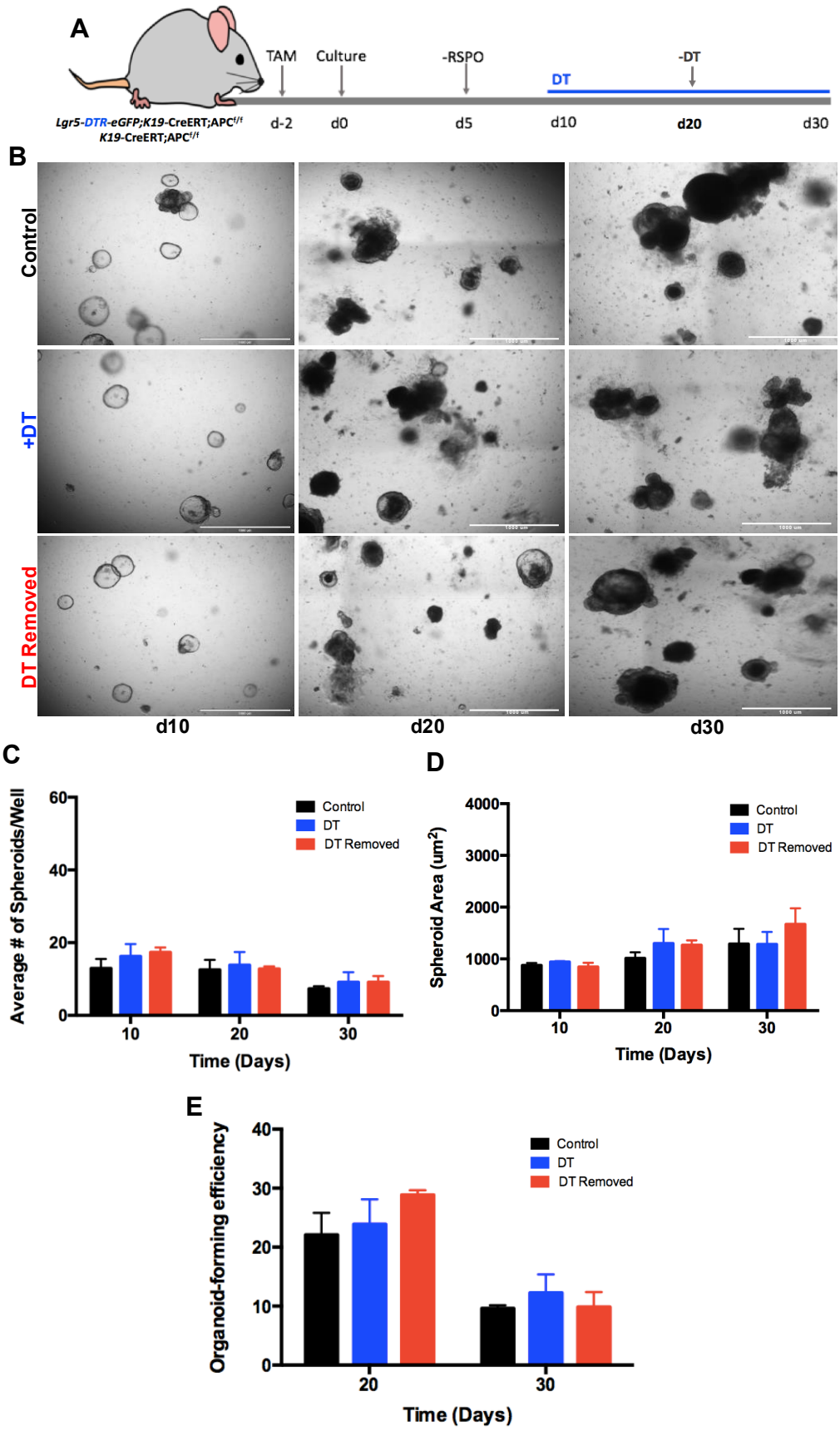
A
TAM
Culture
-RSPO
DT
-DT
Lgr5-DTR-eGFP;K19-CreERT;APC f/f
K19-CreERT;APC f/f
d-2
d0
d5
d10
d20
d30
B
Control
+DT
DT Removed
d10
d20
d30
C
Average # of Spheroids/Well
Control
DT
DT Removed
Time (Days)
D
Spheroid Area (um2)
Control
DT
DT Removed
Time (Days)
E
Organoid-forming efficiency
Control
DT
DT Removed
Time (Days)

Figure 23 | **Diphtheria toxin has no effect on WT colonic spheroids**. (A) Experimental protocol. (B) Representative images of organoid cultures (scale bars, 1000 μm). (C) Quantification of the number of spheroids, spheroid area (D), and spheroid formation efficiency (E). Results presented as mean ± standard error of the mean; n = 3. No significant differences were observed between treatment groups. A two-way ANOVA followed by Tukey's post-hoc test for multiple comparisons was used for statistical analyses.

# Chapter 4

# DISCUSSION

The purpose of this thesis was to determine if the colorectal cancer stem cell pool encompasses different stem cell phenotypes, much like the normal intestinal epithelium. To identify additional CSCs, I analyzed genetic lineage tracing from K19+ cells *in vivo* in multiple mouse models of CRC. To provide further evidence for the presence of multiple cell types, my experiments were followed by ablation of a known CSCs (marked by Lgr5 expression) in established tumours *in vivo* and *in vitro*. My rationale for this approach was based on accumulating evidence which implicated the role of multiple CSCs in CRC, as well as our lab's preliminary findings that K19 may label a CSC population (unpublished studies). My findings support my initial hypothesis that K19 identifies a CSC population distinct from the previously identified Lgr5+ CSCs. Although further studies are necessary to determine whether K19 is essential for tumour growth, data presented here provides insight into the seemingly diverse CSC pool present in CRC tumours.

## 4.1 K19 labels a CSC population in an APCmin model

Previous data from our lab identified K19 as a stem cell marker in the small intestine and colon, distinct from Lgr5+ cells that can give rise to tumours (Asfaha et al. 2015). Moreover, K19 is amplified in solid tumours making it an ideal candidate CSC marker (Lapouge et al., 2011). As such, I hypothesized that K19 would label a CSC population in a mouse model of FAP-CRC. Genetic lineage tracing was used to evaluate CSC potential (i.e. the ability to self-renew and differentiate) to circumvent the drawbacks of traditional serial transplantation assays.

To determine whether K19 labels a CSC population, I analyzed the percentage of intestinal and colonic tumour area traced over time in K19-CreERT;R26TdTomato;APCmin mice. In the small intestine, I found that a small tumour area (2%) was traced red at 24 hours after tamoxifen administration, indicating that it was derived from the labeled K19 cells. Interestingly, this clonal population expanded significantly to make up approximately 20% of tumours by day 10. No further increases were noted at 4 weeks. These set of results

indicate that single traced clones are capable of giving rise to cell lineages that are labeled long-term. Long-term labeling is suggestive of self-renewal, given the highly proliferative nature of tumours. As is the case with Lgr5+ CSCs, sorted K19+ intestinal tumour cells have not been studied in a serial transplantation assay to determine self-renewal or tumourigenic capacity. It should be noted that applicability of serial transplantation assays to solid tumours is controversial. The appearance of Paneth cells in traced lineages suggests the ability of K19 CSCs to differentiate. However, immunohistochemical staining to confirm the presence of Paneth cells or other differentiated lineages has not been carried out. Regardless, the ability of K19 to form single traced clones capable of giving rise to cell lineages (that appear to contain Paneth cells with eosinophilic granules in histological sections) and are labeled long term suggests multipotency and self-renewal. Consequently, my findings represent the first study to identify K19 as a marker for CSCs in intestinal tumours of APCmin mice.

Interestingly, an elegant study conducted by de Sousa e Melo et al demonstrated that Lgr5+ ablation restricts primary tumour growth but does not result in tumour regression (de Sousa e Melo et al., 2017). The authors go on to propose that tumours may be maintained by an Lgr5 negative population capable of replenishing the Lgr5+ CSC pool, which leads to rapid initiation of tumour growth upon removal of treatment (de Sousa e Melo et al., 2017). This is similar to what has been observed in the normal intestine, where homeostasis is maintained by reserve stem cell populations if Lgr5 cells are lost. In contrast to primary lesions, they found that Lgr5 plays a critical role in the development of metastasis as little evidence of metastatic lesions was found post Lgr5 ablation (de Sousa e Melo et al., 2017). Together, this data highlights that different CSC populations may play different roles in primary versus metastatic tumour growth or even across different stages of CRC. Moreover, when taking into consideration that K19 labels a CSC population in the APCmin model, our data provides support that K19 labels a CSC population in primary tumour sites. The APCmin mouse model does not metastasize and is most representative of early stage CRCs. Of note, the model used in the study by de Sousa e Melo et al contained mutations in APC as well as KRAS. However, it would be highly relevant and interesting for future studies to investigate the role of K19 and Lgr5 at different stages of CRC progression.

Additionally, future studies should investigate whether K19 is essential in primary tumours through genetic ablation studies.

## 4.2 K19 may label a CSC population in the AOM/DSS model of CRC

To investigate whether K19 labels a CSC population in a colitis-associated model of CRC, I analyzed genetic lineage tracing from K19-CreERT;R26TdTomato mice treated with AOM/DSS at various time points post-tamoxifen administration. I hypothesized that K19 would label a CSC population in this model and that K19+ cell-derived clones would expand and persist in tumours. Initially, I observed a small population of clones in the tumours. However, the clones did not expand to give rise to more differentiated cell types over time but persisted. These results were not expected. There are several possible explanations for this observation as the CSC phenotype is likely influenced by a variety of factors, including the tissue microenvironment, and the accumulation of mutations at various progressive stages. A study conducted by de Sousa e Melo et al. demonstrated that Lgr5 labelled CSCs are influenced by both tissue location and tumour microenvironment (de Sousa e Melo et al., 2017). Contrary to their initial expectations, ablation of Lgr5 CSCs in primary tumours did not lead to tumour regression. However, they did find that Lgr5 cells play a role in the establishment of liver metastasis. The authors suggested that different "biological cues" mediated CSCs in primary and metastatic sites leading to proliferation of certain CSC populations. In accordance with this study and the results I obtained using the K19 APCmin model, K19 may play a more important role in the earlier stages of CRC. A key distinction between my studies and that by de Sousa e Melo et al. as well as other is that only APC is mutated in the APCmin model compared to β-catenin as well as KRAS alterations in in the AOM DSS models (Takahashi and Wakabayashi, 2004). These studies highlight the importance of the tumour microenvironment (inflammation, primary vs metastatic sites) and genetic mutations (for example, APC vs APC/KRAS) in contributing to the CSC phenotype observed.

## 4.3 Ablation of Lgr5+ cells has no effect on tumour initiation or growth

Previous research has suggested that the CSC pool likely encompasses different cell phenotypes in a dynamic equilibrium with each other and that elimination of Lgr5+ CSCs might disrupt tumour biology to alter tumour growth but not eradicate disease. These findings, in combination with my results from sections 3.1, prompted me to examine the effects of Lgr5+ CSC ablation on tumour initiation and growth in an AOM DSS model. I hypothesized that ablation of Lgr5 cells would have no effect on tumour initiation or growth. Previously, it was shown that short-term administration of high doses of diphtheria toxin was associated with liver toxicity and subsequent lethality in 10 days (Asfaha et al., 2015). Therefore, it was necessary to first establish a protocol that effectively ablated Lgr5 cells at a lower dose for long-term use. Subsequently, I found that 500 ng of DT administered twice a week effectively ablated Lgr5 cells. This was indicated by the presence of Lgr5-GFP+ cells in the vehicle-treated group versus no Lgr5-GFP+ cells in the DT-treated group (Figure 17). Moreover, no detrimental effect on intestinal or animal viability was observed and ensuing long term experiments on the effects of Lgr5 ablation throughout tumour initiation and growth were conducted.

In support of my hypothesis, I found that Lgr5+ CSCs are dispensable for tumour initiation as well as maintenance. Furthermore, efficiency of ablation was confirmed through analysis of histological sections post-ablation. I observed Lgr5-GFP+ cells in vehicle-treated Lgr5-DTR-eGFP mice, while no Lgr5-GFP+ cells were observed in Lgr5-DTR-eGFP mice treated with DT or untreated controls. The results from this study demonstrate for the first time that more than one CSC population functionally contributes to tumour initiation and growth in a colitis-associated model of CRC. Similarly, these findings are also supported by two recent studies by independent groups that demonstrated little effect on tumours following ablation of Lgr5 cells. In one study de Sousa e Melo et al., showed that ablation of Lgr5 in primary tumours had no effect on tumour growth suggesting an Lgr5 negative population is capable maintaining tumour growth (de Sousa e Melo et al., 2017). In another study, it was shown that Lgr5 ablation was only effective temporarily (Shimokawa et al., 2017). Furthermore, targeted ablation of Lgr5+ cells using an Lgr5 antibody directed chemotherapeutic in the APCmin mouse model had no effect on tumour

burden (Junttila et al., 2015). These studies in combination with my findings demonstrate that in some tumour models, the CSC pool encompasses different cell phenotypes.

Unlike the present study, previous studies investigating the ablation of Lgr5 in tumour models did not focus on tumour initiation or utilize immunocompetent mice. As discussed earlier, the tumour microenvironment plays an important role in regulating CSC function. This is of the utmost importance when considering the phenotype of CSCs, particularly in colitis-associated cancer - as the immune system plays a critical role in regulation of the tissue microenvironment. It is important to note, that animal models do not recapitulate all types of human colorectal cancer and these results do not recapitulate the results that might occur at different stages of CRC. As such, the results obtained in this study are likely reflective of this particular model.

## 4.4 Intestinal and colonic K19+ APC floxed organoids give rise to spheroids

In 2009, Sato et al. demonstrated that single Lgr5-eGFP+ CBC cells isolated using FACS and plated in a Matrigel-based three-dimensional culture system gave rise to self-renewing epithelial organoids (Sato et al., 2009). This method was a monumental breakthrough in the field of intestinal stem cells. Later on, it was adapted to culture Lgr5+ CBC that contained a mutation in the APC gene. Interestingly, loss of APC function in Lgr5 cells gave rise to organoids that had a cystic morphology, compared to the normal budding structure. It was later determined that these organoids were representative of early stage colorectal cancers. Subsequently, the culture protocol was modified, allowing for the addition of several mutations found in later stages of colorectal cancer, as well as the eventual culture of human colorectal tumours (Sato et al., 2011; Shimokawa et al., 2017). Since 2009, multiple “tumour organoid” models have been adapted from this initial protocol.

In particular, Asfaha et al. adapted the Sato protocol to establish a tumour organoid protocol derived from intestinal crypts of K19-CreERT;APCf/f mice. Treatment of these mice with tamoxifen induced loss of APC specifically in K19+ cells, and intestinal crypts

cultured from these mice gave rise to tumour spheroids *in vitro* after 48 hours (Asfaha et al., 2015). However, it remained unclear whether colonic crypts from these mice would give rise to colonic tumour spheroids. Based on the expression of K19+ ISCs in both the normal and intestinal and colonic crypt, I hypothesized that loss of APC in colonic K19 cells would give rise to colonic tumour spheroids, similar to the small intestine. My results showed that when colonic intestinal crypts were cultured two days after *in vivo* tamoxifen administration, large cystic structures appeared. The same phenomenon was observed in intestinal crypts that were cultured identically. As described previously, APC floxed organoids are easily distinguishable from non-recombined crypts that form normal budding structures (as shown in Figure 19). Of note, K19+ APC floxed organoids are maintained in the absence of R-spondin. In normal, non-mutated organoids, R-spondin is required for amplification of Wnt signalling and organoid survival. Accordingly, when R-spondin was removed (Figures 20 and 21) from both intestinal and colonic organoids, only APCf/f spheroids survived. Thus indicating that both colonic and intestinal tumour spheroids were derived from K19-CreERT;APCf/f crypts. It is important to note, however, that nuclear co-localization of β-catenin has not been validated in this model. Despite this limitation, selection of tumour organoids with R-spondin provides functional evidence of APC loss of function.

## 4.5 Ablation of Lgr5+ cells has no effect on intestinal or colonic spheroids

As mentioned in section 4.3, previous research has suggested that the CSC pool likely encompasses a dynamic cell population as elimination of Lgr5+ CSCs in some CRC models has limited effects. My results in a colitis-associated model of CRC are supportive of this notion. However, it remains unknown whether Lgr5 CSCs are dispensable in established tumours representative of early stages of CRC, and unrelated to inflammation. As such, I hypothesized that loss of Lgr5 in established APCf/f tumours (model of early stage CRC) would have no effect on spheroid number, growth or formation efficiency. I crossed K19-CreERT;APCf/f mice to Lgr5-DTR-eGFP mice to generate an Lgr5-DTR-eGFP;K19-CreERT;APCf/f model. As mentioned in the previous section, when intestinal

and colonic crypts are cultured after tamoxifen treatment, cystic tumour organoids form due to the loss of APC in K19+ cells. Additionally, the presence of Lgr5-DTR-eGFP allows for the conditional and specific ablation of Lgr5 cells in established K19+ cell derived APCf/f tumours. Therefore, I treated organoid cultures with DT once tumour organoids were established for 10 days. Following the 10 days, DT was removed from a subset of organoids to determine the effects on growth and stem cell activity. As a control, K19-CreERT;APCf/f mice were cultured at the same time to ensure DT alone did not have an effect on tumour number, organoid area or spheroid formation efficiency. My results show that ablation of Lgr5 cells in intestinal and colonic tumour spheroids had no effect on the number, area or spheroid formation efficiency between control and DT groups across all time points (Figure 20, 21). Importantly, no effect on spheroid number and area indicates that an Lgr5- cell population is contributing to spheroid growth and Lgr5 cells are dispensable in this model. This highlights that another CSC population must reside in these spheroids that allows continuous establishment despite constant ablation of Lgr5+ cells even after passaging. This is consistent with my findings presented in section 3.3.2. Additionally, my results from section 3.1, highlight that in an APCmin model, where only APC is mutated, K19 labels a CSC population, thereby corroborating the existence of another CSC population in the early stages of CRC. Future studies should directly examine K19 lineage tracing in addition to Lgr5 ablation with an APCmin or APCf/f model to conclusively determine this.

Unexpectedly, there was no difference between all groups when DT was removed from a subset of spheroids. This is in contrast to the findings of de Sousa e Melo et al., in which discontinuation of DT mediated Lgr5 ablation led to rapid tumour organoid regrowth (de Sousa e Melo et al., 2017). Importantly, this is likely due to differences in experimental models. Our model is reflective of the early stages of CRC, in which only APC is mutated. In contrast, their model is representative of later stages of CRC and included mutations in the KRAS, p53 and SMAD pathways. These results suggest K19 may be an important target in prevention or treatment of earlier stages of CRC. Although unlikely, another potential explanation is that the dose of DT used did not sufficiently ablate Lgr5+ cells. As such, future studies should confirm ablation of Lgr5+ cells possibly by

immunohistochemical or mRNA analysis of DT-treated vs control organoids. It is important to note, however, that the dose of DT used in my study (20 ng) was determined to effectively ablate Lgr5 CBC cells in intestinal organoids by mRNA analysis (Asfaha et al., 2015). Interestingly, in this published study, mRNA analysis also revealed an increase in K19 mRNA expression upon DT mediated ablation of Lgr5. This suggests that the same phenomenon may be occurring in established APCf/f spheroids *in vitro*, although, this needs further verification. Lastly, no differences were observed between control, DT, or DT removed groups in intestinal and colonic spheroids derived from Lgr5-DTR-eGFP negative K19;APCf/f controls (Figure 22, 23). This suggests that administration of DT alone has no effect on spheroid number, growth or formation efficiency. Taken together, these findings provide evidence that more than one CSC population exists in an early CRC model. This highlights that in some models, the CSC population represents a dynamic cell population in delicate equilibrium.

## 4.6 Implications and future directions

The studies outlined here advance our understanding of cancer biology in two very meaningful ways: (1) I determined that the CSC pool encompasses a variety of cell phenotypes; and (2) I determined the relative contributions of these populations to tumour growth by ablating a known CSC population. These two concepts have important implications for the design of anti-tumour therapies. On the one hand, drugs targeted at malignant sub-populations with CSC properties may have important therapeutic effects. However, these effects may vary depending on how permissive the host tissue is to dynamic interconversion between CSC phenotypes and functional differences that may exist between CSC populations. Therefore, drugs or radiation aimed too narrowly at only one CSC phenotype might translate to only transient, short-lived clinical benefits and eventually fail to cure patients. Although these concepts increase the level of complexity for developing new cancer treatments, my research may lead to an improved understanding of the systems that governs the growth, multi- lineage differentiation, dynamic turnover and regenerative response to tumour tissues. Our lab has developed unique transgenic mouse models that are clinically relevant because they are immunocompetent and allow us

to selectively kill a known cancer stem cell *in vivo*. Moreover, my findings suggest that a diverse population of CSCs exist in early and colitis-associated colorectal cancer mouse models. This may suggest that CSCs are governed by the tumour microenvironment or genetic mutations. Consequently, this improved understanding of CSCs will help define new molecular targets for different phenotypic subgroups of CSCs or block the sources of CSCs simultaneously to achieve complete elimination of cancer.

Despite the insights into colorectal cancer CSCs in this thesis, several questions could not be directly answered. Importantly, although it was demonstrated that K19 labels a cancer stem cell population in the APCmin model, it remains unknown whether K19 is essential for tumour growth or whether K19 is influenced by the tumour microenvironment directly. These questions could be answered through genetic ablation studies of K19 and manipulation of the tumour microenvironment through *in vitro* studies. Additionally, the question of whether K19 CSCs drive chemotherapy or radiation resistance could not be answered in this thesis. Future experiments evaluating the tumorigenicity of K19 in different CRC models could provide more evidence to answer this question.

The results in this thesis warrant further exploration and direct comparison of different CSC phenotypes observed in various CRC models as well as stages of progression. This would help to determine essential therapeutic targets as well as the relative contributions of each population to therapy resistance, metastasis and patient survival. Therefore, future experiments should focus on the identification, evaluation and comparison of verified CSC populations to answer this question.

## 4.7 Limitations

The first aim of this thesis was to determine if K19 labels a cancer stem cell population. A potential limitation of aim one is the confirmation of CSC multipotency in lineage tracing models of CRC. While my initial lineage tracing experiments revealed that K19 labels a CSC population in the APCmin model, possibly capable of giving rise to Paneth cells, further experiments are necessary to determine multipotency. In this sense, immunohistochemical analysis of differentiated cell markers (e.g. lysozyme) in tumours

would complement these studies. Likewise, throughout this thesis, genetic lineage tracing analysis was used to determine stemness. However, it would be interesting to assess the CSC potential of these cell populations using serial transplantation assays as a secondary measure of the ability of these cells to self-renew. Perhaps, this may be conducted in vitro using serial culture of organoids. However, this approach may not be as powerful as genetic lineage tracing. It is also important to note that the cre-lox lineage tracing models utilized in this study demonstrate genetic mosaicism. As a result of this, it is likely that the K19+ population labelled in my studies is reflective of only a subset of the true population. The CSC marker identified in this thesis was not characterized as distinct from Lgr5 cells through the appropriate lineage tracing/genetic ablation studies because of the extensive nature of the studies. Most importantly, the long-term side effects or targeting these novel CSC populations was not investigated. This is an important issue to consider before investigating these novel CSC markers as potential therapeutic targets, as K19+ cells share expression with both normal and cancerous tissues.

The second aim of this thesis was to assess the effects of Lgr5+ cell ablation on tumour growth *in vivo* and *in vitro*. In the *in vivo* model, no effect was observed on tumour initiation and growth. However, the mouse model used in this experiment does not recapitulate all types of human colorectal cancer and at all stages. Therefore, the results obtained are likely only reflective of this particular model. Importantly, this limitation is applicable to every mouse CRC model used in this thesis. As such human colorectal cancer organoids or additional animal models should be used to investigate these processes at various stages and types of CRC.

When analyzing the ablation of Lgr5 *in vitro*, I found no effect on spheroid number, growth or formation efficiency. Although the dose used was previously demonstrated to be effective by Asfaha et al., a potential limitation of this experiment is that confirmation of DT-mediated ablation by mRNA or immunohistochemical analysis was not carried out. Furthermore, it would have been optimal to conduct cell viability assays to determine the appropriate dose of DT. Lastly, in the organoid formation assays clumps of cells were plated rather than individual cells. It may have been more accurate to generate single cell

cultures from organoids which may be achieved by using TrypLE, however, this process is much costlier and time consuming.

## 4.8 Conclusion

The cancer stem cell hypothesis suggests that CSCs are the driving force behind tumour progression and metastasis, making them ideal therapeutic targets. Previous research identified Lgr5 as an important marker of CSCs in CRC. However, effective treatment of CRC patients depends on the identification of cells responsible for tumour initiation and progression. This was precisely the motivation of my studies. I found that K19 labels mouse intestinal CSCs in tumours arising in a model that recapitulates the early stages of human CRC. Moreover, selective ablation of Lgr5 had no effect on tumour initiation or growth *in vivo* or *in vitro*. These results clearly demonstrate that additional CSC populations, beyond Lgr5+ cells, exist in intestinal and colonic tumors and are important for tumour initiation and growth.

## REFERENCES


Afify, A., Purnell, P., & Nguyen, L. (2009). Role of CD44s and CD44v6 on human breast cancer cell adhesion, migration, and invasion. *Experimental and molecular pathology*, *86*(2), 95-100.

Al-Hajj, M., Wicha, M. S., Benito-Hernandez, A., Morrison, S. J., & Clarke, M. F. (2003). Prospective identification of tumorigenic breast cancer cells. *Proceedings of the National Academy of Sciences*, *100*(7), 3983-3988.

Artavanis-Tsakonas, S., Rand, M. D., & Lake, R. J. (1999). Notch signaling: cell fate control and signal integration in development. *Science*, *284*(5415), 770-776.

Asfaha, S., Hayakawa, Y., Muley, A., Stokes, S., Graham, T. A., Ericksen, R. E., ... & Guha, C. (2015). Krt19+/Lgr5− cells are radioresistant cancer-initiating stem cells in the colon and intestine. *Cell stem cell*, *16*(6), 627-638.

Ashton-Rickardt, P. G., Dunlop, M. G., Nakamura, Y., Morris, R. G., Purdie, C. A., Steel, C. M., ... & Wyllie, A. H. (1989). High frequency of APC loss in sporadic colorectal carcinoma due to breaks clustered in 5q21-22. *Oncogene*, *4*(10), 1169-1174.

Bao, S., Wu, Q., McLendon, R. E., Hao, Y., Shi, Q., Hjelmeland, A. B., ... & Rich, J. N. (2006). Glioma stem cells promote radioresistance by preferential activation of the DNA damage response. *Nature*, *444*(7120), 756.

Barker, N., Ridgway, R. A., van Es, J. H., van de Wetering, M., Begthel, H., van den Born, M., ... & Clevers, H. (2009). Crypt stem cells as the cells-of-origin of intestinal cancer. *Nature*, *457*(7229), 608.

Barker, N. (2014). Adult intestinal stem cells: critical drivers of epithelial homeostasis and regeneration. *Nature reviews Molecular cell biology*, *15*(1), 19.

Barker, N., Van Es, J. H., Kuipers, J., Kujala, P., Van Den Born, M., Cozijnsen, M., ... & Clevers, H. (2007). Identification of stem cells in small intestine and colon by marker gene Lgr5. *Nature*, *449*(7165), 1003.

Barker, N., Bartfeld, S., & Clevers, H. (2010). Tissue-resident adult stem cell populations of rapidly self-renewing organs. *Cell stem cell*, *7*(6), 656-670.

Barker, N., van Oudenaarden, A., & Clevers, H. (2012). Identifying the stem cell of the intestinal crypt: strategies and pitfalls. *Cell stem cell*, *11*(4), 452-460.

Bienz, M., & Clevers, H. (2000). Linking colorectal cancer to Wnt signaling. *Cell*, *103*(2), 311-320.

Blank, M., Klussmann, E., Krüger-Krasagakes, S., Schmitt-Gräff, A., Stolte, M., Bornhoeft, G., ... & Riecken, E. O. (1994). Expression of MUC2-mucin in colorectal adenomas and carcinomas of different histological types. *International journal of cancer*, *59*(3), 301-306.

Bonnet, D., & Dick, J. E. (1997). Human acute myeloid leukemia is organized as a hierarchy that originates from a primitive hematopoietic cell. *Nature medicine*, *3*(7), 730.

Bromfield, G., Dale, D., De, P., Newman, K., Rahal, R., & Shaw, A. (2017). Canadian cancer statistics, special topic: Predictions of the future burden of cancer in canada. *Toronto, ON: Canadian Cancer Society, Government of Canada*.

Chen, R., Nishimura, M. C., Bumbaca, S. M., Kharbanda, S., Forrest, W. F., Kasman, I. M., ... & Modrusan, Z. (2010). A hierarchy of self-renewing tumor-initiating cell types in glioblastoma. *Cancer cell*, *17*(4), 362-375.

Chen, J., Li, Y., Yu, T. S., McKay, R. M., Burns, D. K., Kernie, S. G., & Parada, L. F. (2012). A restricted cell population propagates glioblastoma growth after chemotherapy. *Nature*, *488*(7412), 522.

Cheng, H., & Leblond, C. P. (1974). Origin, differentiation and renewal of the four main epithelial cell types in the mouse small intestine V. Unitarian theory of the origin of the four epithelial cell types. *American Journal of Anatomy*, *141*(4), 537-561.

Chu, P., Clanton, D. J., Snipas, T. S., Lee, J., Mitchell, E., Nguyen, M. L., ... & Peach, R. J. (2009). Characterization of a subpopulation of colon cancer cells with stem cell-like properties. *International journal of cancer*, *124*(6), 1312-1321.

Clevers, H. (2011). The cancer stem cell: premises, promises and challenges. *Nature medicine*, *17*(3), 313.

Clevers, H. (2013). The intestinal crypt, a prototype stem cell compartment. *Cell*, *154*(2), 274-284.

Collins, A. T., Berry, P. A., Hyde, C., Stower, M. J., & Maitland, N. J. (2005). Prospective identification of tumorigenic prostate cancer stem cells. *Cancer research*, *65*(23), 10946-10951.

Colnot, S., Niwa-Kawakita, M., Hamard, G., Godard, C., Le Plenier, S., Houbron, C., ... & Perret, C. (2004). Colorectal cancers in a new mouse model of familial adenomatous polyposis: influence of genetic and environmental modifiers. *Laboratory investigation*, *84*(12), 1619.

Cunningham, D., et al. (2010). Colorectal cancer. *Lancet*, *375*(9719), 1030-47.

Dalerba, P., Kalisky, T., Sahoo, D., Rajendran, P. S., Rothenberg, M. E., Leyrat, A. A., ... & Zabala, M. (2011). Single-cell dissection of transcriptional heterogeneity in human colon tumors. *Nature biotechnology*, *29*(12), 1120.

Dalton, W. B., & Yang, V. W. (2007). Mitotic origins of chromosomal instability in colorectal cancer. *Current colorectal cancer reports*, *3*(2), 59-64.

Davies, R. J., Miller, R., & Coleman, N. (2005). Colorectal cancer screening: prospects for molecular stool analysis. *Nature Reviews Cancer*, *5*(3), 199.

Deng, S., Yang, X., Lassus, H., Liang, S., Kaur, S., Ye, Q., ... & Connolly, D. C. (2010). Distinct expression levels and patterns of stem cell marker, aldehyde dehydrogenase isoform 1 (ALDH1), in human epithelial cancers. *PloS one*, *5*(4), e10277.

Driessens, G., Beck, B., Caauwe, A., Simons, B. D., & Blanpain, C. (2012). Defining the mode of tumour growth by clonal analysis. *Nature*, *488*(7412), 527.

Du, L., Wang, H., He, L., Zhang, J., Ni, B., Wang, X., ... & Chen, Q. (2008). CD44 is of functional importance for colorectal cancer stem cells. *Clinical cancer research*, *14*(21), 6751-6760.

e Melo, F. D. S., Kurtova, A. V., Harnoss, J. M., Kljavin, N., Hoeck, J. D., Hung, J., ... & Dijkgraaf, G. J. (2017). A distinct role for Lgr5+ stem cells in primary and metastatic colon cancer. *Nature*, *543*(7647), 676.

Evans, J. P., Sutton, P. A., Winiarski, B. K., Fenwick, S. W., Malik, H. Z., Vimalachandran, D., ... & Kitteringham, N. R. (2016). From mice to men: Murine models of colorectal cancer for use in translational research. *Critical reviews in oncology/hematology*, *98*, 94-105.

Fearon, E. R., & Vogelstein, B. (1990). A genetic model for colorectal tumorigenesis. *Cell*, *61*(5), 759-767.

Foersch, S., & Neurath, M. F. (2014). Colitis-associated neoplasia: molecular basis and clinical translation. *Cellular and molecular life sciences*, *71*(18), 3523-3535.

Foulds, L. (1954). The experimental study of tumor progression: a review. *Cancer research*, *14*(5), 327-339.

Fredebohm, J., Boettcher, M., Eisen, C., Gaida, M. M., Heller, A., Keleg, S., ... & Giese, N. A. (2012). Establishment and characterization of a highly tumourigenic and cancer stem cell enriched pancreatic cancer cell line as a well defined model system. *PloS one*, *7*(11), e48503.

Fujii, M., Shimokawa, M., Date, S., Takano, A., Matano, M., Nanki, K., ... & Uraoka, T. (2016). A colorectal tumor organoid library demonstrates progressive loss of niche factor requirements during tumorigenesis. *Cell Stem Cell*, *18*(6), 827-838.

Gregorieff, A., & Clevers, H. (2005). Wnt signaling in the intestinal epithelium: from endoderm to cancer. *Genes & development*, *19*(8), 877-890.

Grabowski, P., SchÖnfelder, J., AHNERT-HILGER, G. U. D. R. U. N., FOSS, H. D., Stein, H., Berger, G., ... & ScherÜbl, H. (2004). Heterogeneous expression of neuroendocrine marker proteins in human undifferentiated carcinoma of the colon and rectum. *Annals of the New York Academy of Sciences*, *1014*(1), 270-274.

Gryfe, R., Bapat, B., Gallinger, S., Swallow, C., Redston, M., & Couture, J. (1997). Molecular biology of colorectal cancer. *Current problems in cancer*, *21*(5), 233-299.

Groden, J., Thliveris, A., Samowitz, W., Carlson, M., Gelbert, L., Albertsen, H., ... & Sargeant, L. (1991). Identification and characterization of the familial adenomatous polyposis coli gene. *Cell*, *66*(3), 589-600.

Gunawardene, A. R., Corfe, B. M., & Staton, C. A. (2011). Classification and functions of enteroendocrine cells of the lower gastrointestinal tract. *International journal of experimental pathology*, *92*(4), 219-231.

Gupta, P. B., Chaffer, C. L., & Weinberg, R. A. (2009). Cancer stem cells: mirage or reality?. *Nature medicine*, *15*(9), 1010.

Hanahan, D., & Weinberg, R. A. (2011). Hallmarks of cancer: the next generation. *cell*, *144*(5), 646-674.

Huang, E. H., Hynes, M. J., Zhang, T., Ginestier, C., Dontu, G., Appelman, H., ... & Boman, B. M. (2009). Aldehyde dehydrogenase 1 is a marker for normal and malignant human colonic stem cells (SC) and tracks SC overpopulation during colon tumorigenesis. *Cancer research*, *69*(8), 3382-3389.

He, X. C., Zhang, J., Tong, W. G., Tawfik, O., Ross, J., Scoville, D. H., ... & Mishina, Y. (2004). BMP signaling inhibits intestinal stem cell self-renewal through suppression of Wnt–β-catenin signaling. *Nature genetics*, *36*(10), 1117.

Hermann, P. C., Huber, S. L., Herrler, T., Aicher, A., Ellwart, J. W., Guba, M., ... & Heeschen, C. (2007). Distinct populations of cancer stem cells determine tumor growth and metastatic activity in human pancreatic cancer. *Cell stem cell*, *1*(3), 313-323.

Ishikawa, F., Yoshida, S., Saito, Y., Hijikata, A., Kitamura, H., Tanaka, S., ... & Fukata, M. (2007). Chemotherapy-resistant human AML stem cells home to and engraft within the bone-marrow endosteal region. *Nature biotechnology*, *25*(11), 1315.

Jasperson, K. W., Tuohy, T. M., Neklason, D. W., & Burt, R. W. (2010). Hereditary and familial colon cancer. *Gastroenterology*, *138*(6), 2044-2058.

Joo, K. M., Kim, S. Y., Jin, X., Song, S. Y., Kong, D. S., Lee, J. I., ... & Jin, J. (2008). Clinical and biological implications of CD133-positive and CD133-negative cells in glioblastomas. *Laboratory investigation*, *88*(8), 808.

Junttila, M. R., Mao, W., Wang, X., Wang, B. E., Pham, T., Flygare, J., ... & Eastham-Anderson, J. (2015). Targeting LGR5+ cells with an antibody-drug conjugate for the treatment of colon cancer. *Science translational medicine*, *7*(314), 314ra186-314ra186.

Kaestner, K. H., Silberg, D. G., Traber, P. G., & Schütz, G. (1997). The mesenchymal winged helix transcription factor Fkh6 is required for the control of gastrointestinal proliferation and differentiation. *Genes & development*, *11*(12), 1583-1595.

Kemper, K., Prasetyanti, P. R., De Lau, W., Rodermond, H., Clevers, H., & Medema, J. P. (2012). Monoclonal antibodies against Lgr5 identify human colorectal cancer stem cells. *Stem cells*, *30*(11), 2378-2386.

Kettunen, H. L., Kettunen, A. S., & Rautonen, N. E. (2003). Intestinal immune responses in wild-type and Apcmin/+ mouse, a model for colon cancer. *Cancer research*, *63*(16), 5136-5142.

Keysar, S. B., & Jimeno, A. (2010). More than markers: biological significance of cancer stem cell-defining molecules. *Molecular cancer therapeutics*, 1535-7163.

Kinzler, K. W., Nilbert, M. C., Su, L. K., Vogelstein, B., Bryan, T. M., Levy, D. B., ... & McKechnie, D. (1991). Identification of FAP locus genes from chromosome 5q21. *Science*, *253*(5020), 661-665.

Kim, M. P., Fleming, J. B., Wang, H., Abbruzzese, J. L., Choi, W., Kopetz, S., ... & Gallick, G. E. (2011). ALDH activity selectively defines an enhanced tumor-initiating cell population relative to CD133 expression in human pancreatic adenocarcinoma. *PloS one*, *6*(6), e20636.

Kobayashi, S., Yamada-Okabe, H., Suzuki, M., Natori, O., Kato, A., Matsubara, K., ... & Hashimoto, E. (2012). LGR5-positive colon cancer stem cells interconvert with drug-resistant LGR5-negative cells and are capable of tumor reconstitution. *Stem cells*, *30*(12), 2631-2644.

Koo, B. K., & Clevers, H. (2014). Stem cells marked by the R-spondin receptor LGR5. *Gastroenterology*, *147*(2), 289-302.

Kosinski, C., Stange, D. E., Xu, C., Chan, A. S., Ho, C., Yuen, S. T., ... & Chen, X. (2010). Indian hedgehog regulates intestinal stem cell fate through epithelial− mesenchymal interactions during development. *Gastroenterology*, *139*(3), 893-903.

Lapidot, T., Sirard, C., Vormoor, J., Murdoch, B., Hoang, T., Caceres-Cortes, J., ... & Dick, J. E. (1994). A cell initiating human acute myeloid leukaemia after transplantation into SCID mice. *Nature*, *367*(6464), 645.

Lapouge, G., Youssef, K. K., Vokaer, B., Achouri, Y., Michaux, C., Sotiropoulou, P. A., & Blanpain, C. (2011). Identifying the cellular origin of squamous skin tumors. Proceedings of the National Academy of Sciences, 201012720.

Li, Z. (2013). CD133: a stem cell biomarker and beyond. *Experimental hematology & oncology*, *2*(1), 17.

Livet, J., Weissman, T. A., Kang, H., Draft, R. W., Lu, J., Bennis, R. A., ... & Lichtman, J. W. (2007). Transgenic strategies for combinatorial expression of fluorescent proteins in the nervous system. *Nature*, *450*(7166), 56.

Leblond, C. P., & Stevens, C. E. (1948). The constant renewal of the intestinal epithelium in the albino rat. *The Anatomical Record*, *100*(3), 357-377.

Luche, H., Weber, O., Rao, T. N., Blum, C., & Fehling, H. J. (2007). Faithful activation of an extra-bright red fluorescent protein in "knock-in" Cre-reporter mice ideally suited for lineage tracing studies. *European journal of immunology*, *37*(1), 43-53.

Marhaba, R., & Zöller, M. (2004). CD44 in cancer progression: adhesion, migration and growth regulation. *Journal of molecular histology*, *35*(3), 211-231.

Marsh, K. A., Stamp, G. W., & Kirkland, S. C. (1993). Isolation and characterization of multiple cell types from a single human colonic carcinoma: tumourigenicity of these cell types in a xenograft system. *The Journal of pathology*, *170*(4), 441-450.

Mashimo, H., Wu, D. C., Podolsky, D. K., & Fishman, M. C. (1996). Impaired defense of intestinal mucosa in mice lacking intestinal trefoil factor. *Science*, *274*(5285), 262-265.

Medema, J. P., & Vermeulen, L. (2011). Microenvironmental regulation of stem cells in intestinal homeostasis and cancer. *Nature*, *474*(7351), 318.

Medema, J. P. (2013). Cancer stem cells: the challenges ahead. *Nature cell biology*, *15*(4), 338.

Middelhoff, M., Westphalen, C. B., Hayakawa, Y., Yan, K. S., Gershon, M. D., Wang, T. C., & Quante, M. (2017). Dclk1-expressing tuft cells: critical modulators of the intestinal niche?. *American Journal of Physiology-Gastrointestinal and Liver Physiology*, *313*(4), G285-G299.

Miyaki, M., Konishi, M., Kikuchi-Yanoshita, R., Enomoto, M., Igari, T., Tanaka, K., ... & Maeda, Y. (1994). Characteristics of somatic mutation of the adenomatous polyposis coli gene in colorectal tumors. *Cancer research*, *54*(11), 3011-3020.

Moll, R., Franke, W. W., Schiller, D. L., Geiger, B., & Krepler, R. (1982). The catalog of human cytokeratins: patterns of expression in normal epithelia, tumors and cultured cells. *Cell*, *31*(1), 11-24.

Moolenbeek, C., & Ruitenberg, E. J. (1981). The 'Swiss roll': a simple technique for histological studies of the rodent intestine. *Laboratory animals*, *15*(1), 57-60.

Moser A. R., Pitot H. C., Dove W. F. A dominant mutation that predisposes to intestinal neoplasia in the mouse. *Science (Washington DC)*, 247*:* 322-324,1990.

Muñoz, J., Stange, D. E., Schepers, A. G., Van De Wetering, M., Koo, B. K., Itzkovitz, S., ... & Myant, K. (2012). The Lgr5 intestinal stem cell signature: robust expression of proposed quiescent '+ 4'cell markers. *The EMBO journal*, *31*(14), 3079-3091.

Nakanishi, Y., Seno, H., Fukuoka, A., Ueo, T., Yamaga, Y., Maruno, T., ... & Isomura, A. (2013). Dclk1 distinguishes between tumor and normal stem cells in the intestine. *Nature genetics*, *45*(1), 98.

Nguyen, L. V., Vanner, R., Dirks, P., & Eaves, C. J. (2012). Cancer stem cells: an evolving concept. *Nature Reviews Cancer*, *12*(2), 133.

Nowell, P. C. (1976). The clonal evolution of tumor cell populations. *Science*, *194*(4260), 23-28.

O'Brien, C. A., Pollett, A., Gallinger, S., & Dick, J. E. (2007). A human colon cancer cell capable of initiating tumour growth in immunodeficient mice. *Nature*, *445*(7123), 106.

O'Connell, M. J., Campbell, M. E., Goldberg, R. M., Grothey, A., Seitz, J. F., Benedetti, J. K., ... & Sargent, D. J. (2008). Survival following recurrence in stage II and III colon cancer: findings from the ACCENT data set. *Journal of Clinical Oncology*, *26*(14), 2336-2341.

Ogden, A. T., Waziri, A. E., Lochhead, R. A., Fusco, D., Lopez, K., Ellis, J. A., ... & McCormick, P. C. (2008). Identification of A2B5+ CD133− tumor-initiating cells in adult human gliomas. *Neurosurgery*, *62*(2), 505-515.

Pham, P. V., Phan, N. L., Nguyen, N. T., Truong, N. H., Duong, T. T., Le, D. V., ... & Phan, N. K. (2011). Differentiation of breast cancer stem cells by knockdown of CD44: promising differentiation therapy. *Journal of translational medicine*, *9*(1), 1.

Pierce, G. B., Nakane, P. K., Martinez-Hernandez, A., & Ward, J. M. (1977). Ultrastructural comparison of differentiation of stem cells of murine adenocarcinomas of colon and breast with their normal counterparts. *Journal of the National Cancer Institute*, *58*(5), 1329-1345.

Plaks, V., Kong, N., & Werb, Z. (2015). The cancer stem cell niche: how essential is the niche in regulating stemness of tumor cells?. *Cell stem cell*, *16*(3), 225-238.

Polakis, P. (1999). The oncogenic activation of β-catenin. *Current opinion in genetics & development*, *9*(1), 15-21.

Polakis, P. (2000). Wnt signaling and cancer. *Genes & development*, *14*(15), 1837-1851.

Potten, C. S., Booth, C., & Pritchard, D. M. (1997). The intestinal epithelial stem cell: the mucosal governor. *International journal of experimental pathology*, *78*(4), 219-243.

Powell, S. M., Zilz, N., Beazer-Barclay, Y., Bryan, T. M., Hamilton, S. R., Thibodeau, S. N., ... & Kinzler, K. W. (1992). APC mutations occur early during colorectal tumorigenesis. *Nature*, *359*(6392), 235.

Quintana, E., Shackleton, M., Sabel, M. S., Fullen, D. R., Johnson, T. M., & Morrison, S. J. (2008). Efficient tumour formation by single human melanoma cells. *Nature*, *456*(7222), 593.

Radtke, F., Clevers, H., & Riccio, O. (2006). From gut homeostasis to cancer. *Current molecular medicine*, *6*(3), 275-289.

Ragnhammar, P., Hafström, L., Nygren, P., & Glimelius, B. (2001). A systematic overview of chemotherapy effects in colorectal cancer. *Acta oncologica*, *40*(2-3), 282-308.

Ricci-Vitiani, L., Lombardi, D. G., Pilozzi, E., Biffoni, M., Todaro, M., Peschle, C., & De Maria, R. (2007). Identification and expansion of human colon-cancer-initiating cells. *Nature*, *445*(7123), 111.

Richardson, G. D., Robson, C. N., Lang, S. H., Neal, D. E., Maitland, N. J., & Collins, A. T. (2004). CD133, a novel marker for human prostatic epithelial stem cells. *Journal of cell science*, *117*(16), 3539-3545.

Rizk, P., & Barker, N. (2012). Gut stem cells in tissue renewal and disease: methods, markers, and myths. Wiley Interdisciplinary Reviews: Systems Biology and Medicine, 4(5), 475-496.

Rosenberg, D. W., Giardina, C., & Tanaka, T. (2008). Mouse models for the study of colon carcinogenesis. *Carcinogenesis*, *30*(2), 183-196.

Sarkar, F. H., Li, Y., Wang, Z., & Kong, D. (2009). Pancreatic cancer stem cells and EMT in drug resistance and metastasis. *Minerva chirurgica*, *64*(5), 489.

Sangiorgi, E., & Capecchi, M. R. (2008). Bmi1 is expressed in vivo in intestinal stem cells. *Nature genetics*, *40*(7), 915.

Sansom, O. J., Reed, K. R., Hayes, A. J., Ireland, H., Brinkmann, H., Newton, I. P., ... & Clarke, A. R. (2004). Loss of Apc in vivo immediately perturbs Wnt signaling, differentiation, and migration. *Genes & development*, *18*(12), 1385-1390.

Sasaki, N., Sachs, N., Wiebrands, K., Ellenbroek, S. I., Fumagalli, A., Lyubimova, A., ... & Li, V. S. (2016). Reg4+ deep crypt secretory cells function as epithelial niche for Lgr5+ stem cells in colon. *Proceedings of the National Academy of Sciences*, *113*(37), E5399-E5407.

Sato, T., Vries, R. G., Snippert, H. J., Van De Wetering, M., Barker, N., Stange, D. E., ... & Clevers, H. (2009). Single Lgr5 stem cells build crypt–villus structures in vitro without a mesenchymal niche. *Nature*, *459*(7244), 262.

Sato, T., Stange, D. E., Ferrante, M., Vries, R. G., Van Es, J. H., Van Den Brink, S., ... & Clevers, H. (2011). Long-term expansion of epithelial organoids from human colon, adenoma, adenocarcinoma, and Barrett's epithelium. *Gastroenterology*, *141*(5), 1762-1772.

Shachaf, C. M., Kopelman, A. M., Arvanitis, C., Karlsson, Å., Beer, S., Mandl, S., ... & Yang, Q. (2004). MYC inactivation uncovers pluripotent differentiation and tumour dormancy in hepatocellular cancer. *Nature*, *431*(7012), 1112.

Schepers, A. G., Snippert, H. J., Stange, D. E., van den Born, M., van Es, J. H., van de Wetering, M., & Clevers, H. (2012). Lineage tracing reveals Lgr5+ stem cell activity in mouse intestinal adenomas. *Science*, *337*(6095), 730-735.

Schwitalla, S., Fingerle, A. A., Cammareri, P., Nebelsiek, T., Göktuna, S. I., Ziegler, P. K., ... & Rupec, R. A. (2013). Intestinal tumorigenesis initiated by dedifferentiation and acquisition of stem-cell-like properties. *Cell*, *152*(1), 25-38.

Shimokawa, M., Ohta, Y., Nishikori, S., Matano, M., Takano, A., Fujii, M., ... & Sato, T. (2017). Visualization and targeting of LGR5+ human colon cancer stem cells. *Nature*, *545*(7653), 187.

Shmelkov, S. V., Butler, J. M., Hooper, A. T., Hormigo, A., Kushner, J., Milde, T., ... & Chadburn, A. (2008). CD133 expression is not restricted to stem cells, and both CD133+ and CD133–metastatic colon cancer cells initiate tumors. *The Journal of clinical investigation*, *118*(6), 2111-2120.

Sikandar, S. S., Pate, K. T., Anderson, S., Dizon, D., Edwards, R. A., Waterman, M. L., & Lipkin, S. M. (2010). NOTCH signaling is required for formation and self-renewal of tumor-initiating cells and for repression of secretory cell differentiation in colon cancer. *Cancer research*, 0008-5472.

Singh, S. K., Hawkins, C., Clarke, I. D., Squire, J. A., Bayani, J., Hide, T., ... & Dirks, P. B. (2004). Identification of human brain tumour initiating cells. *nature*, *432*(7015), 396.

Spit, M., Koo, B. K., & Maurice, M. M. (2018). Tales from the crypt: intestinal niche signals in tissue renewal, plasticity and cancer. *Open biology*, *8*(9), 180120.

Staal, F. J., Weerkamp, F., Baert, M. R., van den Burg, C. M., van Noort, M., de Haas, E. F., & van Dongen, J. J. (2004). Wnt target genes identified by DNA microarrays in immature CD34+ thymocytes regulate proliferation and cell adhesion. *The Journal of Immunology*, *172*(2), 1099-1108.

Stevens, C. E., & Leblond, C. P. (1947). Rate of renewal of the cells of the intestinal epithelium in the rat. *The Anatomical record*, *97*(3), 373.

Su, Y., Qiu, Q., Zhang, X., Jiang, Z., Leng, Q., Liu, Z., ... & Jiang, F. (2010). Aldehyde dehydrogenase 1 A1–positive cell population is enriched in tumor-initiating cells and associated with progression of bladder cancer. *Cancer Epidemiology and Prevention Biomarkers*, *19*(2), 327-337.

Su L. K., Kinzler K. W., Vogelstein B., Preisinger A. C., Moser A. R., Luongo C., Gould K. A., Dove W. F. Multiple intestinal neoplasia caused by a mutation in the murine homolog of the *APC* gene. *Science (Washington DC),* 256*:* 668-670, 1992

Sullivan, J. P., Minna, J. D., & Shay, J. W. (2010). Evidence for self-renewing lung cancer stem cells and their implications in tumor initiation, progression, and targeted therapy. *Cancer and Metastasis Reviews*, *29*(1), 61-72.

Takahashi, M., Fukuda, K., Sugimura, T., & Wakabayashi, K. (1998). β-Catenin is frequently mutated and demonstrates altered cellular location in azoxymethane-induced rat colon tumors. *Cancer research*, *58*(1), 42-46.

Takahashi, M., Nakatsugi, S., Sugimura, T., & Wakabayashi, K. (2000). Frequent mutations of the β-catenin gene in mouse colon tumors induced by azoxymethane. *Carcinogenesis*, *21*(6), 1117-1120.

Takahashi, M., & Wakabayashi, K. (2004). Gene mutations and altered gene expression in azoxymethane-induced colon carcinogenesis in rodents. *Cancer science*, *95*(6), 475-480.

Takeda, N., Jain, R., LeBoeuf, M. R., Wang, Q., Lu, M. M., & Epstein, J. A. (2011). Interconversion between intestinal stem cell populations in distinct niches. *Science*, *334*(6061), 1420-1424.

Tanaka, T., Kohno, H., Suzuki, R., Yamada, Y., Sugie, S., & Mori, H. (2003). A novel inflammation-related mouse colon carcinogenesis model induced by azoxymethane and dextran sodium sulfate. *Cancer science*, *94*(11), 965-973.

Tanei, T., Morimoto, K., Shimazu, K., Kim, S. J., Tanji, Y., Taguchi, T., ... & Noguchi, S. (2009). Association of breast cancer stem cells identified by aldehyde dehydrogenase 1 expression with resistance to sequential Paclitaxel and epirubicin-based chemotherapy for breast cancers. *Clinical cancer research*, *15*(12), 4234-4241.

Tian, H., Biehs, B., Warming, S., Leong, K. G., Rangell, L., Klein, O. D., & de Sauvage, F. J. (2011). A reserve stem cell population in small intestine renders Lgr5-positive cells dispensable. *Nature*, *478*(7368), 255.

Tomita, H., Tanaka, K., Tanaka, T., & Hara, A. (2016). Aldehyde dehydrogenase 1A1 in stem cells and cancer. *Oncotarget*, *7*(10), 11018.

Van der Flier, L. G., van Gijn, M. E., Hatzis, P., Kujala, P., Haegebarth, A., Stange, D. E., ... & van Es, J. H. (2009). Transcription factor achaete scute-like 2 controls intestinal stem cell fate. *Cell*, *136*(5), 903-912.

Van der Flier, L. G., Sabates–Bellver, J., Oving, I., Haegebarth, A., De Palo, M., Anti, M., ... & Clevers, H. (2007). The intestinal Wnt/TCF signature. *Gastroenterology*, *132*(2), 628-632.

Van Der Flier, L. G., & Clevers, H. (2009). Stem cells, self-renewal, and differentiation in the intestinal epithelium. *Annual review of physiology*, *71*, 241-260.

Van Der Kraak, L., Gros, P., & Beauchemin, N. (2015). Colitis-associated colon cancer: Is it in your genes?. *World journal of gastroenterology*, *21*(41), 11688.

Vermeulen, L., & Snippert, H. J. (2014). Stem cell dynamics in homeostasis and cancer of the intestine. *Nature Reviews Cancer*, *14*(7), 468-480.

Visvader, J. E. (2011). Cells of origin in cancer. *Nature*, *469*(7330), 314.

Wang, J., Sakariassen, P. Ø., Tsinkalovsky, O., Immervoll, H., Bøe, S. O., Svendsen, A., ... & Molven, A. (2008). CD133 negative glioma cells form tumors in nude rats and give rise to CD133 positive cells. *International journal of cancer*, *122*(4), 761-768.

Wang, L., Su, W., Liu, Z., Zhou, M., Chen, S., Chen, Y., ... & Han, Z. (2012). CD44 antibody-targeted liposomal nanoparticles for molecular imaging and therapy of hepatocellular carcinoma. *Biomaterials*, *33*(20), 5107-5114.

West, A. B., Isaac, C. A., Carboni, J. M., Morrow, J. S., Mooseker, M. S., & Barwick, K. W. (1988). Localization of villin, a cytoskeletal protein specific to microvilli, in human ileum and colon and in colonic neoplasms. *Gastroenterology*, *94*(2), 343-352.

Wirtz, S., Neufert, C., Weigmann, B., & Neurath, M. F. (2007). Chemically induced mouse models of intestinal inflammation. *Nature protocols*, *2*(3), 541.

World Cancer Research Fund/American Institute for Cancer Research. (2011). Continuous update project report. Food, nutrition, physical activity, and the prevention of colorectal cancer.

Yamashita, K., Katoh, H., & Watanabe, M. (2013). The homeobox only protein homeobox (HOPX) and colorectal cancer. *International journal of molecular sciences*, *14*(12), 23231-23243.

Yan, K. S., Chia, L. A., Li, X., Ootani, A., Su, J., Lee, J. Y., ... & Sangiorgi, E. (2012). The intestinal stem cell markers Bmi1 and Lgr5 identify two functionally distinct populations. *Proceedings of the National Academy of Sciences*, *109*(2), 466-471.

Yanai, H., Atsumi, N., Tanaka, T., Nakamura, N., Komai, Y., Omachi, T., ... & Tokuyama, Y. (2017). Intestinal cancer stem cells marked by Bmi1 or Lgr5 expression contribute to tumor propagation via clonal expansion. *Scientific reports*, *7*, 41838.

Yoon, C., Park, D. J., Schmidt, B., Thomas, N. J., Lee, H. J., Kim, T. S., ... & Yoon, S. S. (2014). CD44 expression denotes a subpopulation of gastric cancer cells in which Hedgehog signaling promotes chemotherapy resistance. *Clinical cancer research*.

Yu, Y., Ramena, G., & Elble, R. C. (2012). The role of cancer stem cells in relapse of solid tumors. *Front Biosci (Elite Ed)*, *4*(4), 1528-1541.

Zasadil, L. M., Britigan, E. M., Ryan, S. D., Kaur, C., Guckenberger, D. J., Beebe, D. J., ... & Weaver, B. A. (2016). High rates of chromosome missegregation suppress tumor progression but do not inhibit tumor initiation. *Molecular biology of the cell*, *27*(13), 1981-1989.

Zeuner, A., Todaro, M., Stassi, G., & De Maria, R. (2014). Colorectal cancer stem cells: from the crypt to the clinic. *Cell stem cell*, *15*(6), 692-705.

## APPENDIX I: CHEMICAL LIST AND SUPPLIERS

| CHEMICAL | SUPPLIER |
|---|---|
| **TAMOXIFEN** | Sigma |
| **DAPI** | Fisher |
| **AOM** | Sigma |
| **DIPHTHERIA TOXIN** | Sigma |
| **TAQQ FROGGAMIX** | FroggaBio |
| **TAE** | Fisher |
| **NUCLEASE FREE H2O** | FroggaBio |
| **AGAROSE** | Fisher |
| **ETHIDIUM BROMIDE** | Sigma |
| **DSS** | Gojira |
| **CORN OIL** | Sigma |
| **PBS** | Fisher |
| **4% PFA** | Santa Cruz |
| **OCT** | Fisher |
| **EOSIN** | Fisher |
| **HEMATOXYLIN** | Cedarlane |
| **XYLENES** | Fisher |
| **MOUNTING MEDIUM DAPI** | Vectashield |
| **MOUNTING MEDIUM H&E** | Toluene - Fisher |
| **EDTA** | Fisher |
| **TRITON X 100** | Fisher |
| **FBS** | Fisher |
| **DMEM** | Life Tech |
| **GLUTAMAX** | Life Tech |

| | |
|---|---|
| **HEPES** | Life Tech |
| **PEN/STREP** | Life Tech |

# APPENDIX II: PREPARATION OF SOLUTIONS

**Tail Lysis Buffer – 25mM NaOH/0.2mM EDTA**

| | |
|---|---|
| 10M NaOH | 125mL |
| 0.5M EDTA | 20 mL |
| MilliQ Water | 49.8 mL |

1. Add 125 mL of 10M NaOH + 20mL 0.5M EDTA to 50 mL centrifuge tube.
2. Fill up to 50 mL of MilliQ water.

**Tail Neutralization Buffer – 40mM Tris HCL (pH 5.5)**

| | |
|---|---|
| Tris HCL | 315.12 mg |
| MilliQ water | 50 mL |

1. Add 315.12 mg of Tris HCL to 50 mL centrifuge tube.
2. Fill MilliQ water up to 45 mL
3. Adjust pH to 5.5 using 10M NaOH and HCL
4. Fill milliQ water up to 50 mL

## APPENDIX III: PCR CONDITIONS AND PRIMERS

**K19-CreERT**

| CYCLE STEP | TEMP (°C) | TIME | CYCLES |
|---|---|---|---|
| Initial Denaturation | 94 | 5min | 1 |
| Denaturation | 94 | 30s | 35 |
| Annealing | 55 | 30s | |
| Extension | 72 | 30s | |
| Final Extension | 72 | 7min | 1 |
| Hold | 4 | ∞ | |

Primers:

F- TCTCCCTCCTCATCATGTCC
R- CATGTTTAGCTGGCCCAAAT

**APCf/f**

| CYCLE STEP | TEMP (°C) | TIME | CYCLES |
|---|---|---|---|
| Initial Denaturation | 94 | 5min | 1 |
| Denaturation | 94 | 30s | 35 |
| Annealing | 60 | 30s | |
| Extension | 72 | 30s | |
| Final Extension | 72 | 7min | 1 |
| Hold | 4 | ∞ | |

Primers:
F- GAGAAACCCTGTCTCGAAAAAA
R- AGTGCTGTTTCTATGAGTCAAC

**Rosa26-tdTomato**

| CYCLE STEP | TEMP (°C) | TIME | CYCLES |
|---|---|---|---|
| Initial Denaturation | 94 | 5min | 1 |
| Denaturation | 94 | 30s | 35 |
| Annealing | 61 | 30s | |
| Extension | 72 | 30s | |

| | | | |
|---|---|---|---|
| Final Extension | 72 | 7min | 1 |
| Hold | 4 | ∞ | |

Primers:
WT F – AAG GGA GCT GCA GTG GAG TA
WT R - CCG AAA ATC TGT GGG AAG TC

Mut F – GGC ATT AAA GCA GCG TAT CC
Mut R - CTG TTC CTG TAC GGC ATG G

**Lgr5-DTR**

| CYCLE STEP | TEMP (°C) | TIME | CYCLES |
|---|---|---|---|
| Initial Denaturation | 94 | 5min | 1 |
| Denaturation | 94 | 30s | 35 |
| Annealing | 61 | 30s | |
| Extension | 72 | 30s | |
| Final Extension | 72 | 7min | 1 |
| Hold | 4 | ∞ | |

Primers:
F – AGAAGCCGGTGGAGAAGAG
R - GCTTGTGGCTTGGAGGATAA

**APCmin**

| CYCLE STEP | TEMP (°C) | TIME | CYCLES |
|---|---|---|---|
| Initial Denaturation | 94 | 5min | 1 |
| Denaturation | 94 | 30s | 35 |
| Annealing | 55 | 30s | |
| Extension | 72 | 1min | |
| Final Extension | 72 | 1min | 1 |
| Hold | 4 | ∞ | |

Primers:
F – TTC TGA GAA AGA CAG AAG TTA
R - TTC CAC TTT GGC ATA AGG C

**Lgr5**

| CYCLE STEP | TEMP (°C) | TIME | CYCLES |
|---|---|---|---|
| Initial Denaturation | 94 | 5min | 1 |
| Denaturation | 94 | 30s | 35 |
| Annealing | 58 | 40s | |
| Extension | 65 | 1:10 min | |
| Final Extension | 65 | 3min | 1 |
| Hold | 4 | ∞ | |

Primers:
F - CACTGCATTCTAGTTGTGG
R – CGGTGCCCGCAGCGAG

# CURRICULUM VITAE

**Name:** Amber Harnett

**Post-secondary Education and Degrees:**
The University of Western Ontario
London, Ontario, Canada
2016-2018 M.Sc.

University of Guelph
Guelph, Ontario, Canada
2011-2016 B.Sc.

**Honours and Awards:**
Western Graduate Research Scholarship (WGRS)
2016-2017, 2017-2018

Cancer Research and Technology Transfer (CaRTT) Scholarship
2017-2018

Bruce Holub Prize
2016

**Publications:**

Wilkin A.M., **Harnett A***, Underschult M, Cragg C, Meckling K. (2018). Role of the ERp57 protein (1,25D3-MARRS receptor) in murine mammary gland growth and development. *Steroids, 135,* 63-68.

Roke K, Walton K, Klingel S, **Harnett A***, Dang S, Haines J, Mutch, D. (2017). Evaluating changes in omega3 fatty acid intake after receiving personal FADS1 genetic information: a randomized nutrigenetic intervention. *Nutrients,* 9(3*),* 240.